Vascular Endothelial Growth Factor-A Expression and Role in Uveal Melanoma

by

Patrick Logan, B.Sc., M.Sc.

Department of Pathology

McGill University

Montreal, Canada

November 2012

A thesis submitted to the Faculty of Graduate Studies and Research in partial fulfillment of the requirements of the degree of Doctor of Philosophy

Abstract

Introduction: Uveal melanoma (UM) is an intraocular tumor that affects 4-6 people per million in the United States, 40% of which will develop liver metastasis within five years. Vascular endothelial growth factor A (VEGF-A) has been extensively studied in cancer due to the requirement for additional vasculature in tumors. Bevacizumab is a humanized monoclonal antibody that binds VEGF-A and is approved for the treatment of various malignancies. Herein, we investigated the expression of VEGF-A in three UM cell lines and the effects of inhibiting VEGF-A on their functional abilities. We also determined if positive VEGF-A expression can predict metastasis in a UM model and in patients.

Materials and Methods: VEGF-A secretion was evaluated in three UM cell lines using sandwich ELISA. Proliferation, migration, and invasion assays were performed before and after the administration of bevacizumab and cytokine expression was assessed by ELISA. One cytokine that was upregulated following bevacizumab treatment (CCL3) was knocked down using siRNA, and the functional assays were repeated using CCL3 siRNA and combination treatments.

Uveal melanoma tumors (n = 27) from an animal model and tumors from human patients (n = 29) were immunostained for VEGF-A. Two different custom immunostaining quantification algorithms implemented with ImageJ software were used to automatically count positive cells and positive staining area. Binary logistic regression was performed to determine if positive staining could predict metastases. $P < 0.05$ was considered significant.

Results: All three UM cell lines produced and secreted VEGF-A and expressed VEGF-R2. Bevacizumab usurped VEGF-A and reduced phosphorylated-VEGF-R2. Proliferation and migration were reduced following bevacizumab treatment ($p < 0.05$ for one cell line, and $p < 0.05$ for two cell lines, respectively).

Both CCL3 and MMP-9 were significantly upregulated after bevacizumab treatment in all cell lines ($p < 0.05$). Proliferation was significantly reduced in all three cell lines following CCL3 siRNA and combination treatments ($p < 0.05$). Migration was significantly reduced in all three cell lines after combination treatment ($p < 0.05$) and invasion was significantly reduced in two cell lines following siRNA ($p < 0.05$). In general, combination therapy was more effective than bevacizumab monotherapy for inhibiting UM functional abilities.

In both rabbit and human tissue, VEGF-A positivity could be used to significantly predict metastasis ($p > 0.05$).

Conclusions: Auto and paracrine VEGF-A signalling is abundant in UM cell lines, but inhibiting VEGF-A has only moderate effects on their functional abilities. This is attributable to compensatory effects, including the upregulation of CCL3. In addition, VEGF-A staining correlated with metastatic development in our patient cohort.

VEGF-A is a powerful cytokine that may play a role in UM development and progression. However, compensatory effects induced by bevacizumab suggest that dual or multiple therapies may be required to effectively treat this tumor.

French Abstract

Introduction: Le mélanome uvéal (MU) est une tumeur intra-oculaire qui affecte 4 à 6 personnes par million aux États-Unis, dont 40% développeront des métastases du foie dans les cinq ans. Le facteur de croissance vasculaire endothélial A (VEGF-A) a été largement étudié sur le cancer en raison de l'exigence de la vascularisation des tumeurs supplémentaires. Le bevacizumab est un anticorps monoclonal humanisé qui se lie au VEGF-A et il est approuvé pour le traitement de diverses tumeurs malignes. Ici, nous avons étudié l'expression du VEGF-A dans trois lignées cellulaires du MU et les effets de l'inhibition du VEGF-A sur leurs capacités fonctionnelles. Nous avons également déterminé si VEGF-A positif d'expression ne peut prédire les métastases dans un modèle UM et chez les patients.

Matériaux et méthodes: VEGF-A sécrétion a été évaluée dans trois lignées cellulaires du MU en utilisant ELISA en sandwich. Des tests de prolifération, la migration et l'invasion ont été réalisés avant et après l'administration de l'expression des cytokines et bevacizumab a été évaluée par ELISA. Une cytokine qui a été régulée à la hausse après le traitement bevacizumab (CCL3) a été renversée à l'aide de siRNA, et les tests fonctionnels ont été répétés en utilisant CCL3 siRNA et des traitements combinés.

Des tumeurs de MU (n = 27) provenant d'un modèle animal et des tumeurs provenant de patients humains énucléés (n = 29) ont été immunocolorées pour le VEGF-A. Deux différents algorithmes de quantification immunomarquage mis en

œuvre avec le logiciel ImageJ ont été utilisés pour compter automatiquement des cellules positives pour la région et une coloration positive. La régression logistique binaire a été effectuée pour déterminer si une coloration positive pouvait prédire les métastases. P <0,05 était considérée comme significative. **Résultats:** Les trois lignées cellulaires de MU ont produites et sécrétées du VEGF-A et ont exprimées du VEGF-R2. Le bevacizumab usurpé VEGF-A et réduit phosphorylée-VEGF-R2. La prolifération et la migration ont été réduites à la suite du traitement par le bevacizumab (p <0,05 pour une lignée cellulaire, et p <0,05 pour les deux lignées cellulaires, respectivement).

Les deux CCL3 et MMP-9 étaient significativement augmentés à la hausse après le traitement par le bevacizumab dans toutes les lignées cellulaires (p <0,05). La prolifération a été réduite de façon significative dans les trois lignées cellulaires à la suite CCL3 siRNA et des traitements combinés (p <0,05). La migration a été significativement réduite dans les trois lignées cellulaires après le traitement combiné (p <0,05) et l'invasion a été considérablement réduite dans les deux lignées cellulaires suivantes siRNA (p <0,05). En général, la thérapie combinée était plus efficace que la monothérapie bevacizumab pour inhiber les capacités fonctionnelles du MU.

Dans les deux lapins et les tissus humains, la présence du VEGF-A pourrait être utilisée pour prédire de façon significative des métastases (p> 0,05). **Conclusions:** La signalisation autocrine et paracrine du VEGF-A est abondante dans les lignées cellulaires du MU, mais l'inhibition du VEGF-A n'a que des effets modérés sur ses capacités fonctionnelles. Cette situation est attribuable à des

effets compensatoires, y compris la régulation positive du CCL3. En outre, le VEGF-A coloration peuvent être utilisées pour identifier les patients prédisposés au développement métastatique.

Le VEGF-A est une cytokine puissante qui peut jouer un rôle dans le développement et la progression du MU. Cependant, les effets compensatoires induits par le bevacizumab suggèrent que les thérapies doubles ou multiples peuvent être nécessaires pour traiter efficacement ce type de tumeur.

Acknowledgments

The famous quantum physicist Richard Feynman once said, “The first principle [of science] is that you must not fool yourself, and you are the easiest person to fool.” Therefore, I humbly admit that the work herein would not have been possible without the help of others not indicated on the spine; science is a discipline of collaboration and I would be remiss to not acknowledge at least some of the people without whom this work would never have been completed. To Dr. Miguel Burnier Jr., without your support, guidance, and leadership I would have never had the courage to embark on this sometimes meandering adventure. I often hear students, after many years of working together, kindly refer to their supervisor as a colleague, but for me, this is far too perfunctory a designation; you are my mentor and my friend, and what you have taught me both professionally and personally has made me a better person.

To Dr. Zorychta and my two advisors, Dr. Richardson and Dr. Siegel, you have supported me and offered guidance without which I would have been unable to balance idealism and pragmatism.

The old adage decrees that a house is not a home; a house is a physical structure while a home is a place for family and friends filled with love and respect. It is unfortunate there isn’t a similar poetic distinction for a laboratory because The Henry C. Witelson Ocular Pathology Lab has become my home and its members, past and present, are my family. If what I learned about science can

be folded into a blade of grass, the life lessons I learned there cannot be contained by an entire field. Lexicographers, you are on notice.

To my parents, it has been said that every journey begins with the first step, but I disagree; nurturing the desire for knowledge and striving for answers starts long before one can walk. Thus, my journey began when I was an infant, and you deserve credit for encouraging my continual inquisitions.

To my wife Ashley, it behooves me to affirm that you are the most important driving force behind all my endeavours. You have supported me indefinitely and without you I would not have accomplished a fraction of what I have. Thank you for always being available to listen, and although you may not have understood all of my scientific exploits, you understand me, which is undoubtedly far more important.

Finally, I would like to thank all scientists that preceded me, in particular the authors attributed to the over 200 publications listed in the reference section, for without them laying the groundwork of this pyramid we call science, this work would never have been possible.

This thesis is for all of you, as it is, in fact, your work. Enjoy.

Table of Contents

Publications and Abstracts

Journal Publications

1. Logan P, Burnier, J., Burnier, M.N. Jr. VEGF-A expression and inhibition in uveal melanoma cell lines. 2012;(Under Review).

2. Logan P, Antecka, E., Burnier, M.N. Jr. Correlation between VEGF-A expression in a rabbit model of uveal melanoma and human patients using novel digital immunohistochemistry quantification methods. 2012;(Under Review).

3. Maloney SC, Marshall JC, Antecka E, Orellana ME, Fernandes BF, Martins C, et al. SPARC is expressed in human uveal melanoma and its abrogation reduces tumor cell proliferation. Anticancer research. 2009;29(8):3059-64. Epub 2009/08/08.

4. Maloney SC, Fernandes BF, Castiglione E, Antecka E, Martins C, Marshall JC, et al. Expression of cyclooxygenase-2 in choroidal neovascular membranes from age-related macular degeneration patients. Retina. 2009;29(2):176-80. Epub 2008/10/02.

5. Fernandes BF, Logan P, Zajdenweber ME, Santos LN, Cheema DP, Burnier MN, Jr. Histopathological study of 49 cases of keratoconus. Pathology. 2008;40(6):623-6. Epub 2008/08/30.

6. Logan PT, Fernandes BF, Di Cesare S, Marshall JC, Maloney SC, Burnier MN, Jr. Single-cell tumor dormancy model of uveal melanoma. Clinical & experimental metastasis. 2008;25(5):509-16. Epub 2008/03/13.

7. Bakalian S, Marshall JC, Logan P, Faingold D, Maloney S, Di Cesare S, et al. Molecular pathways mediating liver metastasis in patients with uveal melanoma. Clinical cancer research : an official journal of the American Association for Cancer Research. 2008;14(4):951-6. Epub 2008/02/19.

8. Cools-Lartigue JJ, McCauley CS, Marshall JC, Di Cesare S, Gregoire F, Antecka E, et al. Immunomagnetic isolation and in vitro expansion of human uveal melanoma cell lines. Molecular vision. 2008;14:50-5. Epub 2008/02/05.

9. Fernandes BF, Marshall JC, Di Cesare S, Logan P, Maloney S, Burnier MN, Jr. Amfenac increases the radiosensitivity of uveal melanoma cell lines. Eye (Lond). 2008;22(5):701-6. Epub 2007/12/01.

10. Di Cesare S, Marshall JC, Fernandes BF, Logan P, Antecka E, Filho VB, et al. In vitro characterization and inhibition of the CXCR4/CXCL12

chemokine axis in human uveal melanoma cell lines. Cancer cell international. 2007;7:17. Epub 2007/11/16.

11. Santos LN, Fernandes BF, de Moura LR, Cheema DP, Maloney S, Logan P, et al. Histopathologic study of corneal stromal dystrophies: a 10-year experience. Cornea. 2007;26(9):1027-31. Epub 2007/09/26.

12. Bakalian S, Marshall JC, Faingold D, Logan P, Antecka E, Burnier MN, Jr. Expression of nm23-H1 in uveal melanoma. Melanoma research. 2007;17(5):284-90. Epub 2007/09/22.

13. Zajdenweber ME, Muccioli C, Moraes RT, Logan P, Fernandes BF, Burnier MN, Jr. Localized retinal ischemia as an ocular manifestation of primary antiphospholipid syndrome. Canadian journal of ophthalmology Journal canadien d'ophtalmologie. 2007;42(3):479-80. Epub 2007/05/18.

14. Fernandes BF, Odashiro AN, Saraiva VS, Logan P, Antecka E, Burnier MN, Jr. Immunohistochemical expression of melan-A and tyrosinase in uveal melanoma. Journal of carcinogenesis. 2007;6:6. Epub 2007/04/21.

15. Marshall JC, Fernandes BF, Di Cesare S, Maloney SC, Logan PT, Antecka E, et al. The use of a cyclooxygenase-2 inhibitor (Nepafenac) in an ocular and metastatic animal model of uveal melanoma. Carcinogenesis. 2007;28(9):2053-8. Epub 2007/04/17.

16. Di Cesare S, Marshall JC, Logan P, Antecka E, Faingold D, Maloney SC, et al. Expression and migratory analysis of 5 human uveal melanoma cell lines for CXCL12, CXCL8, CXCL1, and HGF. Journal of carcinogenesis. 2007;6:2. Epub 2007/01/31.

Book Chapters

1. Logan P. Haematogenous Models of Metastases. In: Burnier Jr, MN, Burnier, J, eds. *Experimental and Clinical Metastasis: A Comprehensive Review*. [In Press]: Springer; 2012.
2. Logan P. Spontaneous, Induced, and Transgenic Models of Metastasis. In: Burnier Jr, MN, Burnier, J, eds. *Experimental and Clinical Metastasis: A Comprehensive Review*. [In Press]: Springer; 2012.
3. Logan P. Animal Model Imaging Techniques. In: Burnier Jr, MN, Burnier, J, eds. *Experimental and Clinical Metastasis: A Comprehensive Review*. [In Press]: Springer; 2012.

Book Section Editor

1. Animal Models of Metastasis. Logan P, ed. In: *Experimental and Clinical Metastasis: A Comprehensive Review*. Burnier Jr, MN, Burnier J, eds. [In Press]: Springer; 2012.

Peer Reviewed Abstracts

1. Logan PT, Hari S, Balazsi M, F de Souza D, Martins C, Burnier MN. Bevacizumab In Combination With The Downregulation Of CCL3 Inhibits The Functional Dynamics Of Uveal Melanoma Cell Lines. ARVO Meeting Abstracts. 2012;53(6):3393.

2. Di Cesare S, Fernandes BF, Balazsi M, Granner TJ, Logan PT, Burnier MN. Transcriptional Changes in Human Lens Epithelial Cells Secondary to Intraocular Lens Exposure. ARVO Meeting Abstracts. 2012;53(6):3065.

3. Briccoli TA, Fernandes BF, Logan P, Maloney SC, Odashiro AN, Burnier MN. Comparison of Different IOLs in Secondary Cataract Assessment. ARVO Meeting Abstracts. 2012;53(6):3064.

4. Bower TN, Fernandes BF, Cheema D, Deschenes J, Logan PT, Burnier MN. A Study On Recurrent Corneal Stromal Dystrophies: Fifteen Years Of Penetrating Keratoplasty. ARVO Meeting Abstracts. 2012;53(6):6051.

5. Tavares ACF, DE Souza D, Martins C, Logan PT, Morcos MW, Burnier MN. The Expression Of Dbc1 In Uveal Melanoma. ARVO Meeting Abstracts. 2011;52(6):1450.

6. Porraccio TE, Martins C, Logan PT, Bakalian S, Faingold D, Burnier MN. The Expression of Preferentially Expressed Antigen of Melanoma in Uveal Melanoma. ARVO Meeting Abstracts. 2011;52(6):1451.

7. Logan PT, Miyamoto C, Granner TJ, Frota Tavares AC, Di Cesare S, Burnier MN. The Effects of Bevacizumab on the In Vitro Characteristics of Uveal Melanoma Cell Lines. ARVO Meeting Abstracts. 2011;52(6):1448.

8. Balazsi M, Odashiro PR, Di Cesare S, Morcos M, Logan P, Burnier MN. Expression of Secreted Frizzled-Related Protein 1 (SFRP-1) in Retinoblastoma. ARVO Meeting Abstracts. 2011;52(6):2475.

9. Tsoukas PA, Di Cesare S, Logan P, Faingold D, Bakalian S, Burnier MN. The Effects of Curcumin on the Chemokine Receptor CXCR4 in Human Uveal Melanoma Cell Lines. ARVO Meeting Abstracts. 2009;50(5):3393.

10. Sanft D-M, Kwee R, Logan P, Martins C, Antecka E, Burnier MN. The Correlation Between KAI1 Expression and Uveal Melanoma Prognosis. ARVO Meeting Abstracts. 2009;50(5):5769.

11. Martins C, Logan P, Abdulmannan D, Isenberg J, Solari HP, Burnier MN. Expression of KISS1 in Primary and Metastatic Uveal Melanoma in an Animal Model. ARVO Meeting Abstracts. 2009;50(5):5775.

12. Maloney SC, Antecka E, Orellana ME, Logan P, Abourbih D, Burnier MN. Toll-like Receptor 3 is Expressed in RPE cells of Choroidal Neovascular Membranes. ARVO Meeting Abstracts. 2009;50(5):2950.

13. Fernandes BF, Di Cesare S, Logan P, Belfort RN, Martins CC, Burnier MN. The Effects of Imatinib Mesylate in an Animal Model of Uveal Melanoma. ARVO Meeting Abstracts. 2009;50(5):5759.

14. Abourbih DA, Di Cesare S, Logan P, Orellana ME, Solari H, Burnier MN. Lysyl Oxidase: A Potential Metastasis Promoting Gene in Uveal Melanoma. ARVO Meeting Abstracts. 2009;50(5):5774.

15. Qian CX, Fernandes BF, Martins CM, Logan P, Bakalian S, Burnier MN. Expression of Timp-3 in Uveal Melanoma and Its Correlation With Outcome. ARVO Meeting Abstracts. 2008;49(5):59.

16. Miyamoto C, Belfort RN, DiCesare S, Belfort R, Logan P, Burnier MN. The Use of CD-25 as an Immunohistochemical Marker for Acquired Ocular Toxoplasmosis. ARVO Meeting Abstracts. 2008;49(5):3896.

17. Maloney SC, Isenberg J, Logan P, Di Cesare S, Young M, Burnier MN. Resveratrol Induces Proliferation of Mouse Retinal Progenitor Cells in a Dose-Dependent Manner. ARVO Meeting Abstracts. 2008;49(5):3558.

18. Logan PT, Abourbih D, Martins C, Faingold D, Bakalian S, Burnier MN. In vitro and in vivo Classification of the Protease Activated Receptor Family and the Consequences of Thrombin Induced Receptor Activation in Uveal Melanoma. ARVO Meeting Abstracts. 2008;49(5):74.

19. Isenberg J, Di Cesare S, Abourbih D, Faingold D, Logan P, Burnier MN. Gene Expression Profiling of CXCL12, CXCL8, CXCL1, and HGF in an Ocular and Metastatic Animal Model of Uveal Melanoma. ARVO Meeting Abstracts. 2008;49(5):69.

20. Di Cesare S, Maloney S, Belfort RN, Fernandes BF, Logan P, Burnier MN. SPARC Expression Correlates with Proliferative and Invasive Potential in Uveal Melanoma Cell Lines. ARVO Meeting Abstracts. 2008;49(5):61.

21. Zajdenweber ME, Marshall JC, Logan P, Bakalian S, Belfort Neto R, Belfort R, et al. Type 1 and Type 2 Toxoplasma Gondii Strains: Differences in Growth and Invasive Abilities. ARVO Meeting Abstracts. 2007;48(5):5135.

22. Oliver KM, Di Cesare S, Marshall J-C, Logan P, Faingold D, Burnier MN. Effects of 17-Allylamino-17-Demethoxygeldanamycin (17-AAG), Imatinib, and Amfenac on the Cellular Proliferation of 5 Human Uveal Melanoma Cell Lines. ARVO Meeting Abstracts. 2007;48(5):4770.

23. Maloney SC, Martins C, Antecka E, Logan P, Faingold D, Burnier MN. Expression of COX-2 in Choroidal Neovascular Membranes From Age Related Macular Degeneration Patients. ARVO Meeting Abstracts. 2007;48(5):3018.

24. Logan P, Marshall J-CA, Fernandes BF, Bakalian S, Martins C, Burnier MN. MMP-2 and MMP-9 Secretion by Human Uveal Melanoma Cell Lines in Response to Different Growth Factors and Chemokines. ARVO Meeting Abstracts. 2007;48(5):4766.

25. Fernandes BF, Marshall J-C, di Cesare S, Logan P, Bakalian S, Burnier MN. The Effect of a COX-2 Inhibitor on the Radiosensitivity of Uveal Melanoma Cell Lines. ARVO Meeting Abstracts. 2007;48(5):4752.

26. Di Cesare S, Marshall J-C, Maloney S, Logan P, Fernandes BF, Burnier MN. The Effect of a COX-2 Inhibitor on Circulating Malignant Cells in an Ocular Melanoma Animal Model. ARVO Meeting Abstracts. 2007;48(5):5253.

27. Logan P, Marshall J-CA, Fernandes BF, Maloney S, Saraiva V, Burnier MN. In vivo Imaging of Fluorescently Labeled Human Uveal Melanoma Cells in Nude Mice. ARVO Meeting Abstracts. 2006;47(5):2230.

28. Di Cesare S, Logan P, Marshall JC, Gregoire FJ, Faingold D, Burnier MN. Migratory and Immunohistochemical Analysis of 5 Human Uveal Melanoma Cell Lines Towards CXCL-12, CXCL-8, CXCL-1, and HGF. ARVO Meeting Abstracts. 2006;47(5):2229.

29. Burnier MN, Marshall J-CA, Gregoire FJ, Di Cesare S, Logan P, Al-Kandari A. The Effect of a Cox-2 Inhibitor on an Ocular Melanoma Animal Model. ARVO Meeting Abstracts. 2006;47(5):2218.

30. Bakalian S, Marshal JC, Faingold D, Logan P, Frota AC, Burnier MN. The Effect of Curcumin on the Proliferation Rate of Human Uveal Melanoma Cell Lines. ARVO Meeting Abstracts. 2006;47(5):2246.

Abbreviations

ANG-2 – Angiopoietin 2

ANOVA – Analysis of Variance

ARMD – Age-Related Macular Degeneration

BAP1 – BRCA1-associated Protein 1

bFGF – Basic Fibroblast Growth Factor

BTK – Bruton's Tyrosine Kinase

CCL – Chemokine (C-C motif) Ligand

CCR – Chemokine (C-C motif) Receptor

cDNA – Complementary DNA

CMC – Circulating Melanoma Cells

CNV – Choroidal Neovascularization

COMS – The Collaborative Ocular Melanoma Study Group

COX-2 – Cyclooxygenase 2

CSF1R – Colony Stimulating Factor-1 Receptor

Ct – Cross Threshold

DNA – Deoxyribonucleic Acid

EGF – Epidermal Growth Factor

ELISA – Enzyme-Linked Immunosorbent Assay

FBS – Fetal Bovine Serum

GIST – Gastro-Intestinal Stromal Tumor

GM–CSF – Granulocyte-Macrophage Colony-Stimulating Factor

GRO – Growth-Regulated Protein

H&E – Hematoxylin and Eosin

HB-EGF – Heparin-Binding EGF-Like Growth Factor

HCC – Hepatocellular Carcinoma

HGF – Hepatocyte Growth Factor

HIF-1a – Hypoxia Inducible Factor Alpha

IFN – Interferon

IGF-1 – Insulin-Like Growth Factor 1

IL – Interleukin

IOL – Intraocular Lens

ISO – International Standards Organisation

JPG – Joint Photographic Group

MCP – Monocyte Chemotactic Protein

MHC – Major Histocompatibility Complex

MIP – Macrophage Inflammatory Protein

MMP – Matrix Mettaloproteinase

mRCC – Metastatic RCC

NF-º B – Nuclear Factor Kappa-Light-Chain-Enhancer of Activated B Cells

NSCLC – Non-Small Cell Lung Cancer

OD – Optical Density

P1GF – Placental Growth Factor

PDGF-BB – Platelet-Derived Growth Factor Subunit B

PDGFR-² – Platelet-Derived Growth Factor Receptor Beta

PI – Propidium Iodide

RANTES – Regulation upon Activation, Normal T-Cells Expressed, and Secreted

RCC – Renal Cell Carcinoma

RET – Rearranged During Transfection

RNA – Ribonucleic Acid

RPE – Retinal Pigment Epithelium

RT-qPCR – Quantitative Real-Time Polymerase Chain Reaction

siRNA – Small Interfering RNA

TAM – Tumor-Associated Macrophages

TIL – Tumor-Infiltrating Lymphocytes

TNF – Tumor Necrosis Factor

UM – Uveal Melanoma

VEGF – Vascular Endothelial Growth Factor

VEGFR – VEGF Receptor

List of Figures and Tables

Literature Review

Uveal Melanoma

General Background

Uveal melanoma (UM) is a malignancy of the uveal tract, which is composed of the pigmented portions of the eye: the iris, the ciliary body, and the choroid. Of these anatomical structures, the choroid is the most common location from which uveal melanomas arise, accounting for roughly 85% of cases[1]. Irrespective of location of origin, all melanomas arise from melanocytes, the pigmented cells that produce melanin, which are responsible for the chromaticity of the eye, skin, and hair. Unlike its more common counterpart, melanoma of the skin, which affects nearly 10,000 per million people in North America, uveal melanoma is a rare entity affecting approximately 4.3 people per million in the United States, the vast majority of which are Caucasians males[2]. Despite its paucity, UM is the most common primary intraocular tumor in adults. As with most malignancies, age is the greatest predisposing factor and incidence estimates considering only individuals over 70 years of age are roughly 25 and 18 per million in males and females, respectively[2].

Choroidal and ciliary body uveal melanomas are typically diagnosed on routine ophthalmological examination. Clinically, the diagnostic accuracy of UM by either slit-lamp biomicroscopy or indirect ophthalmoscope and the use of an ultrasound B-scan exceeds 99%[3-5]. Occasionally, rapidly growing tumors and those proliferating in close proximity to the macula may affect vision and thus the resulting symptoms will expedite prompt evaluation by an ophthalmologist. Iris

melanomas, on the other hand, are usually diagnosed earlier owing to their more visible, anterior location.

In contrast to cutaneous melanoma that has a clear causal relationship with UV-A and UV-B ray exposure, the pathogenesis of uveal melanoma remains unclear. However, exposure to blue light has been proposed as a possible contributing factor for disease initiation and progression[6,7]. An interesting caveat to this hypothesis is the impact that the recent ubiquity of cataract surgeries, in which the opacified or damaged biological lens is removed from the eye and replaced with an artificial intraocular lens (IOL), may contribute to the development of uveal melanoma; as we age, the lens naturally yellows and this tinting blocks some of the incoming blue light. Furthermore, it has been demonstrated that blue light can generate free radicals in the retinal pigment epithelium (RPE)[8]. As well as being a risk factor for the development of age-related macular degeneration (ARMD), the unimpeded penetrance of blue light into eyes with IOLs that lack blue-light filtering properties may contribute to the development or initiation of uveal melanoma[9]. This theory is supported by the fact that one of the most prominent risk factors for developing uveal melanoma is fair skin color and light colored irises[10]. In individuals with such features, it is hypothesized that the reduced melanin results in unabsorbed photons that can generate free-radicals and subsequently damage ocular cells and structures, including the uveal tract. Melanocytes in particular are susceptible to UV-A and UV-B induced DNA damage, both of which can cause photodimers and, eventually, melanoma[10]. Moreover, welders have a higher incidence of uveal

melanoma, likely stemming from the aforementioned relationship of exposure to high intensity wavelengths of light[11]. In addition, melanocytes are more susceptible to spontaneous, non-light induced mutations as they lack some of the DNA repair mechanisms present in a variety of other cell types[12].

Pre-existing nevi are also considered a risk factor for uveal melanoma[13]. Nevi are usually present either at birth or are acquired during the first few decades of life. These benign, asymptomatic lesions, often referred to as freckles, are the result of an accumulation of melanocytes and are diagnosed by fundus examination. Support for the theory that nevi can be precursors to uveal melanoma include histopathological studies that reveal melanoma-like cells at nevi borders[14]. However, the incidence of nevi in the population is much greater than is uveal melanoma, and estimates indicate that only between approximately four and eight percent of nevi transform into uveal melanoma[15,16]. The Collaborative Ocular Melanoma Study Group (COMS) has identified additional criteria that influence nevi growth, and thus differentiate melanoma from nevi, which include: 1) greater apical tumor thickness, 2) larger initial basal diameter, 3) presence of orange pigment, 4) absence of drusen, and 5) absence of retinal pigment epithelial changes adjacent to the tumor[17]. Advanced imaging techniques and methodologies, such as internal quiet zone on B-scan ultrasonography, have also proved helpful for identifying growing masses and thus for potentially differentiating between nevi and small or intermediate uveal melanomas[18]. Ultimately, the gold standard for distinguishing nevi from melanoma remains fine-needle aspiration biopsy; however, due to the location of these lesions within

the eye, the low rate of transformation, and the potential for infection and other complications, it is not always practical nor prudent to biopsy these entities. Typically, most ophthalmologists will take a wait-and-see approach with respect to suspicious masses, as usually only melanomas will grow over time; however, in very rare cases, nevi will increase in size without undergoing malignant changes[19].

Treatment and Disease Course

Approximately 40% of people with uveal melanoma will develop metastases within 5 to 10 years of diagnosis[20,21]. In the unfortunate instances in which metastases arise, the majority occur in the liver, and 90% of patients will succumb to these sequelae in less than three months[22-25]. Iris melanomas, which are more easily detected and treated due to their location at the front of the eye, carry a much lower risk of metastasizing.

In the past, enucleation – the removal of the entire globe – was the standard treatment for uveal melanoma. It was believed that removing the fully contained tumor would lessen the chances of metastasis. However, research has shown that there is no correlation between the choice of primary tumor treatment and clinical outcome for the patient[26]. Thus, methodologies for treating choroidal tumors have changed dramatically over the past few decades with a new focus on retaining visual function and cosmetic appeal in the affected eye as opposed to the more barbarous and callow method of enucleation. Currently, tumors that are less

than 16 mm by largest dimension are treated with brachytherapy, which involves suturing a plaque with radioactive material, often Iodine-125, to the outside of the eye in juxtaposition to the tumor for several days[27,28]. Other, more advanced surgical techniques, including exoresection, such as sclerouvectomy and lamellar sclerouvectomy, and endoresection have been used with varying degrees of success, primarily for anteriorly located tumors[29-31]. The former technique involves dissecting the tumor after either removing a portion of the sclera and replacing it with donor material or suturing it back in place afterwards, while the latter involves using a vitreous cutter to remove the tumor during pars plana vitrectomy. Depending on tumor location, all of the aforementioned treatment modalities can potentially result in sight retention in the affected eye, which is clearly not possible with enucleation. Therefore, due to the fact that clinical course, in particular the development of metastasis, is unaffected by primary tumor treatment, the current goal of an ophthalmologist is to maintain vision when possible, reserving enucleation for extremely large tumors in blind, painful eyes. Furthermore, a recent study reported a better quality of life for patients that receive brachytherapy as opposed to enucleation; thus, current research should focus on adjuvant treatments to reduce the size of the primary tumor, rendering the aforementioned conservative treatment methods applicable[32].

Treating iris melanomas is typically uncomplicated and involves local resection. However, the aforementioned treatments for choroidal melanomas, including enucleation and brachytherapy, are employed for large or diffuse iris melanomas[33].

Despite technical advances in treating the primary tumor, the incidence of metastasis has remained relatively unchanged over the past four decades[34]. Several hypotheses have been proposed to account for this peculiarity, but an important attribute of this disease is that the time of tumor onset is usually unknown. Unlike melanomas of the skin that appear in conspicuous areas and permit a relatively accurate history and time of onset, intraocular tumors are usually asymptomatic and usually develop several years before they are noticed on routine ophthalmological examination. Further confounding this issue is the consideration that these tumors may have begun as nevi, making it difficult to determine when malignant transformation occurred. In fact, it has been estimated that, on average, uveal melanoma tumors exist for 10 years before clinical diagnosis[35]. Therefore, it is assumed that uveal melanoma cells from choroidal and ciliary body tumors in particular, have already extravasated the globe, and metastatic seeds have been established at the time of diagnosis[36]. As the eye lacks lymphatic vessels, invading and migrating tumor cells must escape and disseminate hematogenously. To study this process, several studies have focussed on identifying, quantifying, and classifying uveal melanoma cells circulating in the blood (circulating melanoma cells; CMCs)[36-38]. These studies reveal that that almost 90% of uveal melanoma sufferers have detectable CMCs regardless of primary tumor treatment modality[36].

Much research has focussed on identifying the microbiological or genetic properties of metastatic clusters that facilitate their development into liver metastases. For example, researchers have identified monosomy 3 as an indicator

of metastatic potential and recent work has identified that mutation of the BAP1 gene on chromosome 3 is at least partially responsible for the correlation between monosomy 3 and metastasis[39]. Another study successfully categorized uveal melanoma tumors as class 1 or class 2 tumors using gene profiling analysis, the latter being more likely to metastasize[40-42].

The primary, and often exclusive, affinity for metastatic growth in the liver in uveal melanoma patients has drawn considerable interest from cancer researchers. Clearly, identifying factors that contribute to this seemingly magnetic predilection will provide valuable clues regarding disease pathogenesis in addition to elucidating important pharmaceutical targets. For instance, several studies have demonstrated that uveal melanoma cells express high levels of the c-Met receptor whose ligand, aptly named hepatocyte growth factor (HGF), is produced in large quantities in the liver, suggesting a possible role for this receptor-ligand interaction in 'homing' to the liver[43,44]. Other molecules, such as IGF-1, have also been implicated in the homing process, but based on the understanding that malignant cells likely leave the primary tumor on disease inception, the value of understanding these proposed 'homing' mechanisms is predicated on which cells are capable of developing into overt metastases; i.e., if cells that leave the eye upon inception populate the liver and remain dormant, as research regarding patients that undergo enucleation and develop metastases many years later suggests, understanding how cells 'homed' to the liver would afford little value or opportunity for pharmaceutical or clinical intervention[44,45].

In a recently reported mouse model of uveal melanoma, in which uveal melanoma cells were fluorescently tagged and injected into the circulation of mice, the final destination of malignant cells was determined by physical restrictions based on the size of the cells relative to the small capillaries[46]. This study also revealed that these cells were capable of remaining dormant in the liver of immunocompromised mice with little or no cellular division for up to seven weeks[46]. Although this study was performed on immunocompromised mice, the situation in human patients may be analogous: cells leave the primary tumor and populate several organs yet are only capable of surviving in the liver, where they remain dormant. As a result of this and other studies, researchers are now spending considerable efforts to identify the molecular fuses that trigger the proliferative explosion of these metastatic seeds.

Unlike the primary tumor, for which many efficacious and conservative treatments are available, limited and markedly less-successful treatments exist for overt liver metastases. In fact, there are no guidelines or standard treatments for liver metastasis derived from uveal melanoma tumors; typical systemic chemotherapy agents were tried and met with limited success[47]. Although surgical resection can increase the life-span of patients suffering from liver metastasis, the tendency for multiplicity and diffusivity of uveal melanoma liver metastases renders this treatment applicable for only a small percentage of patients[25,48-50].

Gross Pathology and Histopathology

On gross pathology, choroidal uveal melanoma tumors can be either pigmented, amelanotic, or be composed of both pigmented and amelanotic fractions. Choroidal melanomas grow from the choroid inward, pushing against Bruch's membrane and, should the tumor grow large enough, break through Bruch's membrane to assume a characteristic mushroom-shaped appearance (Figure 1). Choroidal melanomas also occasionally appear as diffuse, general thickenings of the choroid. Iris melanomas share the same variable pigmentation as choroidal melanomas and typically present as an archetypal thickening of the iris[51]. Conversely, ciliary body melanomas appear ring-shaped and are difficult to diagnose based on their conspicuous nature[52].

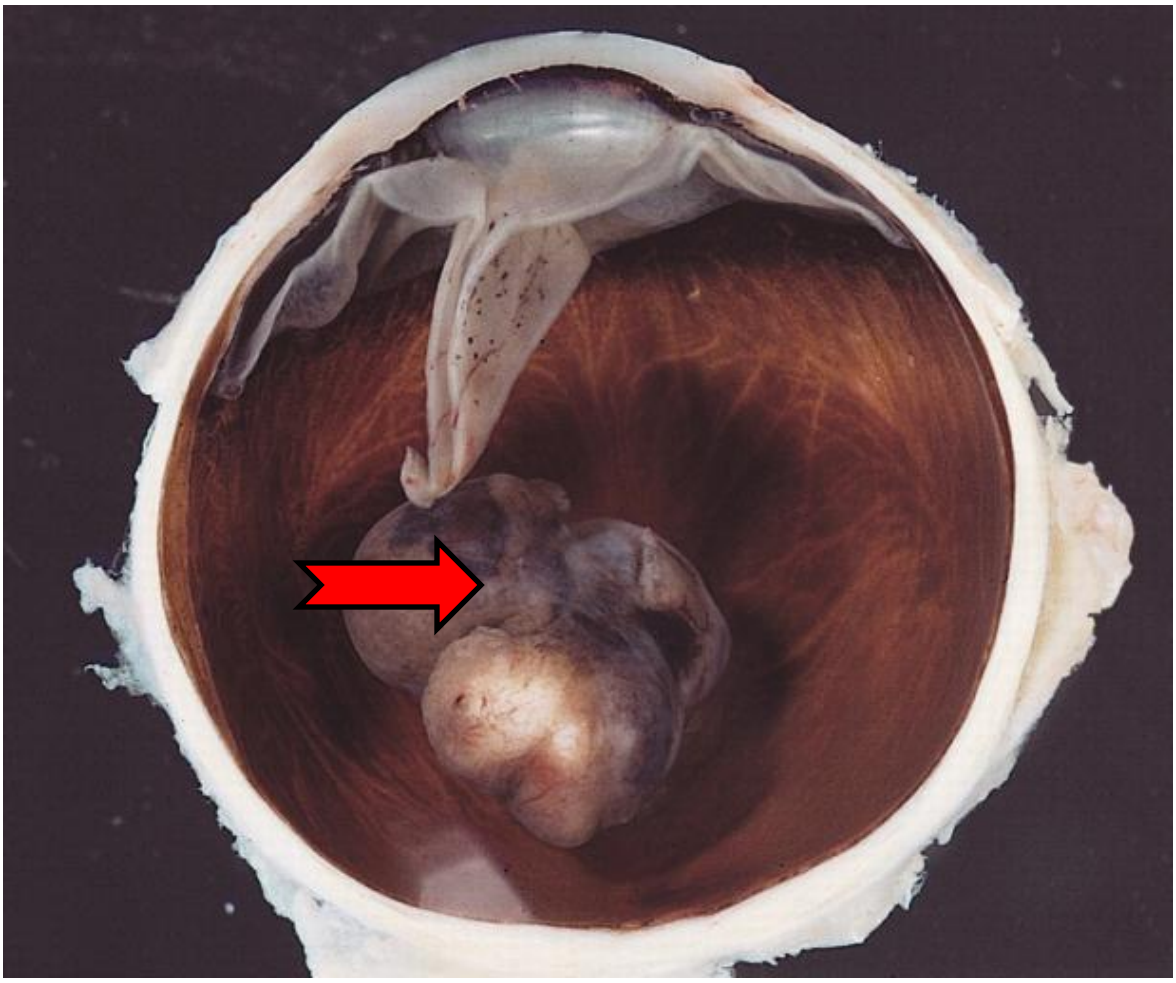

Figure 1. A representative image of a choroidal uveal melanoma that has broken through Bruch's membrane. The arrow indicates the tumor, which has both melanotic and amelanotic portions.

Histopathologically, uveal melanomas are comprised of two cell types: spindle and epithelioid. Generally, spindle cells have minute amounts of cytoplasm and have an organized, 'sheet-like' appearance. Spindle cell melanomas are further subdivided into spindle A and spindle B sub-classifications, the latter possessing a more circular appearance and a round

nucleolus. Conversely, epithelioid cells have larger and more heterochromatic nuclei, are rounder, have more cytoplasm, and are less organized. In Callender's original classification scheme proposed in 1931, the malignancy of the different uveal melanoma cell types are organized from nearly benign to highly malignant in the order in which they are described above[53]. However, because uveal melanoma tumor cells represent a cytologic continuum, this classification scheme requires subjective evaluation and thus generates inter- and occasionally intra-pathologist disagreements[54,55]. Several alternative, objective methods have been proposed to determine histopathological criteria to ascertain patient outcome. Folberg, et al. 1993, investigated vascular patterns within uveal melanoma tumors and, after defining nine specific patterns, determined that the presence of a vascular network, defined as a minimum of three back-to-back closed-loops, strongly correlated with metastasis[56]. At the turn of the century, it was demonstrated that uveal melanoma cells are capable of forming perfusion channels lined by melanoma cells instead of endothelial cells either de novo or connecting to existing tumor vasculature, a process dubbed 'vasculogenic mimicry'[57,58]. The presence of such vascular channels in tumor sections is an indicator of poor prognosis, likely because these features aid the diffusion of oxygen and nutrients in the absence of angiogenesis and present as additional avenues for tumor cell extravasation into haematogenous circulation[59].

Further objective criteria have been proposed with the intention of objectifying Callender's classification, including using a digitized interactive overlay system to determine the standard deviation of nuclear area, mean nuclear

size, and standard deviation of the shortest nuclear axis, among others, several of these tumor characteristics correspond well with Callender's classification system[60].

Immunohistochemical studies have revealed a plethora of molecules that exhibit some degree of prognostic significance. For instance, intense staining of the translational product of the metastasis suppressor gene *nm23-H1* in primary tumor samples was found to correlate with increased survival[61]. Also, Figuieredo et al. discovered that the expression of cyclooxenase-2 (COX-2), an inducible prostaglandin synthase, can be used to sub-classify mixed tumor cell types, is associated with vascular closed loops, and is a negative prognostic indicator[62]. The expression of insulin-like growth factor-1 receptor, CXC chemokine receptor-4, and phospho-akt, among a host of other factors, has also been shown to correlate with metastases[63-65]. Further, the presence of tumor-associated macrophages (TAMs) or tumor-infiltrating lymphocytes (TILs) in uveal melanoma is an indication of poor prognosis[66]. This is in stark contrast with skin melanoma, in which the presence of immune cells confers a survival advantage.

Currently, the problem inherent with using the aforementioned prognostic indicators is the acquisition of tumor tissue from the patient required to perform the diagnostic investigation. Several decades ago, this was feasible due to the overwhelming prevalence of enucleation. However, due to the lack of survival implications with this surgery, enucleation is no longer performed with regularity, and this has limited the number of cases for which these prognostic evaluation techniques can be ascribed. However, more ophthalmologists are resorting to

tissue collection via fine-needle aspiration biopsy, although this is not necessarily a quietus as the small sampling of cells obtained by this technique may not be indicative of the cytological characteristics of a heterogeneous tumor[67]. Based on the magnitude of research performed in this area over the last three decades, it is unlikely that the largest tumor dimension, as first described by Shammas in 1977, will be usurped as the best non-invasive method for predicting patient outcome[68]. Nevertheless, information garnered from tissue studies are critically important for increasing our understanding of tumor pathogenesis, which will prove invaluable for the development of new, patient-specific treatment modalities to conserve vision, improve quality of life, and lengthen disease free-survival.

Vascular Endothelial Growth Factor

General Background

Vascular endothelial growth factor (VEGF) is the most potent angiogenic stimulator in mammals. First identified in 1971 by Folkman et al., this signalling molecule is involved in both physiological and pathological angiogenesis[69-72]. VEGF fundamentally describes a family of five homodimer signalling molecules that include VEGF-A through VEGF-D and placental growth factor (P1GF)[73]. Although all five molecules influence steps of the angiogenic process to differing degrees, including blood vessel lumen formation and endothelial cell migration and proliferation, VEGF-A is commonly branded with the generic term VEGF as

it is responsible for the majority of the physiological functions of this family[73]. Subdivisions of the VEGF family of molecules becomes increasingly more complex as splice variants are considered; for example, VEGF-A exists as VEGF121, VEGF165, VEGF189, and VEGF205[73]. Of these, VEGF165 is the most biologically active for both physiological and pathological, including tumor, angiogenesis[73]. VEGF signalling also plays a critical role in embryogenesis, and a mutation in any VEGF-A allele is embryonic lethal[74].

Almost all cell types are capable of producing VEGF-A, primarily under hypoxic conditions[75]. Under said conditions, a transcription factor, hypoxia inducible factor 1 (HIF-1) is stabilized and transcription of the *VEGFA* gene, among others, is increased. The subsequent increase in the production and secretion of VEGF-A results in the migration and proliferation of endothelial cells and increased tubule formation, the overall consequence of which is amplified vessel formation and a return to a normoxic state[76]. In addition, VEGF-A increases vascular permeability, which can inhibit drug diffusion to the center of a tumor[77].

VEGF Receptors

Like their ligands whereby they are activated, VEGF receptors share redundancies and multiplicities. Currently, three VEGF receptors have been described: VEGF receptor 1 (VEGFR-1/Flt-1), VEGF receptor 2 (VEGFR-2/Flt-2/KDR), and VEGF receptor 3 (VEGFR-3/Flt-4), all of which are seven-

transmembrane receptor tyrosine kinases[78-82]. Although the consequences of individually activating each receptor are partially redundant, generally VEGFR-1 activation inhibits embryonic angiogenesis, VEGFR-2 activation generates physiological activity, including wound repair and muscle growth, and some embryonic angiogenesis, and VEGFR-3 signalling controls lymphangiogenesis. The role of the different VEGF signalling molecules are primarily defined by the receptor to which they bind: VEGF-B and P1GF bind VEGFR-1 and VEGF-C and VEGF-D bind VEGF-R3[73]. VEGF-A, the primary regulator of angiogenesis, promiscuously binds both VEGF-R1 and VEGF-R2 and, to further complicate VEGF and VEGFR function, although VEGF-A has a higher affinity for VEGF-R1, VEGF-R2 induces substantially greater tyrosine kinase activity and subsequent angiogenic response[83]. Finally, VEGFR-2 activation on endothelial cells induces proliferation, migration, tubule formation, and enhances vessel permeability[73].

VEGF and Cancer

Physiologically, a tumor requires oxygen and nutrients to grow larger than 2-3 mm in diameter[84], and this phenomenon has been termed the angiogenic switch, and is a major research interest for most solid tumors. For most locations, a tumor 2-3 mm in diameter will either not dramatically influence a patient's quality of life or can easily be resected. The allure of VEGF and their receptors as potential therapeutic targets for cancer treatment is compounded by the knowledge that these receptors are typically inactive during normal physiological

conditions and thus their inhibition is generally well tolerated[85]. Furthermore, the consequence of VEGF signalling in a variety of tumors extends beyond merely recruiting endothelial cells and forming perfusion channels; signalling through both VEGF-R1 and VEGF-R2 have been implicated in cancer progression, together contributing to tumor cell invasion, migration, proliferation, and metastasis. VEGF-R1 is also expressed on macrophages and monocytes, which, upon activation, produce a host of pro-angiogenic factors, including VEGF-A, in order to appease the requisite for increased oxygen and nutrients[86,87].

VEGF and Uveal Melanoma

Recent studies have shown that patients with uveal melanoma have elevated levels of VEGF-A in both the aqueous humor and vitreous[88]. In the aqueous humor, increased VEGF-A production is attributed to both the retina and tumor cells and thus presents as a potential therapeutic target[89]. In vitro studies have also revealed that UM cell lines produce VEGF-A in normal culture and production increases under hypoxic conditions[90,91]. Furthermore, in an animal model of uveal melanoma, increased VEGF-A levels were detectable in serum, and these escalations correlate with increased metastasis[92]. Reports vary with regard to VEGF-A expression in primary UM tumors, ranging from 22 to 84% positivity, and conflicting reports exist regarding correlations between expression levels and tumor size, vascularization, or metastasis[93,94].

Anti-VEGF Therapy

Based on the importance and implication of VEGF-A in both local and metastatic growth in a wide spectrum of malignancies, it is unsurprising that several pharmaceutical VEGF inhibitors have been developed. The first anti-angiogenic drug, a monoclonal antibody targeting all isoforms of VEGF-A named bevacizumab, was approved in 2003 for the treatment of metastatic colorectal cancer[95]. Later, this same drug was approved for the treatment of non-small cell lung cancer and metastatic breast cancer[96,97]. Recently, a soluble chimeric receptor mimicking both VEGF-R1 and VEGF-R2 named VEGF-$Trap_{R1R2}$ has been developed and shows a greater affinity than bevacizumab for scavenging VEGF-A[98]. Additional small molecule inhibitors of VEGF-R have been developed and are undergoing various stages of clinical trials (Table 1).

Table 1. VEGF receptor tyrosine kinase inhibitors and their indications in cancer patients. Adapted from Shojaei, et al. 2012[99]. Used with permission.

Compound	Target(s)	Indications
Sunitinib (SU11248)	VEGFRs, PDGFR-², CSF1R, c-Kit	RCC, GIST
Pazopanib (Votrient)	VEGFRs, PDGFRs and c-kit	RCC,
Sorafenib (Bay 43-9006; Nexavar®)	VEGFR-2 and -3, PDGFR-², Flt-3, c-kit, Raf kinases	RCC, Inoperable HCC
Vendatanib (Caprelsa)	VEGFRs and EGFRs, RET-tyrosine kinases	Late-stage Medullary Thyroid Cancer
Cabozantinib (XL184)	VEGFRs Met	Prostate Cancer
Tivozanib (AV-951, KRN-951)	VEGFRs	RCC
Axitinib (AG-013736)	VEGFRs	mRCC
Linifanib (ABT-869)	VEGFRs, PDGFR-², CSF1R	RCC, NSCLC

Despite the initial success of anti-angiogenic compounds and the development of inhibitors of various aspects of the signalling cascade (ligand sequestering to receptor inhibition), recent studies have revealed tenuous promise of this approach. It has been hypothesized that for most solid tumors, the main benefit of anti-VEGF therapies is the repair of tumor vasculature rendered leaky

due to VEGF; this stabilizing effect inherently enhances delivery of chemotherapy or other cytotoxic compounds[100]. Further complicating the assessment of the efficacy of anti-angiogenic therapies is the fact that susceptible tumors often become resistant to anti-VEGF therapies. Although the mechanisms of resistance can vary, there is mounting evidence indicating that refractory and compensatory production of other angiogenic factors, such as P1GF and HGF, by both tumor cells and stromal cells may be the culprit[99,101].

Distressingly, new research demonstrates that for some tumors, anti-angiogenic therapy can be pro-metastatic; that is, inhibiting VEGF makes these tumors more aggressive, thereby leading to a greater incidence of metastasis. For instance, in murine models of pancreatic neuroendocrine carcinoma, glioblastoma, and breast cancer, after initial anti-tumor effects, animals were encumbered with more invasive tumors and additional metastases following anti-angiogenic treatment[102,103]. While the exact cause of this paradoxical consequence is unknown, it has been hypothesized that it may be the result of either one or several of the following: 1) refractory or compensatory production of other angiogenic factors, 2) selecting for a clone of hypoxia insensitive tumor cells, or 3) hypoxia engendered invasion[102,104,105].

Unsurprisingly, anti-VEGF therapies have also been explored for the treatment of uveal melanoma. In 2010, Yang et al. demonstrated that bevacizumab reduced intraocular tumor size and the number of micrometastases in a short-term mouse model of uveal melanoma[106]. This same group also reported a reduction of in vitro and in vivo angiogenesis and in vitro invasive capabilities

using the same model construct[106]. A clinical trial using intravitreal bevacizumab injections to reduce the size of uveal melanoma tumors is currently underway[107]. Attributable to the aforementioned appeal of using bevacizumab's vessel stabilizing properties in conjunction with other pharmacological agents, several clinical trials using combination therapies are also being conducted[108]. Although the results of these trials are pending, bevacizumab use in eyes afflicted with other ocular pathologies that were later discovered to harbour occult uveal melanomas revealed no effects on tumor growth[109].

Reported side-effects of intravenously injected bevacizumab include impaired wound healing, arterial hypertension, renal insufficiency, and congestive heart failure[110].

Bevacizumab in Ophthalmology

Although not specifically approved for ophthalmological use, bevacizumab has been the off-label choice for the treatment of various ocular pathologies since 2005[111]. Many studies report positive effects of intravitreal injections of bevacizumab for the treatment of proliferative diabetic retinopathy, choroidal neovascularization (CNV) secondary to age-related macular degeneration, macular edema in central vein occlusion, and retinal and iris neovascularization[111-115]. All of the aforementioned studies report either none or limited side-effects from intravitreal bevacizumab treatment and attest to the

ability of the antibody to penetrate retinal tissues. Other studies report rare consequences, such as intraocular inflammation or retinal pigment epithelium (RPE) tears[116,117]. In a recent, 12-month study including 1,265 patients treated with intravitreally injected bevacizumab for various ocular pathologies, adverse systemic effects occurred in only 1.5% of patients[118]. Generally, intravitreous bevacizumab injections are considered well tolerated and systemic and ocular side-effects are only rarely reported[118].

Ranibizumab is a truncated form of the bevacizumab monoclonal antibody that possesses a greater affinity for binding VEGF-A and is approved for the intraocular treatment of wet ARMD[119,120]. However, based on the dramatic difference in pricing of bevacizumab compared to ranibizumab ($17 compared to $1950 per dose, respectively), clinicians often administer bevacizumab over ranibizumab[121]. In defence of this decision, physicians often cite a two-year study that concluded that the efficacy for treating neovascular ARMD did not differ significantly between these compounds[122].

Conclusion

Uveal melanoma is a devastating tumor and roughly 40% of patients will die from liver metastases between five and 10 years after diagnosis. Conservative treatments for the primary tumor can often preserve the eye and vision provided the tumor does not exceed a certain size. In order to proliferate beyond a few millimeters, tumors require new blood vessels, a process that is primarily governed by the powerful angiogenic cytokine, VEGF-A. Inhibition of VEGF-A, predominantly through the use of the monoclonal antibody bevacizumab, either as a mono or as part of combination therapy, has been explored for the treatment of many different cancers. While the efficacy of this approach is undeniable for some tumors, others become more aggressive in response to treatment. In ophthalmology, bevacizumab is efficaciously used to treat various ocular pathologies, including ARMD, with limited side-effects. Coupled with preliminary in vitro and in vivo data, bevacizumab presents as an auspicious treatment modality for uveal melanoma.

Chapter 1: VEGF-A Expression and Inhibition in Uveal Melanoma Cell Lines

Introduction

Based on the effectiveness of anti-angiogenic therapy in several cancers, we assessed whether three uveal melanoma cell lines produced VEGF-A in culture as well as the primary receptor for this ligand, VEGF-R2. We also sought to determine if the VEGF-R2 receptor was activated on these cells by auto or paracrine signalling and if this process could be abrogated using the commercially available VEGF-A inhibitor, bevacizumab. We also examined what effect this inhibition has on the production of other pro-angiogenic cytokines and the transcriptional levels of VEGF-A. Finally, the consequences of bevacizumab on UM cell cycle and potential cytotoxic effects were also evaluated.

Ascribed by evidence from UM and other cancers, we predict that our cell lines produce VEGF-A, which subsequently activates the receptor. In addition, we hypothesize that inhibiting this process will result in the upregulation of VEGF-A transcription and the secretion of other angiogenic factors with limited perniciousness.

Materials and Methods

Cell Lines and Culture

Three UM cell lines, 92.1 (Dr. Jager; University Hospital Leiden, The Netherlands), OCM-1 (Dr. Albert; University of Wisconsin-Madison, USA), and UW-1 (Dr. Albert) were used in this study. The functional characteristics of these cell lines are described elsewhere[123-125]. Briefly, the former two cell lines were initially extracted and cultured from human uveal melanomas whereas the latter is a transformed human melanocyte cell line. The cell lines are listed according to their ability to form intraocular tumors, listed from most to least capable, which has been confirmed in an animal model and in in vitro studies[124,126]. During normal culture periods, cells were incubated at 37°C in a humidified 5% CO_2-enriched atmosphere (Thermo Forma Series II Water Jacketed CO_2 Incubator; Fisher Scientific Limited, Ontario Canada). Cells were cultured in RPMI 1640 medium (Invitrogen, Ontario, Canada) that was supplemented with 5% heat inactivated fetal bovine serum (FBS; Invitrogen), 1% fungizone (Invitrogen), and 1% penicillin-streptomycin (Invitrogen) as a monolayer in 25 cm^2 flasks (Fisher), and the media was changed twice weekly. Cells were observed at media change for normal growth by phase contrast microscopy. Cell viability was determined using the trypan blue exclusion test[127]. For experiments requiring serum-starved cells, normal culture media was removed and cells were washed in phosphate buffered saline (PBS) and recultured in RPMI 1640 medium supplemented with 1% fungizone (Invitrogen) and 1% penicillin-streptomycin (Invitrogen).

Multiplex Sandwich Enzyme Linked Immunosorbent Assay (ELISA)

In order to determine if the three cell lines produced VEGF and other pro-angiogenic cytokines, we used a commercially available multiplex sandwich ELISA (Quantibody® Human Angiogenesis Array I; RayBiotech, Inc., Norcross, GA, USA). We also investigated whether the administration of bevacizumab affected the production of these factors using ELISA.

First, 500,000 cells from each cell line were cultured separately in 6-well plates with 5% FBS-supplemented media for 24 hours. Serum media was then removed, and cells were washed twice with PBS, and serum-free media was added to the wells. For the experimental condition, 100µg/mL of bevacizumab (Avastin®; Roche; Laval, QC, Canada) was also added to the wells. Twenty-four hours after changing to serum free media with or without the addition of bevacizumab, 500µL of concentrated, conditioned media was extracted from each well for multiplex sandwich ELISA analysis (Quantibody® Human Angiogenesis Array I; RayBiotech, Inc., Norcross, GA, USA). This platform provides quantitative data pertaining to 10 cytokines: Angiogenin, ANG-2, EGF, bFGF, HB-EGF, HGF, Leptin, PDGF-BB, P1GF, and VEGF. ELISA experiments were performed as per the manufacturer's instructions. Briefly, 100µL of Sample Diluent (blocking solution) was added to each well of the glass slide with bound capture antibody. After blocking for 30 min, 100µL of standard cytokines or samples (conditioned media) were added to each well and incubated on an orbital

shaker for two hours at 4°C. The slide was then washed five times with Wash Buffer I followed by two washes with Wash Buffer II. Next, 80µL of detection antibody cocktail was added to each well for two hours followed by the identical, aforementioned washing procedure. After washing, 80µL of Cy3 dye-conjugated streptavidin was added to each well followed by incubation in the dark for one hour. The glass slide was then washed five times with 150µL of Wash Buffer I. After drying, slides were sent to RayBiotech Inc. for fluorescent analysis with the Quantibody® Q-Analyzer software. All conditions were repeated in quadruplicate and normal, unconditioned media with and without the addition of 100ug/mL of bevacizumab were used as negative controls.

Immunocytochemistry

To initially determine if the three cell lines produced the primary VEGF-A receptor VEGF-R2, we performed cytospins and immunostained for this protein.

After growing to 80% confluency in conditions described above, cells were prepared for immunocytochemistry by first detaching them from the flask using 0.05% trypsin in EDTA (Fisher) and, after neutralizing the trypsin with supplemented media, cells were resuspended in PBS at a concentration of 1,000,00 cells/mL. Cytospins were then preformed using Cytospin® 3 (Thermo Shandon Inc.; Cheshire, England) as per the manufacturer's instructions. Briefly, 300µL of the PBS diluted cell suspension were added to the Cytofunnel™ and the

machine spun the samples for three minutes at 500RPM. This process forced the cells onto a glass slide, suitable for immunocytochemistry and other applications.

Immunocytochemistry was performed using the Ventana BenchMark fully automated machine (Ventana Medical System Inc., AZ, USA). The automated processing of barcode labeled slides included baking of the slides, solvent-free deparaffinization, and CC1 (Tris/EDTA buffer pH 8.0) antigen retrieval. Slides were incubated with a monoclonal mouse anti-human VEGFR2/KDR-1/Flt-1 antibody (Millipore, Temecula, MA; 1:50 dilution) for 30 min at 37°C, followed by application of a biotinylated secondary antibody (8 min at 37°C) and an avidin/streptavidin enzyme conjugate complex (8 min at 37°C). Finally, the antibody was detected by Fast Red chromogenic substrate and counterstained with hematoxylin. Cytospins were independently graded as either positive or negative for VEGFR2 expression by two different pathologists, and there were no inter-observer conflicts. This process is described elsewhere[128]. For negative controls, the process was repeated using the identical procedure save the omission of the primary antibody.

Western Blot

Next, in order to determine if the VEGF-R2 receptors are activated by endogenous VEGF-A, a western blot for the phosphorylated version of the protein was performed. This process was executed on control cells and those in which VEGF-A was inhibited with 100ug/mL bevacizumab. Cells were grown in a 6-

well plate with 5% supplemented serum media to a total density of 500,000 cells, after which they were grown in serum-free media for 24 hours prior to protein extraction. The experimental group was incubated with 100ug/mL of bevacizumab (Roche) for 24 hours prior to protein extraction. Cells were removed from the flask using trypsin as previously described, and pelleted. Next, protein was extracted from the pellets using cOmplete Protease Inhibitor Cocktail Tablets (Roche), PhosSTOP Phosphatase Inhibitor Tablets (Roche), and lysis buffer (150mM NaCl, 50mM HEPES, pH 7.4, 1mM EGTA, 1mM Na3VO4, 10mM NaF, 1mM phenylmethylsulfonyl fluoride, 5% glycerol, and 1% Triton X-100) as per the manufacturers' instructions. After extraction, protein quantification was determined using the Micro BCA Protein Assay Kit (Thermo Scientific; Rockford, IL, USA) as per the manufacturer's instructions and read using the Bio-Tek EL-800 Universal plate reader (Bio-Tek Instruments, Winooski, VT, USA) at a wavelength of 560nm. Protein from all samples was standardized to 15ng/uL. Next, 30µL of control and experimental samples were subjected to SDS-PAGE on 8% acrylamide separating gel before transferring to nitrocellulose membranes (Invitrogen) and incubating overnight at 4°C with Phospho-VEGFR2 (1:500; Cell Signalling Technology; Beverly, MA, USA) and ² -Actin (1:1000; Abcam plc; Cambridge, MA, USA). Film was developed using Pierce ECL Western Blotting Substrate (Thermo Scientific) and Kodak Biomax XAR film (Kodak; Rochester, NY, USA), as per manufacturers' instructions; film was exposed for 30 seconds. For negative controls, the aforementioned process was repeated save omission of the primary antibody.

In order to objectively compare activated VEGF-R2 protein levels between control cells and those treated with bevacizumab, the optical density (OD) of the positive bands from the western blot were analyzed using ImageJ Software (ver. 1.46d; National Institutes of Health [NIH], USA)[129,130]. After scanning the film and generating a JPG image, lanes were individually selected using the Analyze > Gels command. Next, plots of the relative densities of the content of each lane were generated and the data from each plot area were calculated and exported to Microsoft Excel (2010). This process was repeated for every control and experimental condition for both ² -actin and Phospho-VEGFR2. To normalize all lanes for loading discrepancies, the densest (highest value determined by ImageJ) ² -actin lane was given a relative value of 1 and all other ² -actin values were normalized to the density of this lane. Next, all Phospho-VEGFR2 bands were normalized according to their respective loading controls. Finally, relative expression of VEGF-R2 before and after bevacizumab treatment was determined for each cell line by dividing the normalized OD of the control by the normalized OD of the experimental condition.

Flow Cytometry

In order to assess the effect of bevacizumab on cell cycle, flow cytometry in conjunction with propidium iodide (PI) staining was performed. Succinctly, all three cell lines were grown in regular culture conditions 24 hours prior to PI staining. One day prior to experimentation, the media was removed and the cells were washed in and then incubated in serum free media. For the experimental

groups, 100µg/mL of bevacizumab (Roche) was added to the media. Twenty-four hours later, cells were harvested and resuspended in PBS at a concentration of 100,000 cells/mL and fixed with cold ethanol. After fixation, cells were added to a PI staining solution (3.8mM sodium citrate, 50µg/mL PI) and 10µg/mL RNAse solution (Promega; Madison, WI, USA). This cell solution was then analyzed using a 488nm laser and fluorescence (> 600 nm), and side scatter were obtained using the BD FACS Calibrator (BD Biosciences; San Jose, CA, USA). For each sample, 30,000 events were captured and the Dean/Jett/Fox Algorithm was used in order to measure the number of cells in the following states: %G1, %S, %G2, % > G2, and % < G1. The percentage of cells in phase < G1 were considered an indication of apoptosis. For negative controls, no PI solution was added to the cells prior to flow cytometry.

Quantitative Real-Time Polymerase Chain Reaction (RT-qPCR)

To determine the effects of bevacizumab on the transcription rate of VEGF-A, RT-qPCR was performed. The three cell lines were grown in 6-well plates in regular culture media until they reached a total of 500,000 cells per well. Twenty-four hours prior to harvesting, supplemented media was replaced with serum free media and the experimental group was augmented with 100ug/mL of bevacizumab. Cells were harvested and RNA was extracted using the Qiagen RNeasy kit (Qiagen, Mississauga, Ontario, Canada) as per the manufacturer's instructions. Briefly, cells were disrupted and homogenized using lysate buffer

and, after mechanical separation using a syringe, insoluble material was removed by centrifugation. The lysate solution was mixed with one volume of 70% ethanol before adding the solution to RNeasy minicolumns, which were centrifuged and then washed twice using the included buffer solutions. Finally, total cellular RNA was eluted using RNase-free water.

Next, the RNA was converted to a cDNA library using iScript™ Reverse Transcription Supermix for RT-qPCR (Bio-Rad Laboratories; Hercules, CA) as per the manufacturer's instructions. After adding the Supermix to each RNA sample, a Chromo4 thermocycler (MJ Research, Waltham, Massachusetts, USA) was used to incubate the mixture with the following settings: priming, 5m at 25°C, reverse transcription, 30m at 42°C, and RT inactivation, 5m at 85°C. All future experiments used the cDNA generated using the techniques described above. For negative controls, the process was repeated without the addition of the reverse transcription.

The iQ™ SYBR® Green Supermix (Bio-Rad Laboratories) was then added to the cDNA from each sample. Each sample was prepared in triplicate using both ² -actin and VEGF-A primers (QuantiTect® Primer Assay; Qiagen) and the following settings were programmed into the Opticon Monitor software (Bio-Rad Laboratories) and run using the Chromo4 thermocycler: 15m at 95°C, 15s at 94°C, 30s at 55°C, 30s at 72°C, followed by a plate read. This process was repeated a total of 40 times.

For all comparisons between treated and untreated cells, the Pfaffl fold-change method was used[131]. This method was selected as it accounts for potential differences in primer efficiency and non-perfect transcript doubling. First, standard curves were generated using the two primers (² -actin [Invitrogen] and VEGF-A [Invitrogen]) and known quantities of RNA and, from this standard curve, the slope of the line was calculated. This data was used to determine primer efficiency, which was calculated using the following formula:

Efficiency = 10 ^ (-1/slope)

Next, the fold change in expression (" Ct) was calculated using the following formula:

$$\text{" Ct} = (\text{Efficiency}^{\text{ACTIN}} \wedge [\text{Ct}^{\text{VEGFcontrol}} - \text{Ct}^{\text{VEGFexp}}]) / \text{Efficiency}^{\text{VEGF}} \wedge [\text{Ct}^{\text{ACTINcontrol}} - \text{Ct}^{\text{ACTINexp}}])$$

The suffixes control and exp represent the values obtained from the mean of three experiments using untreated cells and those treated with bevacizumab, respectively.

The assay was performed in triplicate for each gene of interest, and product validation was achieved using melting curve analysis.

Statistical Analysis

The Student's t-test was used for all comparisons, and a p-value of < 0.05 was considered statistically significant (Microsoft Excel). All data is presented as means ± standard deviation (SD).

Results

Multiplex Sandwich Enzyme Linked Immunosorbent Assay (ELISA)

All three cell lines produced VEGF-A in culture (mean ± SD): 92.1, 11785.5 ± 231.8 pg/µL; OCM-1, 4608.0 ± 324.0 pg/µL; UW-1, 8309.3 ± 634.5 pg/µL. After bevacizumab administration, there was no detectable VEGF-A in the serum produced by any cell line; a difference that was significant ($p < 0.001$) for all (Figure 2).

With respect to other pro-angiogenic cytokines, angiogenin was significantly reduced in the OCM-1 and UW-1 cell lines following bevacizumab treatment (1562.0 ± 16.9 pg/µL vs. 1401.2 ± 16.2 pg/µL and 4980.9 ± 187.6 pg/µL vs. 1736.8 ± 101.1 pg/µL, respectively; Student's t-test; $p < 0.05$, for both). EGF expression was significantly reduced following bevacizumab treatment of the UW-1 cell line (33.3 ± 2.0 pg/µL vs. 23.7 ± 2.4 pg/µL, respectively; Student's t-test; $p < 0.05$). Similarly, both HB-EGF and P1GF were significantly reduced in the UW-1 cell line after bevacizumab administration (366.4 ± 47.3 pg/µL vs. 59.1 ± 4.2 pg/µL and 64.6 ± 4.4 pg/µL vs. 22.1 ± 2.1 pg/µL, respectively; Student's t-test; $p < 0.05$, for both). No significant expression changes in any other cytokines were noted after bevacizumab treatment. Although not significant, it is of note that bevacizumab induced an increase in EGF and HB-EGF in the OCM-1 cell line. There was no detectable VEGF-A in serum-free media with or without the addition of bevacizumab (0.0 pg/µL, for all).

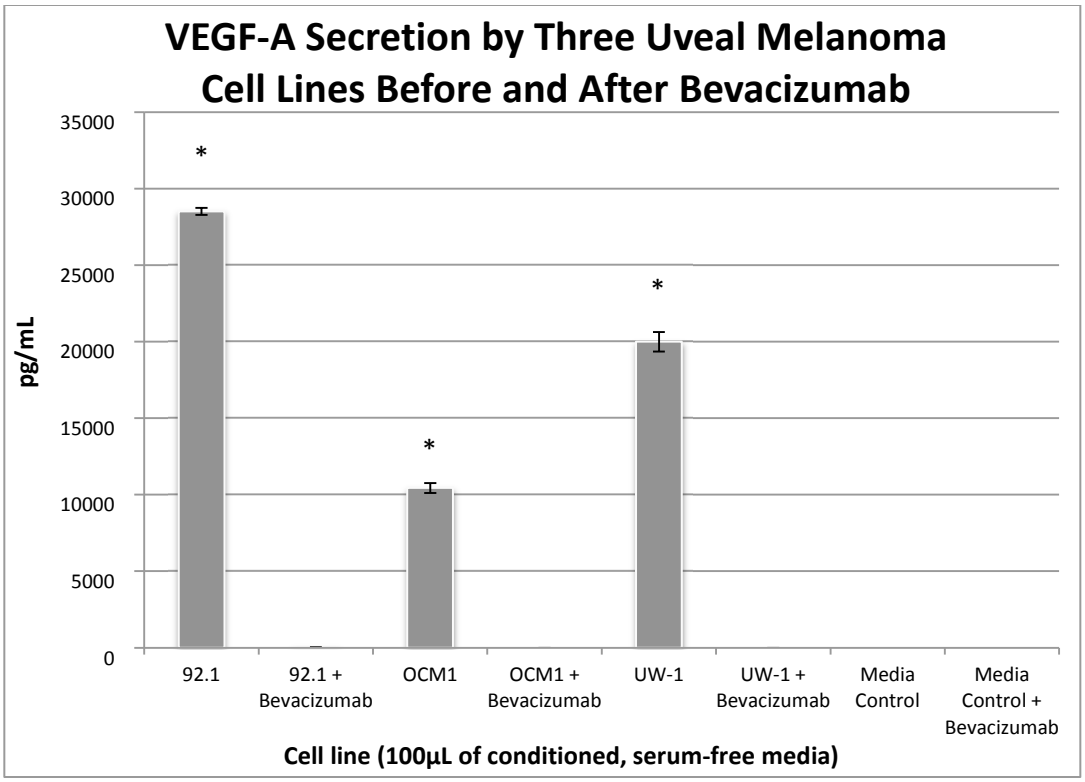

Figure 2. VEGF-A secretion by three uveal melanoma cell lines (92.1, OCM-1, and UW-1) into conditioned media before and after the administration of 100ug/mL of bevacizumab (+ bevacizumab), as determined using a sandwich ELISA. Normal media with and without bevacizumab were used as controls. *p < 0.05; Student's t-test.

Immunocytochemistry

Cytospins of all three cell lines were positive for VEGF-R2. Immunostaining was primarily cytoplasmic/membrane, but nuclear positivity was also identified in the OCM-1 and UW-1 cell lines (Figure 3).

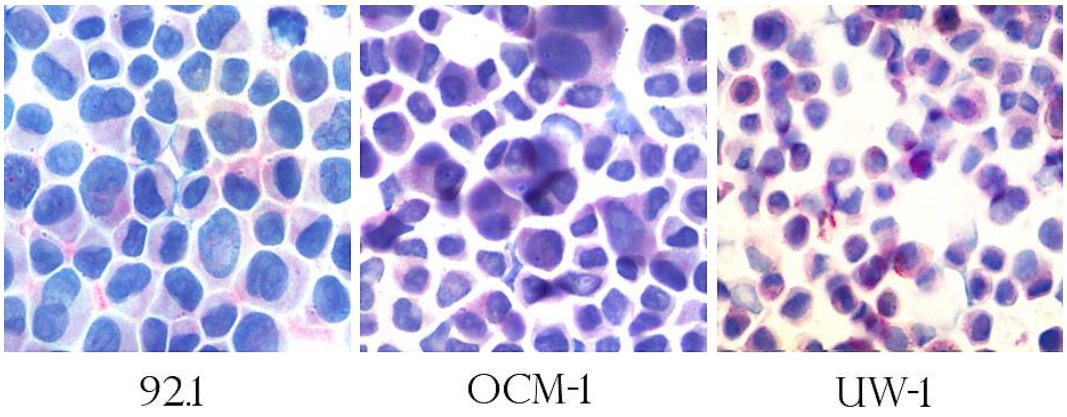

Figure 3. Immunocytochemistry of three uveal melanoma cell lines for the expression of VEGF-R2. Pink: Positive immunostaining; Blue: Hematoxylin counter staining.

Western Blot

Activated VEGF-R2 was detectable in all three cell lines under control conditions. The ODs after correcting for loading bias were as follows: 92.1 = 107525.2 ± 8602.0, OCM-1 = 46587.3 ± 4192.9, and UW-1 = 60394.3 ± 4026.4. After bevacizumab administration, activated VEGF-R2 levels significantly dropped to 1% (1024.5 ± 98.2), 28% (12821.1 ± 1666.7), and 14% (6908.2 ± 607.2) of the 92.1, OCM-1, and UW-1 controls, respectively (Student's t-test; $p < 0.05$; Figure 4).

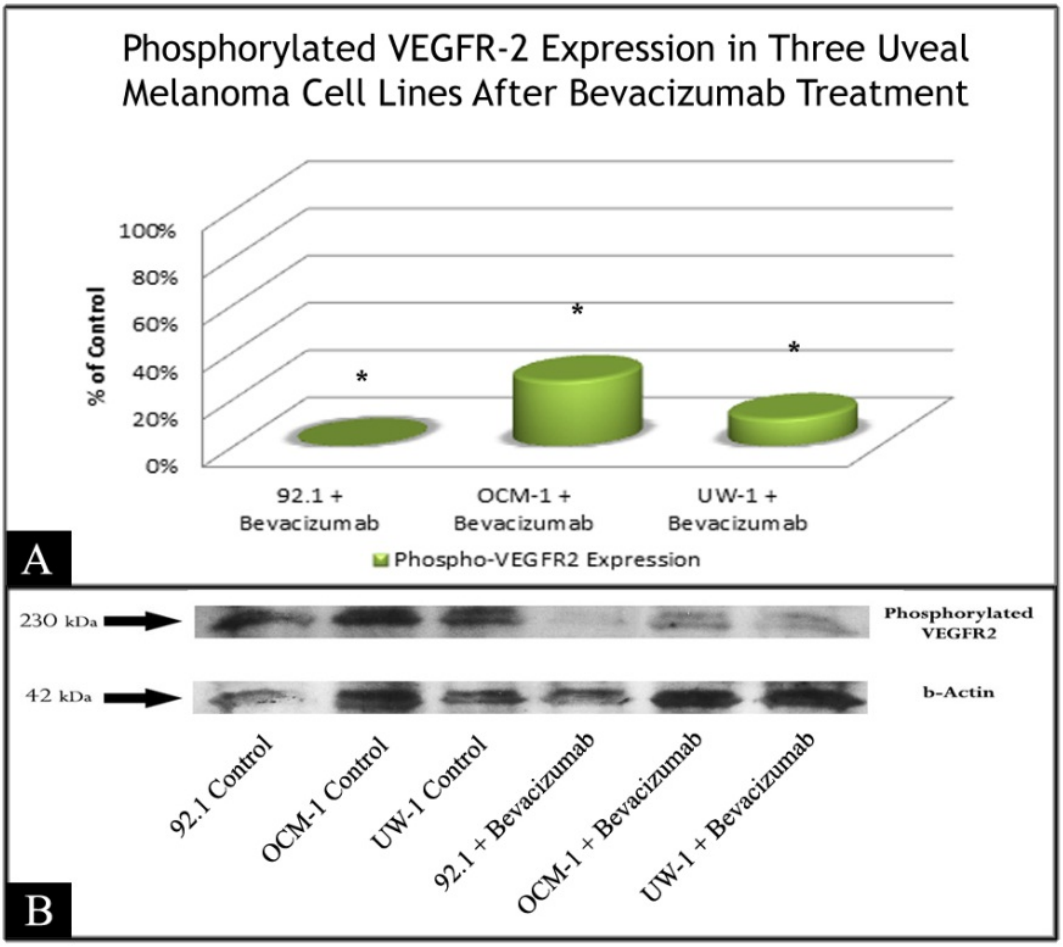

Figure 4. A. Expression of phosphorylated-VEGF-R2 before and after bevacizumab treatment expressed as a percentage of the control. Optical density of the western blots was quantified using ImageJ software (NIH). *p < 0.05; Student's t-test. B. Representative western blot of phosphorylated-VEGF-R2. ² -Actin was used as a loading control.

Flow Cytometry

The use of bevacizumab at a concentration of 100µg/mL did not statistically influence either cell cycle or cell death. In general, less than 1% of

cells had fragmented DNA representative of apoptosis, irrespective of cell line or treatment (Table 2). These data suggest that any changes in proliferation or other functional abilities addressed later in the thesis will not be attributable to bevacizumab-induced cell cycle changes or toxicity.

Table 2. Dean/Jett/Fox algorithm applied to the flow cytometry results displaying the percentage of cells in the different phases of the cell cycle, as determined using propidium iodide staining. Individual percentages are obtained by dividing the number of events for that category by the total number of events (30,000). The %<G1 represents the population of cells that have undergone apoptosis. G: gap phase; S: synthesis gap phase.

	%G1	%S	%G2	%<G1	%>G2	TOTAL
92.1 Control	51.4	25.5	21	0.51	0.52	98.93
92.1 + Bevacizumab	50.3	29.4	17.8	0.28	0.56	98.34
OCM-1 Control	64	22.3	11	0.31	0.74	98.35
OCM-1 + Bevacizumab	61.9	20.4	14.9	0.31	1.23	98.74
UW-1 Control	50.1	32	13.2	0.91	1.6	97.81
UW-1 + Bevacizumab	51.2	26	18.3	1.05	1.87	98.42

Quantitative Real-Time Polymerase Chain Reaction (RT-qPCR)

Inhibition of VEGF-A with 100ug/mL of bevacizumab caused a slight yet consistent upregulation of VEGF-A across all three cell lines. VEGF-A mRNA increased 1.14, 1.18, and 1.37 fold, for the 92.1, OCM-1, and UW-1 cell lines, respectively.

Discussion

Based on recent studies describing the importance of VEGF-A for tumor growth and development, we investigated VEGF-A status in three uveal melanoma cell lines of varying metastatic potential. Currently, there are limited studies in the literature investigating VEGF-A expression in UM, and fewer still assessing the inhibition of this cytokine in animal models, thus comprehensive studies regarding VEGF-A in multiple UM cell lines are needed[92,93,106,132]. In the present study, we determined that three UM cell lines produced copious amounts of VEGF-A (between 4600 and 12000 pg/mL). It is of note that this exceeds the amount of VEGF-A detected in the serum of patients with UM, which ranged between approximately 40 and 2000 pg/mL[133]. Although direct comparisons between culture experiments and serum from patients should be considered with reservation, our data indicates that the VEGF-A produced by our cell lines might represent a clinically relevant concentration.

All three cell lines tested also produced the primary VEGF-A receptor involved in tumor angiogenesis, VEGF-R2, suggesting that both the cytokine and its receptor may be involved in UM development or progression. To better ascertain the functional consequences of this activation, we chose to inhibit VEGF-A using a commercially available inhibitor, bevacizumab. The decision to select bevacizumab over other inhibitors was based on the fact that bevacizumab is currently the most commonly used anti-angiogenic pharmaceutical used to treat various ocular conditions[112,121,134,135]. As expected based on previous reports, bevacizumab did not affect cell cycle or induce cell death at 100ug/mL[106]. This

clinically relevant dosage was capable, however, of completely inhibiting VEGF-A from activating VEGF-R2 in these cell lines. Taken together, these data suggest that UM cell lines use the VEGF-A/VEGF-R2 signalling cascade for autocrine and paracrine processes, a proceeding that can be abolished with bevacizumab administration.

Autocrine signalling is not uncommon for malignant cells, and has been seen in UM. For example, it has been shown that the FGF2/FGFR1 autocrine loop induces cell proliferation and survival in UM cells[136]. Furthermore, in many cancers, including ovarian carcinoma, breast cancer, and prostate cancer, VEGF-A signalling can operate in an autocrine manner and induce cell growth[137-139].

We also determined that our UM cells increase VEGF-A mRNA production in response to inhibition with exogenous bevacizumab. This is to be expected, as recognition of decreased VEGF-R2 signalling should subsequently result in upregulation of ligand transcription in the cell lines. However, based on the abundant production of both the receptor and ligand, a paltry maximum increase of 40% in VEGF-A mRNA by these cell lines seems unexpectedly low. A previous study analyzing VEGF-A production in neutrophils demonstrated that they harbor an intracellular pool of VEGF-A that can be released in response to various factors[140]. Although we did not test this hypothesis directly, it is possible that our UM cells did not radically increase VEGF-A mRNA when activation of the receptor was significantly reduced because they released pooled VEGF-A from intracellular compartments. Unfortunately, the antibody based detection methods (ELISA) used in our study would not detect this process unless the

exogenous bevacizumab was saturated, which was evidently not the case. In this scenario, it is reasonable to assume that if this initial compensatory mechanism failed to restore VEGFR-2 activation, increased transcription of VEGF-A would ensue. Future studies in which uveal melanoma cells experience prolonged exposure to bevacizumab beyond 24 hours would be useful to address this hypothesis.

Alternatively, we initially considered that UM cells may increase the production of other angiogenic or growth factors in response to bevacizumab treatment, as is the case in colorectal cancer cells after chronic treatment with bevacizumab[141]. This compensatory process was also detected in a study investigating bevacizumab treatment for other ocular conditions in the clinic. In that study, the authors concluded that bevacizumab therapy induced significant upregulation of IL-8 and TGF-b[142]. However, our data investigating 10 pro-angiogenic cytokines does not support this hypothesis as none of the factors tested were significantly upregulated following bevacizumab administration. We did note, however, a non-significant increase in EGF and HB-EGF following treatment; thus, we suggest that it is possible that other cytokines that do not possess intrinsic angiogenic properties, and were therefore not included on the ELISA array, may be upregulated following bevacizumab therapy.

The discrepancy between our in vivo data and in vitro data from other studies described above may also be a consequence of a lack of oxygen restrictions in the latter relative to the former. In vivo, tumor cells must compete with a host of other cell types for oxygen, whereas in culture, UM cells only

compete with other UM cells in a self-limiting manner. In addition, cells grow as a monolayer in culture, and thus do not suffer the same surface area to volume diffusion restrictions experienced by three-dimensional tumors. Despite the aforementioned discrepancies in oxygen acquisition restrictions between in vitro and in vivo settings, our experiments were performed in serum-free media and thus competition for sustenance may be similar between the two cohorts. Therefore, in culture, VEGF-A may be employed more for its growth factor characteristics than for its pro-angiogenic influence, and thus refractory cytokine production following inhibition may reflect growth requirements as opposed to being hypoxia motivated. Therefore, future studies should investigate the compensatory upregulation of growth factors and other cytokines following bevacizumab treatment.

Conclusion

In this chapter, we demonstrated that three uveal melanoma cells produce VEGF-A and the primary receptor VEGF-R2 in culture. We also showed that the receptor is activated in both a paracrine and autocrine fashion, which can be inhibited by a non-lethal dose of bevacizumab. Although VEGF-A generally acts as a mitogen and induces proliferation in other malignancies, there are limited studies investigating the consequences of this effect in UM. Because producing ligands and receptors requires the expenditure of valuable energy resources, VEGF may play an important role in UM progression. Therefore, the present results and preceding work in this field provide an impetus for future studies focusing on the downstream and functional effects of this signalling process in uveal melanoma.

Chapter 2: The Effects of VEGF-A Signalling and Inhibition in UM Cell Lines

Introduction

In this chapter, we explore and expand on the findings of chapter 1; mainly, the consequences of auto- and paracrine signalling of VEGF-A through VEGF-R2, and inhibition of said signalling with bevacizumab in UM. Moreover, we investigate the effects of VEGF-A inhibition on a large panel of complementary cytokines to determine if they are upregulated to offset the reduced receptor tyrosine kinase activity.

We hypothesize that inhibiting VEGF-A signalling in our UM cell lines will reduce their ability to proliferate, migrate, and invade. Furthermore, we postulate that other cytokines will be upregulated by bevacizumab and that dual inhibition of VEGF-A and select compensatory cytokines will result in further depression of the functional abilities of UM cells.

Materials and Methods

Cell Lines and Culture

Cell lines and cell culture were maintained exactly as described in the complementary section in Chapter 1.

Multiplex Sandwich Enzyme Linked Immunosorbent Assay (ELISA)

In order to establish whether bevacizumab treatment influenced the production of additional cytokines, a multiplex ELISA assay was performed using the same methodology and equipment listed in the dizygotic section in Chapter 1. In this chapter, we analyzed the production of 20 human cytokines using the Quantibody® Human Cytokine Array 1 (Raybiotech, Inc.), which detects secreted levels of IL-1a, IL-2, IL-5, IL-8, IL-12p70, GM-CSF, IFNy, CCL3, MMP-9, TNF-a, IL-1b, IL-4, IL-6, IL-10, IL-13, GRO, MCP-1, MIP-1b, RANTES, and VEGF. All conditions were repeated in quadruplicate and expression before and after treatment with 100µg/mL of bevacizumab (Roche) was compared. Serum-free media with and without added bevacizumab (Roche) were used as controls.

Gene Knockdown using siRNA

Based on the results of the cytokine ELISA, we selected one cytokine (CCL3) that was consistently upregulated following bevacizumab for inhibition (*see* Chapter 2: Results). In order to knockdown the expression of CCL3, we used

the ON-TARGET plus SMARTpool Human CCL3 siRNA (Thermo Fisher Scientific; Lafayette, CO, USA) with DharmaFECT® siRNA transfection reagent 1 (Thermo Fisher Scientific) employing the manufacturer's instructions. All cell lines were seeded at 300,000 cells per well in a 6-well plate in serum and antibiotic free media. Five microliters of transfection reagent 1 (Thermo Fisher Scientific) was diluted with 195µL of antibiotic free media and 10µL of the 5uM concentration of either SMARTpool Human CCL3 (Thermo Fisher Scientific), SMARTpool Human GAPDH (positive control; Thermo Fisher Scientific), or On-TARGET plus Non-Targeting Plus (negative control; Thermo Fisher Scientific) was mixed with 190µL of antibiotic free media. These two mixtures were combined with 1600µL of complete, antibiotic free media and added to the individual wells. After 24 hours, the media was removed from the wells and new, antibiotic free media with serum was added, and these transfected cells were used for further experiments. In total, each cell line (92.1, OCM-1, and UW-1) was separately transfected with three different siRNAs: CCL3 (experimental condition), GAPDH (positive control), scramble sequence (negative control). All experiments were repeated in triplicate.

Quantitative Real-Time Polymerase Chain Reaction (RT-qPCR)

In order to determine the efficiency of the knockdown of CCL3 using the siRNA described above, RT-qPCR was performed. This procedure was executed in an identical manner as described in the corresponding section in Chapter 1,

save the use of the following PCR primers: CCL3 (Qiagen) and GAPDH (Qiagen). GAPDH was used to evaluate both the positive and negative siRNA controls. ² -actin was used as the internal control for all experiments.

In addition, RT-qPCR was performed to determine if the UM cell lines produced the primary receptor for CCL-3 (CCR-1) using a CCR-1 primer (Qiagen). Furthermore, MMP-9 expression was also evaluated using this same technique. The expression levels of all the proteins were tested under the following conditions: control, siRNA transfected, bevacizumab treated, and siRNA transfected and bevacizumab treated (combination). All experiments were performed in triplicate, and the previously described Pfaffl fold-change method was used to evaluate expression differences between conditions.

Protein Expression

To determine CCL3 protein secretion before and after bevacizumab treatment and to assess the effectiveness of CCL3 siRNA to reduce protein secretion, we used the Quantikine® Human CCL3/MIP-1a (R&D Systems; Minneapolis, MN, USA), an ELISA based system. To determine serum protein levels, UM cell lines (either controls or siRNA transfected) were incubated in a 6-well culture plate at a density of 333,000 cells per well with 1mL of serum-free media. For experimental conditions that required bevacizumab, the drug was added 24 hours prior to assaying. For cells treated with siRNA, experiments

commenced immediately following incubation in complete media (24 hours after beginning the transfection). Therefore, for all conditions, cells were seeded and treated (where required) 24 hours prior to conditioned media acquisition.

As per the manufacturer's instructions, 200µL of serum from each condition was added to the individual wells provided with the assay and incubated for two hours. Next, wells were aspirated and washed three times and 200µL of CCL3 conjugate was added. After 1 hour, the wells were once again aspirated and washed three times. Then, 200µL of Substrate Solution was added to each well, and the cells were incubated in the dark for 20 minutes. Finally, 50µL of stop solution was added, and all wells were read with a plate reader (Bio-Tek Instruments) at a wavelength of 450nm after 15 min of color development. The following conditions were tested for all three cell lines: control, bevacizumab treated (100µg/mL), CCL3 siRNA, and bevacizumab and CCL3 siRNA (combination).

To assess the effects of bevacizumab, CCL3 siRNA, and combination treatments on MMP-9 protein secretion, we used the Quantikine® Human MMP-9 (R&D Systems) kit. Samples were prepared and the assay was performed using identical procedures as outlined above for CCL3. For all ELISA experiments, conditions were repeated in triplicate and controls included serum-free media with and without added bevacizumab.

Functional Assays

In order to determine the effects of various treatments on the functional abilities of UM cells, we compared the following conditions: serum-free media (control), 100µg/mL bevacizumab, CCL3 siRNA, and the combination of both treatments. The goal of the latter set of experiments was to determine what effect CCL3 siRNA has on the functional abilities and whether inhibiting this cytokine would increase the efficacy of bevacizumab.

Proliferation Assay

Cell proliferation was calculated using the Sulforhodamine B based in vitro toxicology assay kit (TOX-6; Sigma; St. Louis, MI, USA), executed as per the manufacturer's instructions. Sulforhodamine B stains cellular proteins; thus, the amount of dye incorporation is an indirect measure of total biomass and, consequently, cell number[143]. Briefly, 25,000 cells from each condition were grown in 96-well plates in serum free media. For experimental conditions, 100µg/mL of bevacizumab was added to the wells. After 24 hours, cells were fixed using trichloroacetic acid for one hour before washing with water. Next, Sulforhodamine B Solution was added to the cells, and they were allowed to stain for 30 minutes. After residual solution was removed by washing, dye was solubilized with the provided Sulforhodamine B Assay Solubilization Solution and wells were agitated for five minutes. After visual confirmation that the dye was dissolved, the absorbance of the wells was determined at 565nm using the

Bio-Tek EL-800 Universal plate reader (Bio-Tek). Data was collected using KC Junior software (Bio-Tek). All experiments were repeated in triplicate. Media with and without added bevacizumab were used as controls.

Migration Assay

Conceptually, the migration assay functions by seeding serum starved cells into an upper chamber that has a porous, membrane base. With the addition of a chemoattractant in the lower chamber, cells will migrate towards the attractant and, after staining, the number of migrated cells can be counted and compared between conditions.

Migration assays were performed using the QCM ™ 24-well Colorimetric Cell Migration Assay (EMD Millipore; Billerica, MA, USA) as per the manufacturer's instructions. Briefly, 300,000 cells were serum starved for 24 hours prior to adding them in serum free media into the upper chamber. For a chemoattractant, serum supplemented media was added to the lower. For experimental conditions, 100μg/mL of bevacizumab was added to the upper chamber with the cells. Cells were then placed back into the incubator under normal culture conditions to allow migration. After 24 hours, non-migrating cells from the upper chamber were removed by pipetting, and the lower portion of the upper chamber was incubated in Cell Stain for 20 minutes. Residual, non-migrating cells from the upper chamber were removed by swabbing. The bottom of the chamber, containing the stained, migrated cells, was incubated in

Extraction buffer. After transferring 100µL of this solution to a 96-well plate, the OD at 560nm was determined using the Bio-Tek EL-800 Universal plate reader (Bio-Tek). All experiments were repeated in triplicate. Media with and without added bevacizumab were used as controls.

Invasion Assay

The Colorimetric QCM ECMatrix Cell Invasion Assay (EMD Millipore) was used to determine the invasive ability of UM cell lines. This assay functions similarly to the migration assay described above; the cells were prepared in the same manner, and the technical aspects of the kit are identical. However, while the migration assay has a membrane with 8µm holes for the cells to migrate through, in the invasion assay, these pores are covered with a basement membrane (ECMatrix™). This membrane is designed to represent the extracellular matrix present in vitro; in this context, the cells must actively degrade this membrane in order to migrate into the lower chamber, in a manner mimicking physiological extracellular matrix. Only cells that accomplish this task will be subsequently detected by the plate reader. Media with and without added bevacizumab were used as controls.

Statistical Analysis

To compare between multiple means, such as for the multiple conditions used in the proliferation, migration, and invasion assays, and for comparing CCL3 and MMP-9 protein secretion, we first determined homogeneity of variance using Levene's statistic. If Levene's statistic was < 0.05, indicating that the assumption of homogeneity of variance was not met, we performed Brown-Forsythe and Welch tests to determine if differences were significant. If Levene's statistic was > 0.05, we performed a one-way analysis of variance analysis (ANOVA). Tukey post-hoc analysis was used to determine where differences were significant between treatment conditions for each cell line. To compare experimental conditions to the controls, Dunnett's 2-sided tests were used for post-hoc analysis. Analyses were performed using SPSS ver. 20 (IBM Corporation).

The Student's t-test was used to determine differences for all tests requiring the comparison of only two means (Microsoft Excel).

For all statistical analyses, a p-value of < 0.05 was considered statistically significant. All data is presented as means ± standard deviations (SD).

Results

Multiplex Sandwich Enzyme Linked Immunosorbent Assay (ELISA)

Of the 20 cytokines tested, only four were significantly affected following bevacizumab treatment: IL-4, GM-CSF, CCL3, and MMP-9; the former two were downregulated and the latter two upregulated. The following data pertaining to these cytokines are displayed as means ± SD.

IL-4 secretion was significantly reduced in the 92.1 and OCM-1 cell lines after bevacizumab treatment (223.00 ± 35.44 pg/mL vs. 124.33 ± 16.74 pg/mL; 213.50 ± 31.93 pg/mL vs. 114.25 ± 19.03 pg/mL, respectively; Student's t-test; $p < 0.05$ for both). GM-CSF secretion was also significantly reduced in the OCM-1 cell line following bevacizumab therapy (167.00 ± 11.43 pg/mL vs. 109.50 ± 21.01 pg/mL; control vs. bevacizumab; Student's t-test; $p < 0.05$).

Only CCL3 and MMP-9 were significantly upregulated following bevacizumab treatment across all three cell lines. For CCL3, the values were: 1072.50 ± 18.77 pg/mL vs. 1281.00 ± 72.34 pg/mL; 22.5 ± 7.85 pg/mL vs. 62.00 ± 9.16 pg/mL; 20.33 ± 6.35 pg/mL vs. 35.00 ± 6.22 pg/mL; control vs. bevacizumab; 92.1, OCM-1, and UW-1, respectively; Student's t-test; $p < 0.05$ for all (Figure 5).

For MMP-9, the values were: 25.50 ± 5.47 pg/mL vs. 88.25 ± 13.38 pg/mL; 19.75 ± 4.14 pg/mL vs. 45.25 ± 8.36 pg/mL; 3.25 ± 1.09 pg/mL vs. 19.25

± 3.77 pg/mL control vs. bevacizumab; 92.1, OCM-1, and UW-1, respectively; Student's t-test; $p < 0.05$ for all (Figure 5).

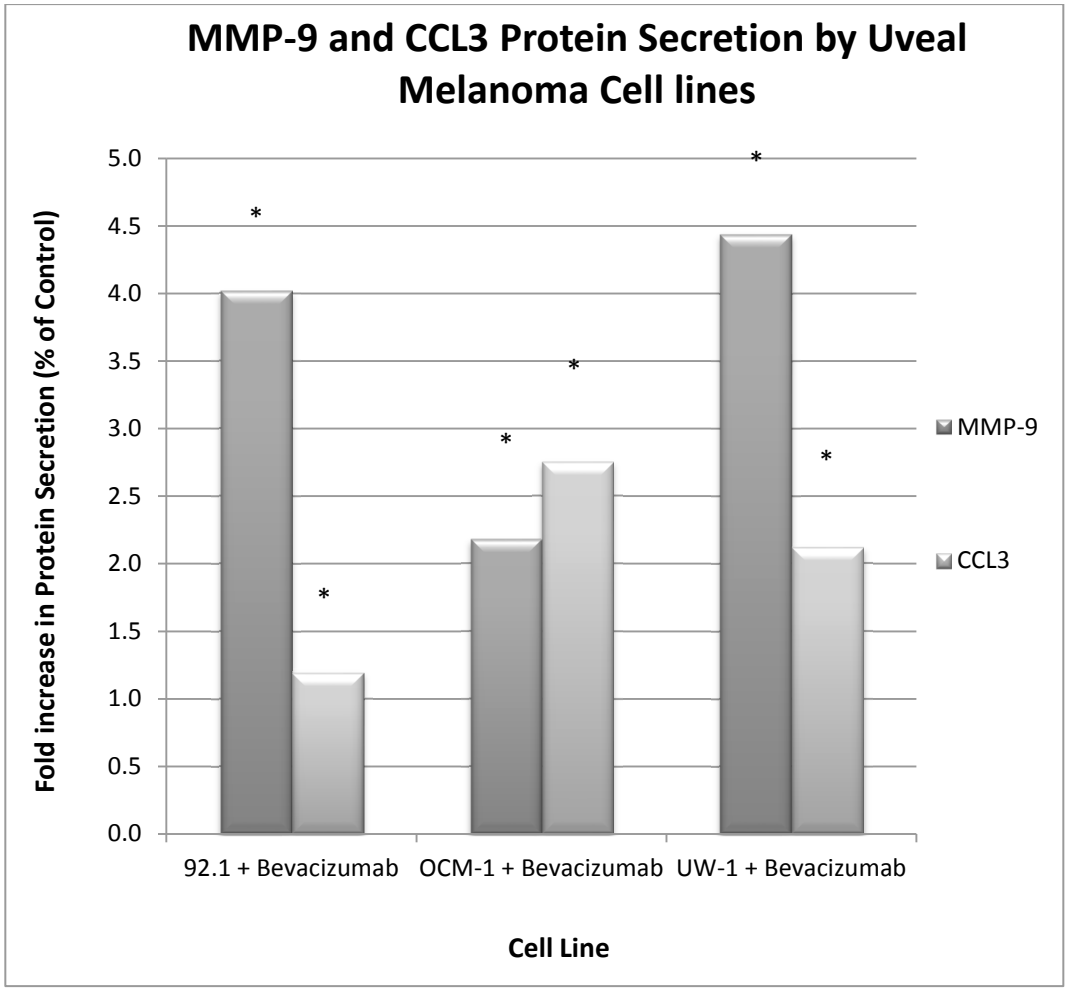

Figure 5. Secretion of CCL3 and MMP-9 by three uveal melanoma cell lines following treatment with 100µg/mL of bevacizumab. Results are shown as fold change in expression relative to the control. *$p < 0.05$; Student's t-test (compared to control).

Gene Knockdown using siRNA

Quantitative Real-Time Polymerase Chain Reaction (RT-qPCR)

Based on the results of the ELISA revealing that MMP-9 and CCL3 were ubiquitously upregulated following bevacizumab treatment, we decided to knockdown one of these cytokines to determine their effect on the functional abilities of the UM cells. MMP-9 is a downstream effector of the CCL3 signalling cascade[144]; we therefore silenced CCL3 to assess the impact of the loss of function of this pathway.

All qPCR data is expressed as fold change according to the previously described Pfaffl method, unless otherwise noted.

Transcriptional reduction of CCL3 was successfully accomplished using siRNA. After treatment, the fold reduction of CCL3 transcripts in the 92.1, OCM-1, and UW-1 UM cell lines, was 23, 21, and 23, respectively. To determine whether this was a specific downregulation, we compared ² -actin expression between the control and siRNA treated cells; no significant differences were detected for 92.1, OCM-1, or UW-1 (18.80 ± 0.19 vs. 19.19 ± 0.17; 18.66 ± 0.28 vs. 19.15 ± 0.16; 18.74 ± 0.31 vs. 18.90 ± 0.29, respectively; control vs. CCL3 siRNA; Student's t-test; $p > 0.05$ for all; all data expressed as Ct).

In order to ensure that the aforementioned downregulation was attributed to the specific sequence used and not the process of incorporating the siRNA, we compared ² -actin expression from one cell line that was transfected with scramble

sequence siRNA to the control; no significant differences were determined in ^{2} -actin expression for the UW-1 cell line (18.56 ± 0.04 vs. 18.86 ± .0.39; control vs. scrambled; Student's t-test; $p > 0.05$, for all; all data expressed as Ct).

Surprisingly, after bevacizumab treatment, transcription of CCL3 and MMP-9 were not drastically upregulated in any cell line despite the significant changes in protein secretion: fold changes in transcription for 92.1, OCM-1, and UW-1 cell lines were 1.95, 1.08, and 0.97 for CCL3 and 1.48, 1.67, and 1.02 for MMP-9, respectively. This result was consistent for VEGF-A transcript production, as well (1.14, 1.18, and 1.37, for 92.1, OCM-1, and UW-1, respectively).

Transcripts of the primary CCL3 receptor, CCR1, were detected in all three cell lines and this production increased slightly following bevacizumab treatment (1.20, 1.83, and 1.24 fold increase for 92.1, OCM-1, and UW-1, respectively).

The CCL3 siRNA caused a drastic reduction in MMP-9 transcript production in all cell lines, affirming our notion that CCL3 upregulation was, at least in part, responsible for the MMP-9 increase following bevacizumab treatment (6.5, 8.8, and 6.7 fold reduction, for 92.1, OCM-1, and UW-1, respectively).

Protein Expression

After confirming that CCL3 siRNA treatment successfully downregulated the transcription of CCL3, we investigated if the same were true for protein secretion.

With respect to CCL3 and MMP-9 secretion, only the UW-1 cell line passed the homogeneity of variance test ($p > 0.05$; Levene's statistic); for both proteins, the one-way ANOVAs were significant ($p < 0.05$). For the other cell lines, homogeneity of variance was violated ($p < 0.05$; Levene's statistic), and thus both Welch and Brown-Forsythe tests were used, both of which were statistically significant for all ($p < 0.05$). Based on these data, we concluded that there were significant changes in both CCL3 and MMP-9 secretion in all cell lines.

After siRNA treatment, CCL3 expression was significantly reduced in all cell lines compared to controls (0.937 ± 0.042 vs. 0.040 ± 0.010; 0.240 ± 0.022 vs. 0.025 ± 0.006; 0.073 ± 0.005 vs. 0.022 ± 0.002; control vs. CCL3 siRNA treated; 92.1, OCM-1, and UW-1, respectively; Dunnett's test; $p < 0.05$, for all; values OD; Figure 6). This confirms that our siRNA treatment successfully reduced CCL3 secretion.

We also determined that bevacizumab and CCL3 siRNA together (combination) treatment did not significantly alter CCL3 protein secretion compared to CCL3 siRNA monotherapy (0.050 ± 0.008 vs. 0.040 ± 0.010; 0.029 ± 0.001 vs. 0.025 ± 0.006; 0.018 ± 0.003 vs. 0.022 ± 0.002; combination vs. CCL3 siRNA treated; 92.1, OCM-1, and UW-1, respectively; Tukey post-hoc; $p >$

0.05 for all; values OD; Figure 6); however, the combination treatment significantly reduced CCL3 protein secretion relative to bevacizumab for all cell lines (0.050 ± 0.008 vs. 1.147 ± 0.090; 0.029 ± 0.001 vs. 0.900 ± 0.043; 0.018 ± 0.003 vs. 0.150 ± 0.008; combination vs. bevacizumab treated; 92.1, OCM-1, and UW-1, respectively; Tukey post-hoc; $p < 0.05$ for all; values OD; Figure 6).

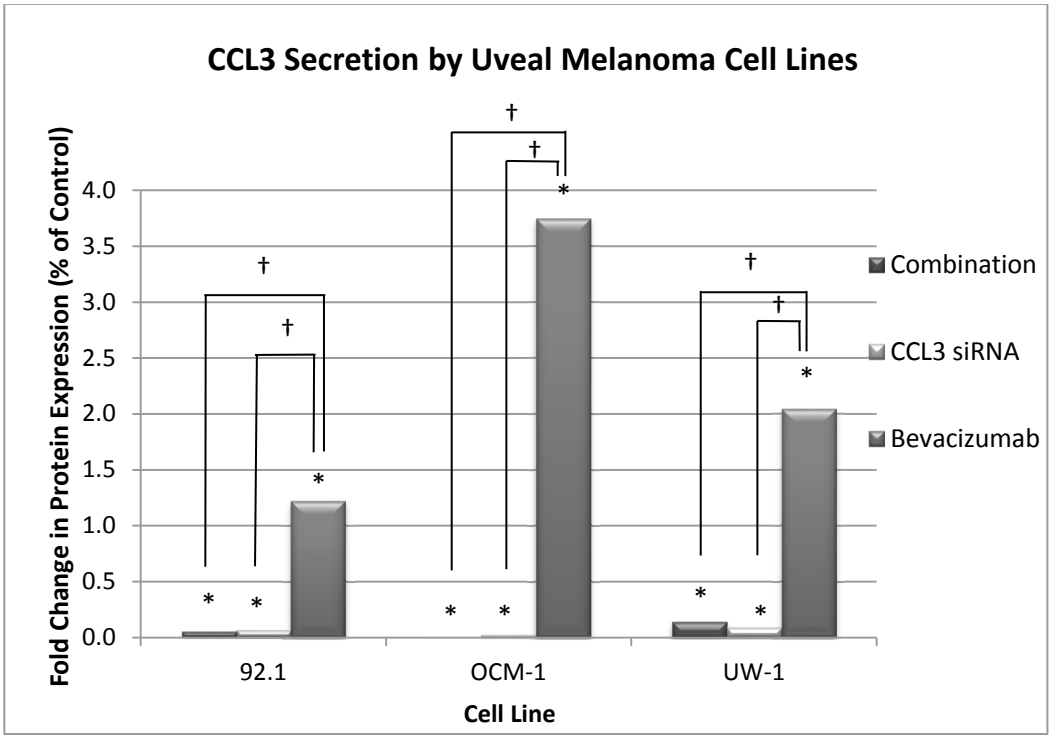

Figure 6. Secretion of CCL3 by three uveal melanoma cell lines following 100ug/mL of bevacizumab, CCL3 siRNA, or the combination of both treatments, as determined by ELISA. Results are shown as fold change in expression relative to the control. *p < 0.05; Dunnett's test (compared to control); †p < 0.05; Tukey post-hoc.

Next, we sought to determine if MMP-9 protein secretion was regulated by CCL3. This was confirmed by the finding that MMP-9 protein expression was significantly reduced after CCL3 siRNA compared to controls (0.630 ± 0.020 vs. 0.042 ± 0.010; 0.170 ± 0.022 vs. 0.028 ± 0.004; 0.570 ± 0.042 vs. 0.022 ± 0.006; control vs. CCL3 siRNA treated; 92.1, OCM-1, and UW-1, respectively; Dunnett's test; $p < 0.05$ for all; values OD; Figure 7).

Perhaps more importantly, the increase in MMP-9 following bevacizumab treatment was significantly reduced after CCL3 siRNA treatment (0.042 ± 0.010 vs. 1.752 ± 0.210; 0.028 ± 0.004 vs. 0.390 ± 0.056; 0.022 ± 0.006 vs. 1.764 ± 0.223; CCL3 siRNA treated vs. bevacizumab treated; 92.1, OCM-1, and UW-1, respectively; Tukey post-hoc; $p < 0.05$ for all; values OD; Figure 7). These results indicate that CCL3 siRNA is capable of offsetting the bevacizumab induced increase in MMP-9.

Unsurprisingly, based on the previously demonstrated influence of CCL3 on MMP-9 secretion, the results for MMP-9 mimicked those of CCL3; i.e., there were no significant differences in combination treatment compared to CCL3 siRNA monotherapy, and combination therapy significantly reduced MMP-9 secretion relative to bevacizumab therapy (0.062 ± 0.005 vs. 0.042 ± 0.010; 0.038 ± 0.003 vs. 0.028 ± 0.004; 0.028 ± 0.003 vs. 0.022 ± 0.006; combination vs. CCL3 siRNA treated; 92.1, OCM-1, and UW-1, respectively; Tukey post-hoc; $p > 0.05$ for all; and 0.062 ± 0.005 vs. 1.752 ± 0.210; 0.038 ± 0.003 vs. 0.390 ± 0.056; 0.028 ± 0.003 vs. 1.764 ± 0.223; combination vs. bevacizumab treated; 92.1,

OCM-1, and UW-1, respectively; Tukey post-hoc; $p < 0.05$ for all; values OD; Figure 7).

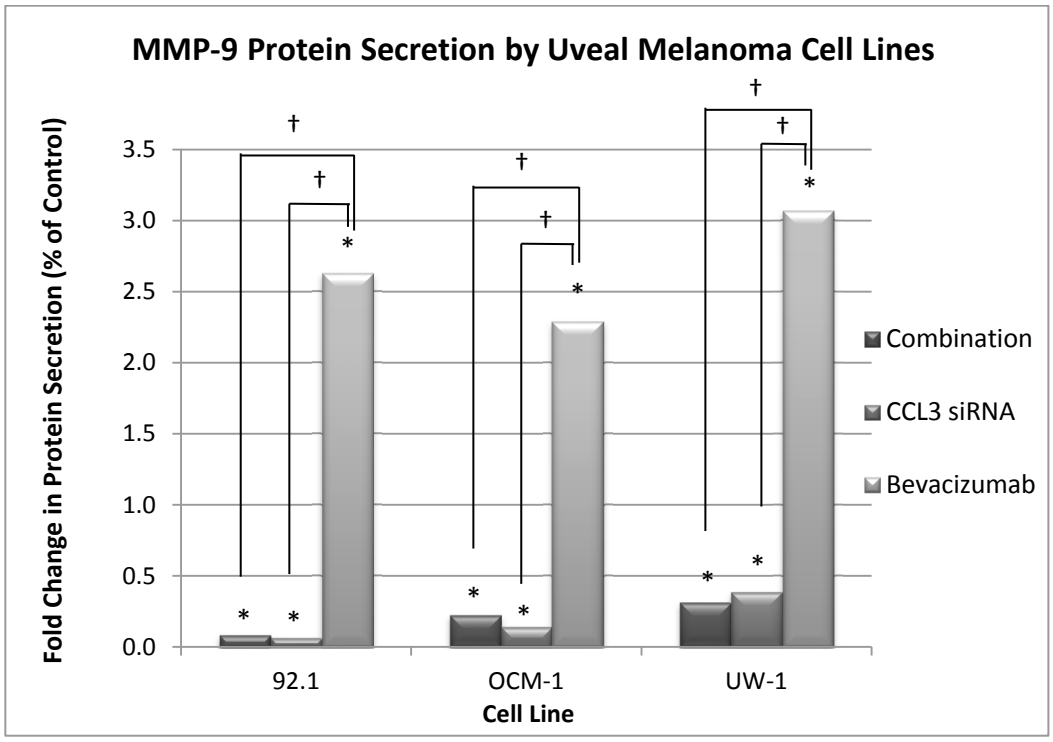

Figure 7. Secretion of MMP-9 by three uveal melanoma cell lines following 100ug/mL of bevacizumab, CCL3 siRNA, or the combination of both treatments, as determined by ELISA. Results are shown as fold change in expression relative to the control. *p < 0.05; Dunnett's test (compared to control); †p < 0.05; Tukey post-hoc.

Proliferation Assay

For the 92.1 cell line, the ANOVA test showed statistical significance and passed the homogeneity of variance test (ANOVA; $p < 0.05$ and Levene's statistic; $p > 0.05$). All conditions significantly reduced proliferation compared to the control (0.405 ± 0.012, 0.361 ± 0.026, 0.219 ± 0.013 vs. 0.509 ± 0.033; bevacizumab, CCL3 siRNA, and combination vs. control; Dunnett's test; $p < 0.05$ for all; all values OD; Figure 8). There were no significant differences between bevacizumab treatment and siRNA treatment; however, the combination of CCL3 siRNA and bevacizumab significantly reduced proliferation compared to both monotherapies (0.219 ± 0.013 vs. 0.405 ± 0.012 and 0.361 ± 0.026; combination vs. bevacizumab and siRNA; Tukey post-hoc; $p < 0.05$, for all; values OD; Figure 8).

Likewise, for the OCM-1 cell line, the ANOVA was statistically significant and it passed the homogeneity of variance test (ANOVA; $p < 0.05$ and Levene's statistic; $p > 0.05$). Only CCL3 siRNA alone and the combination treatment significantly reduced proliferation compared to the control (0.243 ± 0.024 and 0.238 ± 0.004 vs. 0.338 ± 0.027; siRNA and combination vs. control; Dunnett's test; $p < 0.05$ for all; values OD; Figure 8), and there were no significant differences between these two conditions (ANOVA; $p > 0.05$; Figure 8). Combination treatment and siRNA treatment also significantly reduced proliferation compared to bevacizumab treatment (0.243 ± 0.024 and 0.238 ± 0.004 vs. $.0395 \pm 0.040$; siRNA and combination vs. bevacizumab; Tukey post-hoc; $p < 0.05$ for all; values OD; Figure 8).

The ANOVA for UW-1 was also significant and complied with homogeneity of variance (ANOVA; $p < 0.05$ and Levene's statistic; $p > 0.05$). The results for UW-1 mimicked those of OCM-1; siRNA alone and combination treatments significantly reduced proliferation compared to the control, although they were not significantly different from each other (0.249 ± 0.004 and 0.236 ± 0.028 vs. 0.429 ± 0.018; siRNA and combination vs. control; Dunnett's test; $p < 0.05$ and Tukey-post hoc; $p > 0.05$ for all; values OD; Figure 8). Both CCL3 siRNA alone and combination treatments significantly reduced proliferation relative to bevacizumab treatment (0.249 ± 0.004 and 0.236 ± 0.028 vs. 0.450 ± 0.019; CCL3 siRNA and combination vs. bevacizumab; Tukey-post hoc; $p < 0.05$ for all; values OD; Figure 8).

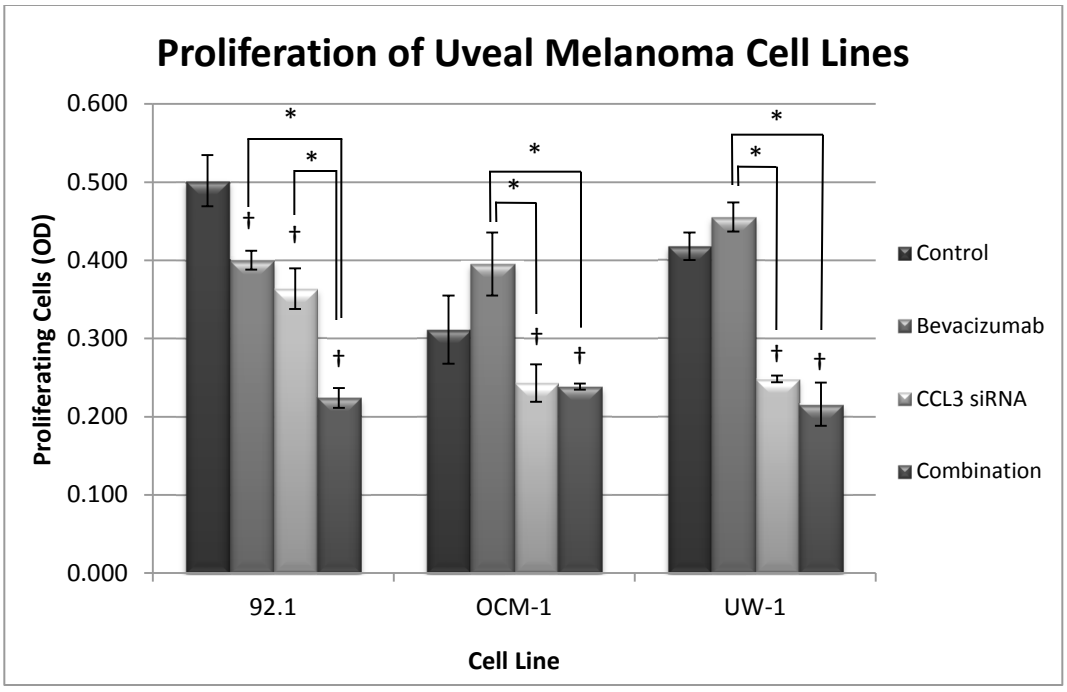

Figure 8. Graphical representation of the effects of different treatment modalities on the proliferative ability of three uveal melanoma cell lines, determined using a Sulforhodamine B based proliferation assay. *p <0.05, Tukey post-hoc; †p <0.05, Dunnett's test (compared to control); Bars: standard deviation.

Migration Assay

The 92.1 cell migration ANOVA was statistically significant and conformed with the homogeneity of variance (ANOVA; $p < 0.05$ and Levene's statistic; $p > 0.05$, respectively). All treatments significantly reduced the ability of 92.1 cells to migrate compared to the control (0.071 ± 0.003, 0.083 ± 0.004, and 0.039 ± 0.002 vs. 0.115 ± 0.003; bevacizumab, CCL3 siRNA, and combination

vs. control; Dunnett's test; $p < 0.05$ for all; values OD; Figure 9). In addition, combination treatment inhibited migration more than either bevacizumab treatment or CCL3 siRNA transfection alone (0.039 ± 0.002 vs. 0.071 ± 0.003 and 0.083 ± 0.004; combination vs. bevacizumab and CCL3 siRNA; Tukey post-hoc; $p < 0.05$ for all; values OD; Figure 9). There was no statistical difference in migration of cells between bevacizumab treatment and CCL3 siRNA transfection (Tukey post-hoc; $p > 0.05$).

The ANOVA for OCM-1 was significant and passed the homogeneity of variance test (ANOVA; $p < 0.05$ and Levene's statistic; $p > 0.05$, respectively). For this cell line, only bevacizumab alone and the combination treatment significantly reduced migration relative to the control (0.049 ± 0.005 and 0.041 ± 0.004 vs. 0.117 ± 0.014; bevacizumab and combination vs. control; Dunnett's test; $p < 0.05$ for all; values OD; Figure 9). No other statistically significant differences were noted (Tukey post-hoc; $p > 0.05$).

As with the other two cell lines, the ANOVA for the UW-1 cell line was significant and passed the homogeneity of variance test (ANOVA; $p < 0.05$ and Levene's statistic; $p > 0.05$). Both the CCL3 siRNA transfection and combination treatment reduced migration relative to the control (0.076 ± 0.003 and 0.036 ± 0.001 vs. 0.141 ± 0.040; CCL3 siRNA and combination vs. control; Dunnett's test; $p < 0.05$ for all; values OD; Figure 9). There were no other statistically significant differences (Tukey post-hoc; $p > 0.05$).

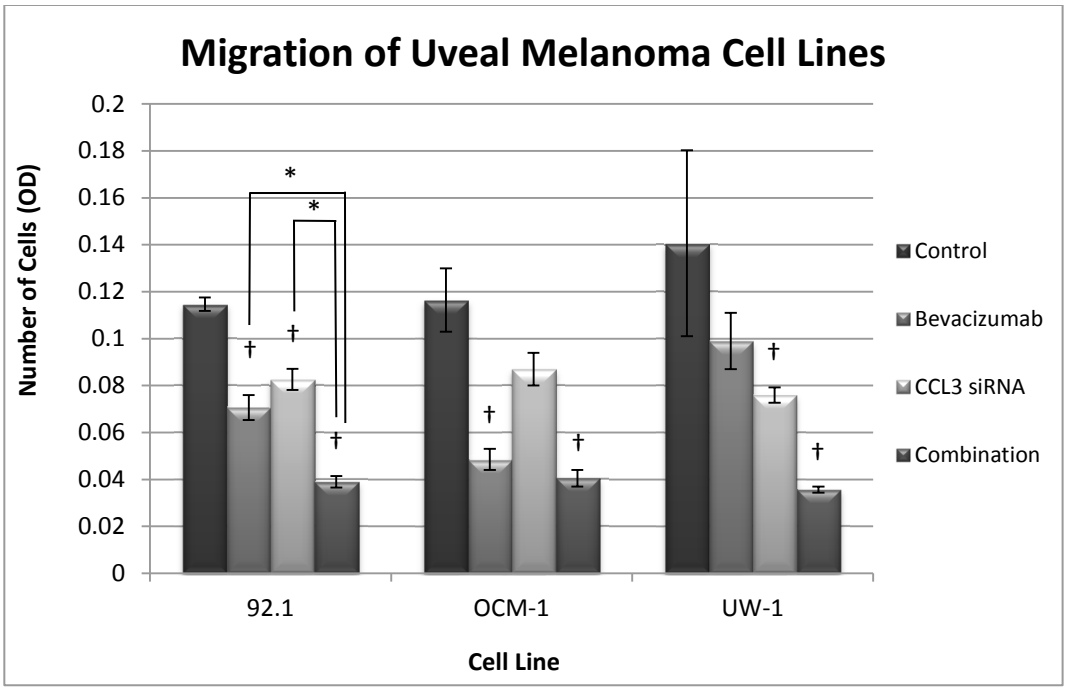

Figure 9. Graphical representation of the effects of different treatment modalities on the migratory ability of three uveal melanoma cell lines, using transwell migration assays with FBS as a chemoattractant. *p <0.05, Tukey post-hoc; †p <0.05, Dunnett's test (compared to control); Bars: standard deviation.

Invasion Assay

The ANOVA for the 92.1 cell line was significant and it passed the homogeneity of variance test (ANOVA; $p < 0.05$ and Levene's statistic; $p > 0.05$). Treatment with CCL3 siRNA significantly reduced invasion relative to the control (0.127 ± 0.006 vs. 0.245 ± 0.018; CCL3 siRNA vs. control; Dunnett's test; $p <$

0.05; values OD; Figure 10). In addition, both the combination treatment and CCL3 siRNA monotherapy significantly reduced invasion relative to bevacizumab treatment (0.188 ± 0.002 and 0.127 ± 0.006 vs. 0.265 ± 0.036; combination and CCL3 siRNA vs. bevacizumab; Tukey post-hoc; $p < 0.05$ for all; values OD; Figure 10).

For the OCM-1 cell line, although Levene's statistic indicated homogeneity of variance, the ANOVA was non-significant (Levene's statistic; $p > 0.05$ and ANOVA; $p > 0.05$). Despite non-significance, the OCM-1 cell line followed the same invasion pattern as the 92.1 cell line, according to the different treatment modalities (Figure 10).

As for the 92.1 cell line, the ANOVA for the UW-1 cell line passed the homogeneity of variance test and was statistically significant (Levene's statistic; $p > 0.05$ and ANOVA; $p < 0.05$). Likewise, CCL3 siRNA treatment significantly reduced invasion relative to the control, and this treatment also significantly reduced invasion relative to bevacizumab treatment (0.106 ± 0.008 vs. 0.145 ± 0.003 and 0.162 ± 0.012; siRNA vs. control and bevacizumab; Dunnett's test and Tukey post-hoc, respectively; $p < 0.05$, for all; values OD; Figure 10). Finally, combination treatment significantly reduced invasion relative to bevacizumab treatment monotherapy (0.121 ± 0.011 vs. 0.162 ± 0.012; combination vs. bevacizumab; Tukey post-hoc; $p < 0.05$; values OD; Figure 10).

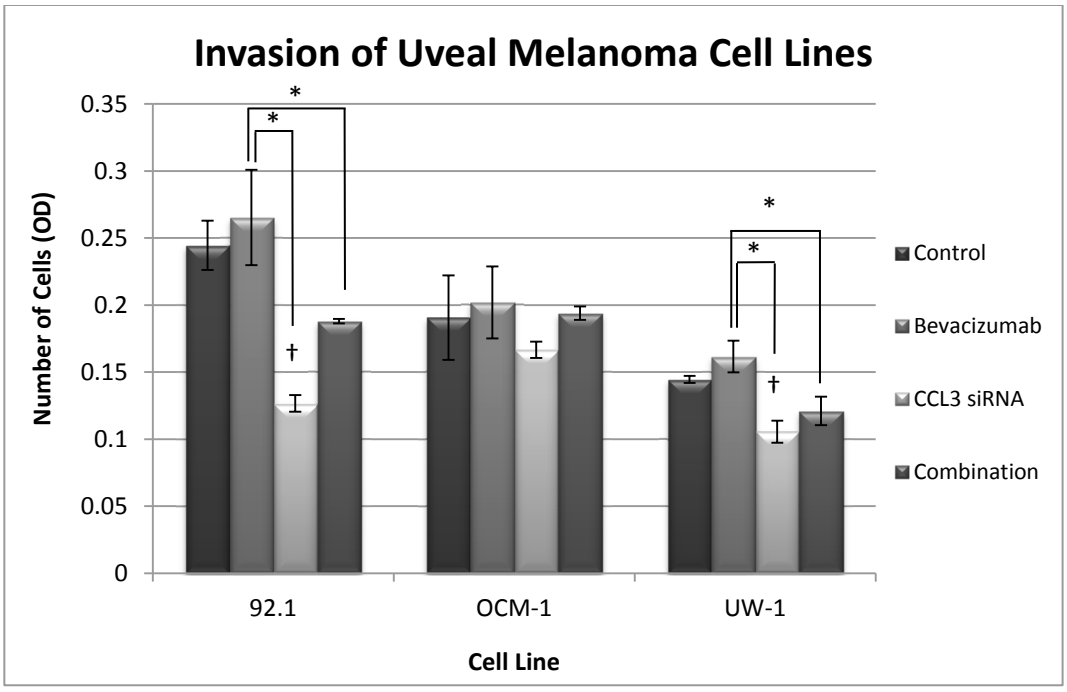

Figure 10. Graphical representation of the effects of different treatment modalities on the invasive ability of three uveal melanoma cell lines. *p <0.05, Tukey post-hoc; †p <0.05, Dunnett's test (compared to the control); Bars: standard deviation.

Discussion

In this chapter, we investigated the consequences of bevacizumab administration and subsequent sequestering of VEGF-A on the functional abilities of and protein secretion by three UM cell lines. We determined that treating our UM cell lines with bevacizumab successfully inhibited activation of the primary VEGF-A receptor, VEGF-R2. It was expected that blocking this signal cascade would cause a substantial, global reduction of all functional abilities, as shown in other malignancies, including breast cancer and VEGF-R2+ melanoma cell lines[145,146]. Our hypothesis was also supported by the positive growth and migratory effects that VEGF signalling imparts on endothelial cells[75]. Surprisingly, despite abundant and ubiquitous production of both VEGF-A and its receptor, usurping VEGF-A with bevacizumab had only moderate inhibitory effects on the functional capacity of UM cells. Furthermore, VEGF-A inhibition caused a slight, non-significant increase in the invasive ability of our cell lines and yet negatively influenced migration. This is in contrast to a previous study showing that bevacizumab significantly reduced the invasive ability of one human and one mouse uveal melanoma cell line[106]. While this discrepancy is peculiar, it is of note that the cell line used in the aforementioned study (Mel290) was different than the three used in our study. Due to the heterogeneous nature of malignant cells in general, and in particular UM cells, this result is not entirely surprising, and may be related to differing internal signalling pathways. For instance, it has been shown that OCM-1 (a cell line used in the present study) produces high levels of notch signalling intermediates, whereas Mel290 expresses

low levels[147]. Moreover, it has been demonstrated in bladder carcinoma and glioblastoma that high DII4/Notch signalling may confer resistance to anti-VEGF therapies, thus offering a potential explanation for the aforementioned discrepancy[148,149].

At first glance, it appears paradoxical that migration was significantly reduced in two cell lines after bevacizumab treatment and yet invasion was not significantly affected, considering that invasion is a process dependent on the former. A potential explanation is provided by recent evidence demonstrating that autocrine VEGF-A signalling through VEGF-R2 in prostate cells can enhance migration[150]. Thus, in our study, we hypothesize that bevacizumab blocked this signalling cascade which subsequently reduced migration; however, bevacizumab also increased MMP-9 secretion, permitting easier digestion of the basement membrane, which is an inherent impediment to migration in invasion assays[150]. In short, even though our UM cells may be less capable of migrating than controls, they digest the basement membrane more readily, and thus the negative implications of bevacizumab on migration are concealed in the invasion assay.

Based on our data, we were forced to reject the hypothesis that bevacizumab would universally inhibit the functional abilities of our cell lines. The current results strongly suggest that acceptance of the null hypothesis is a consequence of compensatory mechanisms mitigating bevacizumab's effects, as two cytokines, CCL3 and MMP-9, were significantly upregulated in the cultured media of all cell lines following treatment. MMP-9 is a collagenase responsible for digesting the extracellular matrix, which is a critical process for migration,

invasion, and tumor growth in vivo. Conceptually, the upregulation and increased secretion of MMP-9 is a plausible reason for the increase in invasive ability that was noted in our study. Although there was no dramatic increase in MMP-9 transcription, it is probable that the increased secretion was a result of post-transcriptional modification, as shown in breast cancer[151]. In the 24-hours that these cells were exposed to bevacizumab, we hypothesize that post-translation and secretory changes were activated as initial cellular responses as these processes occur more rapidly than transcriptional alterations. In addition, it has been demonstrated that high MMP-9 expression in UM tumors is associated with poor prognosis[152].

CCL3, also known as macrophage inflammatory protein 1 alpha, binds to two receptors (CCR1 and CCR5) and is responsible for orchestrating acute and chronic inflammatory responses[153]. Studies report that CCL3 is present in some cutaneous melanoma tumors and in the vitreous of eyes with UM; however, to the best of our knowledge, the present study is the first evidence that UM cells produce CCL3 in culture[154,155]. Based on the fact that our cells produce both CCL3 and CCR1 and that CCL3 signalling is an upstream regulator of MMP-9, we considered that the increased secretion in MMP-9 was a consequence of CCL3/CCR1 signalling[144]. This was confirmed as CCL3 inhibition abolished the bevacizumab induced increase in MMP-9 secretion. Thus, we hypothesize that when the UM cell lines sense a decrease inVEGF-R2 activation following bevacizumab treatment, they respond by upregulating CCL3 secretion. Next, secreted CCL3 activates CCR1 on the host and neighbouring cells, which

subsequently increases MMP-9 production. By employing this cascade, cells degrade the extracellular matrix more readily, thereby potentiating dissemination with the ultimate goal of a return to normoxic conditions. It has also been demonstrated that the ECM can harbour biologically active VEGF isoforms; thus, increased MMP-9 production may also release ECM-bound VEGF in vivo[156].

In general, dual inhibition of CCL3 and VEGF-A had a much greater inhibitory effect on the functional abilities of all three cell lines. With respect to proliferation, dual inhibition in all cell lines resulted in greater inhibition than bevacizumab monotherapy. This is not surprising, as it has been demonstrated that CCR1 signalling in multiple myeloma cells induces proliferation[157]. Thus, by inhibiting both VEGF and CCR1 pathways, it is expected that proliferation would decrease substantially compared to solely inhibiting VEGF.

Considering migration, only combination treatment was capable of significant reduction relative to the control across all cell lines. However, for different cell lines, migratory inhibition was significant with either bevacizumab or CCL3 siRNA monotherapies. Although both VEGF-R2 and CCR1 signalling pathways have been shown to be powerful mitogens, differing internal response mechanisms may account for this discrepancy[157,158].

Although statistical significance was not always reached, all cell lines followed the same invasion pattern in response to the different treatment modalities: bevacizumab increased invasion, CCL3 inhibition decreased invasion, and the combination decreased invasion, yet not to the same level as CCL3

inhibition. These results add further evidence that bevacizumab induced upregulation of CCL3 modulated the increase in invasion through, at least in part, MMP-9 secretion. In summary, VEGF-A inhibition increased MMP-9 secretion via the CCL3/CCR1 signalling axis, which subsequently amplified invasion. Inhibiting CCL3 reduced baseline levels of MMP-9 and negatively impacted invasion, and thus when used in combination, the inverse effects of the two treatment modalities on MMP-9 levels resulted in a slight reduction in secretion and invasion compared to baseline.

In vivo, the increased production of CCL3 following bevacizumab treatment may have greater negative effects beyond MMP-9 and invasion augmentation. For instance, CCL3 is a potent macrophage attractant and, in UM, lymphocytic and macrophage infiltration are associated with poor prognosis[159,160]. In addition, it has been demonstrated that CCL3 enhances VEGF production in macrophages, which further potentiates the compensatory process by which UM cells may counteract a VEGF-A-inhibited environment in vivo[161]. Thus, considered anthropomorphically, UM cells produce VEGF for autocrine signalling as well as to facilitate the formation of blood vessels in order to support continual growth. When this process is challenged or inhibited, they respond by upregulating CCL3 production, which re-establishes autocrine signalling and increases MMP-9 production. Amplification of MMP-9, in turn, allows UM cells to degrade the extracellular matrix and escape the VEGF-A inhibited environment as well as releasing any ECM-bound VEGF. In addition, CCL3 attracts

macrophages to the tumor where they produce VEGF-A and other cytokines, thus circumventing the VEGF-A usurping.

This study is not the first illustrating that bevacizumab can cause compensatory upregulation of pro-angiogenic and metastatic factors. For instance, colorectal cell lines under chronic bevacizumab exposure showed upregulation of VEGF-A, -B, -C, and P1GF[141]. Further, in the same study, it was demonstrated that bevacizumab significantly increased migration and invasion in these chronically treated cells[141]. This atoning phenomenon also extends beyond malignant cells, as it was discovered that treating conjunctival neovascularization with subconjunctival bevacizumab injections can significantly increase the presence of specific cytokines and growth factors in tears[162]. Also, significant increases in a similar cytokine profile in the aqueous humor are evident after intravitreal bevacizumab injections for the treatment of diabetic retinopathy[142].

In summary, in this chapter we showed that bevacizumab inhibited the para and autocrine activation of VEGF-R2 in our UM cell lines, which resulted in a moderate reduction in the proliferative and migratory abilities, yet had an inverse effect on invasion. Future studies should focus on elucidating shared molecular biology pathways that enable cells to defy growth factor inhibition. Following the acquisition of such knowledge, a plausible approach would be to inhibit these internal signalling intermediates, with the intention of preventing cells from inducing compensatory mechanisms.

Conclusion

It is evident that even the most promising and conceptually sound pharmaceutical intervention strategies can incur unwanted and unpredictable side-effects. The ideology that inhibiting a tumor's blood supply undeniably conforms with the aforementioned declaration; however, in UM cell lines, abrogating VEGF-A induces secretory changes in factors that can promote the accumulation of macrophages, which are indicators of poor prognosis, and gelatinases that facilitate hematogenous spreading. Inevitably, dual or multiple therapies are likely required to completely sever all potential compensatory avenues that malignant cells can exploit in response to pharmacological insults. Physicians and researchers alike should be forewarned that exogenous treatments can activate countervailing pathways in highly ploidy cells resulting in the paradoxical generation of more aggressive phenotypes.

Chapter 3: VEGF-A Expression as a Prognostic Marker in a Rabbit Model of Uveal Melanoma

Introduction

Identifying prognostic markers has become an important pursuit of cancer researchers. Generally, these markers serve three valuable purposes: 1) they allow researchers to identify potential therapeutic targets, 2) high and low risk patients can be apportioned and treatment aggressiveness appropriately tailored, and 3) disease pathogenesis may be elucidated potentiating future discoveries.

In UM, many prognostic indicators of varying significance have been discovered, including NM23, monosomy 3, and TILs[61,163,164]. Based on the ability of VEGF-A inhibition to encumber some of the functional abilities of our UM cell lines, we were interested in investigating whether or not expression carries significance in an in vivo setting. To investigate this hypothesis, we immunostained for VEGF-A in UM specimens from a rabbit model. Second, we developed a novel, automated immunohistochemical grading algorithm using ImageJ Software (NIH) to identify positively stained tumor areas. Finally, we determined whether VEGF-A expression correlated with the development of metastasis in these animals.

Materials and Methods

Uveal Melanoma Rabbit Model

Tissue was obtained from two UM rabbit models (n = 27), explicit details of which have been published elsewhere[165,166]. Only tissue from control rabbits was used in our experiments. Briefly, 1×10^6 92.1 UM cells were cultured and injected into the suprachoroidal space of 3kg female New Zealand albino rabbits (Charles River Canada, St-Constant, Quebec, Canada). Due to the fact that these UM cells originated from a human patient, it was necessary to immunosuppress these animals to avoid MHC Class I rejection, and this was accomplished using daily Cyclosporine A injections (Novartis Pharma AG, Basel, Switzerland; 260mg/m^2). The UM cells were allowed to proliferate and develop into tumors for up to 12 weeks in these immunosuppressed animals before sacrifice. After necropsy, eyes were enucleated and fixed in 10% formalin for further processing. Lung and liver tissue were examined both macroscopically and, after staining with hematoxylin and eosin (H&E), microscopically for the presence of metastasis. If a pathologist identified one or more metastatic nodules either macro- or microscopically, irrespective of size, then that tissue was immunostained for the melanoma specific marker HMB-45[167]. Only if the suspected mass was positive for this marker was the animal considered to be afflicted with metastasis; otherwise, the animal was deemed metastasis free.

Immunohistochemistry for VEGF-A

After fixation, rabbit eyes were embedded in paraffin, and 2µm sections were mounted onto glass slides. For the purpose of this study, it was important to minimize as many variables that may affect staining quality as possible. To this end, we chose a fully automated process: tumors were stained with a monoclonal VEGF-A antibody (Novus Biologicals; Littleton CO, USA) using the Ventana Benchmark LT (Ventana Medical Systems, Inc.) fully automated machine. This process is described in greater detail in chapter 1 and elsewhere[128]. Briefly, slides were incubated with the VEGF-A antibody (Novus Biologicals; 1:500) for 30 min at 37°C, followed by the application of the biotinylated secondary antibody for 8 min at 37°C, then the avidin-streptavidin enzyme conjugate complex for 8 min at 37°C. Finally, the antibodies were detected with fast red chromogenic substrate and counterstained with hematoxylin. Placental tissue was used for the positive control and the process was repeated except the primary antibody was omitted for the negative control.

Image Acquisition

All images were obtained using the Olympus BX43 microscope with the DP21 camera (Olympus Canada Inc.; Richmond Hill, ON, Canada) with the following parameters: ISO 200, white balance 5500k, shutter speed 1/50 sec, 200x magnification, 1600 x 1200 TIFF format. Before taking the first image, the bulb

was turned on and the apparatus was allowed to warm up for a minimum of 15 minutes.

Inclusion criteria for the rabbit samples were the following: macroscopic primary tumor, definitive conclusion with respect to presence of metastasis, and a tumor large enough that three representative images occupying a minimum of 90% of the image at a magnification of 200 × with minimal overlap between the images. The microscope operator was blinded to the metastasis status of the rabbit samples. A pathologist confirmed that the positively stained cells were primarily UM cells. In addition, brightfield (no specimen, light passing through the lens) and darkfield (light source on, shutter closed) images were obtained for image processing and correction purposes.

Immunostaining Quantification

Immunostaining quantification was performed using the ImageJ (NIH) software. We selected this software in part because of its freeware nature and the availability of plugins and community-created java code. In order to create a unique algorithm for quantifying immunostaining in UM specimens, we parsed java code freely provided by other users, used the program's built-in modules, and created our own code when existing code was either unavailable or inapplicable.

The first step in our quantification algorithm was to correct the image for bright and darkfield abnormalities; this was accomplished using the brightfield and darkfield images and the Calculator_Plus plugin and code generated by G.

Landini[168]. Simply, the algorithm subtracts the bright and darkfield images from each experimental image, eliminating the influence of the microscope and light source, thus generating a more accurate representation of the stained slide.

Next, in order to further distinguish stained from unstained tissue, image contrast was enhanced using the built-in function. Every image was processed using the same enhancement procedure.

After contrast enhancement, the Color_Deconvolution plugin was used to separate colors according to their three dimensional red green blue (RGB) spectral properties[169]. Custom color vectors were developed by trial and error to ensure optimal separation between the blue hematoxylin nuclei counterstain and the positive pink immunostain. This Color_Deconvolution plugin separates the original images into three new images each containing only one of the custom color vectors that we provided. We isolated the image representing the pink, positive immunostaining and rendered it binary. The built-in Watershed plugin was used to identify and separate cells that were in contact with each other and thus did not previously have defined borders. Finally, we used the built-in Analyze Particles feature to identify all positive cells, which generated two outputs: the number of positively stained cells and the fraction of the entire image that was positively stained. Throughout the entire process, a pathologist was continually consulted to ensure that the subsidiary images were representative of the positive cells as viewed under light microscopy. The java code in its entirety can be found in Appendix I. All images were processed in an identical way using this algorithm.

Statistical Analysis

The number of positive cells and the percentage of the total image that stained positive were averaged for all three images from each rabbit. A student t-test was performed comparing the percentage and number of positive cells in rabbits that developed metastases and those that did not. Next, in order to determine if positive VEGF-A staining could be used to predict metastasis, a binary logistic regression was performed using the presence of metastasis as the dependent variable and the average cell count and average positive staining fraction as independent variables using SPSS ver. 20 (IBM). The Hosmer-Lemeshow test was performed to determine goodness-of-fit of the model. Data are presented as means ± SD.

Results

Immunohistochemistry Quantification

Of the 27 rabbits that met the inclusion criteria, 18 rabbits did not have metastases and nine had confirmed metastatic nodules. The custom immunostaining quantification algorithm successfully isolated positively stained cells and rendered cell counts and area stained for all images (Figure 11).

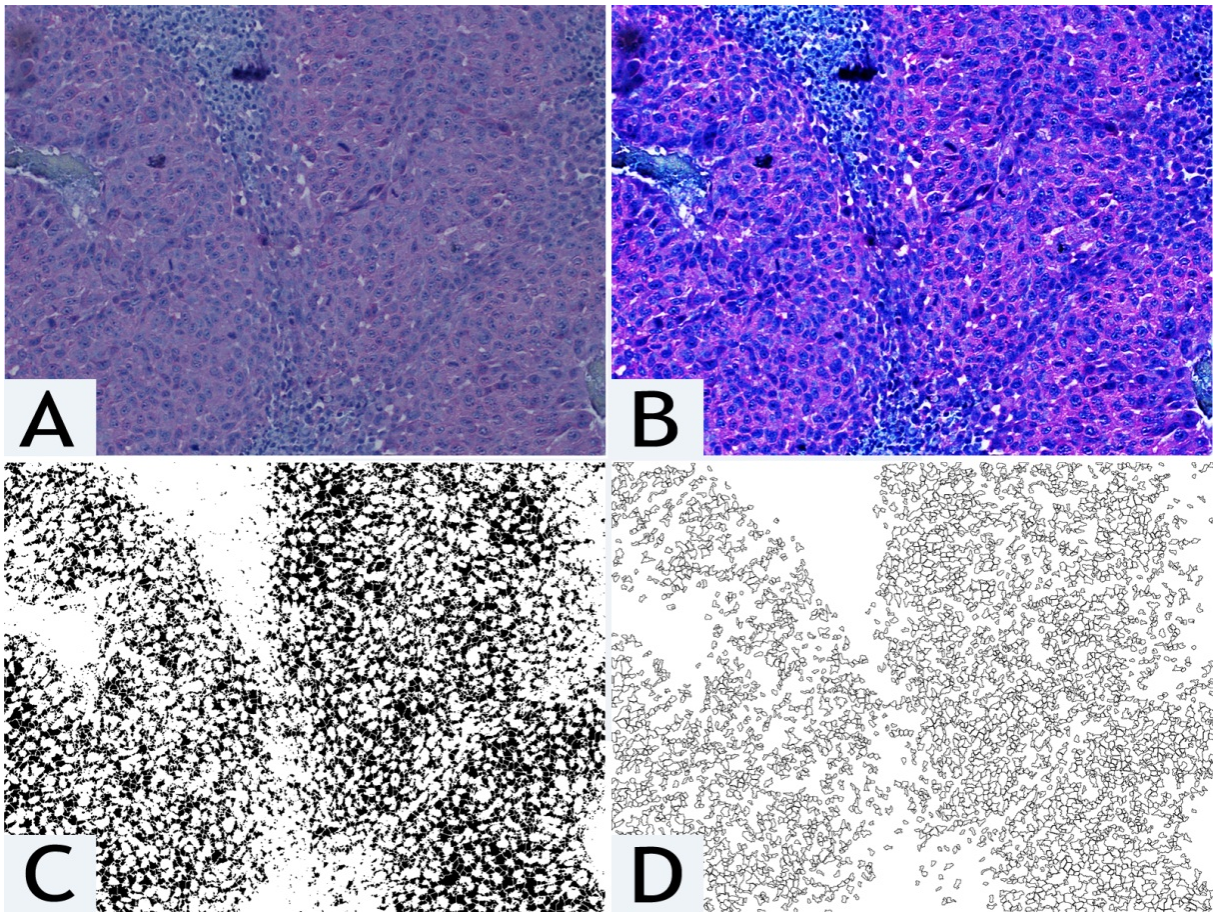

Figure 11. Representative example of the VEGF-A immunostaining quantification algorithm for rabbit tumors. A. The original image immunostained for VEGF-A expression (pink), and counterstained with hematoxylin (blue). B. The image after correction for bright and darkfield abnormalities and enhancement. C. The binary image after color deconvolution, which isolated only the positively stained area. This image was used for the quantification of the positive immunostained area. D. The image after using the watershed plugin and analyzing and outlining positive cells. This image was used for the quantification of the number of positively immunostained cells. Magnification = 200×.

The number of positive cells and the areas stained were averaged for each rabbit. For all images, only the cytoplasm was positive for VEGF-A expression. In the non-metastasis group, the average positive cell count was 376 ± 75 and the average positive staining area was 2.86% ± 0.91%. In the metastasis group, the average positive cell count was 2483 ± 414 and the average positive staining area was 18.64% ± 4.44%. Both differences were statistically significant ($p < 0.05$).

Binary logistic regression using average positive cell count and average positive staining area for VEGF-A resulted in a statistically significant model for predicting metastasis ($p < 0.05$). Without the input of variables (beginning block), assuming that no rabbits had metastases, the model was 63.3% accurate. With the introduction of positive area and positive cell count, the model accuracy increased to 83.3% (Table 3). Hosmer-Lemeshow was non-significant, indicating that the model is a good fit ($p > 0.05$).

Table 3. Predictive value of VEGF-A immunostaining for the presence of metastasis in rabbit uveal melanomas with binary logistic regression.

[a]No variables added to the regression analysis (beginning block).

[b]Average positive area and average positive cell count added to the regression analysis. *p < 0.05. †p < 0.05.

		Average Positive Area ± SD†	Average Positive Cells ± SD†	Predicted[a]			Predicted[b]		
				Metastasis		Percentage Correct	Metastasis		Percentage Correct
				No	Yes		No	Yes	
Metastasis	No	2.86% ± 0.91%	376 ± 75	0	11	0.0	10	1	90.9
	Yes	18.64% ± 4.44%	2483 ± 414	0	19	100.0	4	5	78.9
Overall (Percentage)				63.3			83.3*		

Discussion

In this penultimate chapter, we determined that the expression of VEGF-A in primary UM tumors from a rabbit model could retrospectively predict the development of metastases. Using a custom java script, we objectively quantified both the number of cells and the average area that stained positive in three representative images from each rabbit (n = 27). Using this data, we could retrospectively predict with over 83% accuracy which animals developed metastasis. To the best of our knowledge, this is the first time that VEGF-A expression has been quantified in a rabbit model of UM. The impetus behind our decision to assess expression in a rabbit model was twofold: 1) to determine if expression was related to metastasis in as homogeneous a population as possible and, 2) provide evidence and support for this technique prior to expending precious patient samples.

Only the non-metastasis group had tumors that were completely void of VEGF-A expression, suggesting that this protein may be important in the initial steps of the metastasis cascade. However, there was one tumor in the metastasis negative group that had VEGF-A expression comparable to the highly positive samples from the metastasis group. We considered two possibilities for this anomaly: either there were occult tumors that were not identified on macro or micro analysis of the organs or the animal was sacrificed too early for the cells to have spread to other organs. Initially, we considered that the latter was more likely, as this particular animal was sacrificed in week three of the model, a time-point at which animals are rarely afflicted with metastases[165,170]. Therefore, based

on this information, we ran a regression analysis using week sacrificed as a variable, but this did not yield significant associations with metastasis nor did this data significantly contribute to the overall model (data not shown). As for the former hypothesis, although we meticulously scoured all organs for the presence of metastasis, it is often very difficult to identify single metastatic cells or even small clusters of cells despite the immunohistochemical markers at our disposal[46,167]. Thus, it is possible that metastases were present, but went undetected.

When we began this study, it was not obvious that there would be inter-animal differences in VEGF-A expression, as we have previously shown in this thesis that the 92.1 cell line injected into the animals produces copious amounts of this pro-angiogenic cytokine in culture. Although we controlled for as many variables as possible, including using animals that were genetically similar, using a clonally expanded cell line, and performing strictly regimented injection techniques, inconsistencies in any of these may account for these differences. The fact that not all animals developed identical intraocular tumors or metastasis at the same time, or even during the same week, exemplifies these apparent differences. Moreover, if we consider that, unlike UM development in humans, disease inception can be definitively determined in the rabbits, changes in the primary tumor prior to metastasis, such as VEGF-A expression, may indicate a greater importance in the metastatic cascade. With respect to the human disease, changes in the primary tumor may have occurred after metastatic seeding, thus its implications for metastatic disease may be minimal.

In a previous mouse model of UM, it was discovered that peak and average VEGF levels in serum strongly correlated with the presence and number of metastatic nodules[92]. This same group also showed that bevacizumab suppresses UM primary tumor growth even though the drug was administered via intraperitoneal injection; therefore, it is likely that intraocular injections would have a greater effect on tumor growth[106]. Based on our results and these aforementioned studies, there is strong evidence that VEGF-A is involved in UM tumor growth and influences metastatic development. Therefore, analysis of VEGF-A expression in human tissue and patients is warranted.

There are several limitations to the present study. For instance, this study was performed retrospectively using a relatively modest sample size, which limits generalizations based on our data; our results would invariably benefit from corroboration by other studies that implement a larger sample size using a similar model. One of the major benefits of our quantification algorithm, however, is that it enables direct comparisons between studies, allowing for accurate meta-analyses. Ideally, future studies should apply this algorithm to cells obtained using fine-needle aspiration, with the intention of prospectively identifying rabbits most likely to develop metastasis.

Conclusion

To the best of our knowledge, this study is the first to use an automated immunostaining quantification to evaluate UM specimens from a rabbit model. In addition, this is the only study that has examined VEGF-A expression in primary tumors from an animal model and retrospectively correlated positivity with the presence of metastasis. Although results extrapolated from animal models should always be considered with at least some reservation, the outcomes of the present study offer evidence and support for investigating the relationship between VEGF-A expression and metastasis in human specimens.

Chapter 4: VEGF-A Expression as a Prognostic Marker in Uveal Melanoma Patients

Introduction

There are several studies reporting the prognostic significance of VEGF-A immunostaining in UM; however, there is a lack of consensus over the results. For instance, in 2000, Sheidow et al. reported that broad expression of VEGF in 47 UM tumors did not correlate with metastasis[94]. Another study reports that in 49 UM samples, staining was present, albeit weak, in less than a quarter of samples[93]. Yet a third study with the largest case series including 100 patients, demonstrated that 84% of posterior UMs had VEGF-A expression and that expression was associated with metastasis[171]. Adding to these contradictory and conflicting results, or perhaps an underlying contributor to them, is the fact that all three studies used different, subjective immunostaining grading criteria: a 7-point scale, a 3-point scale, and a disparate 3-point scale, respectively, all of which considered both staining distribution and intensity.

Recently, with the advent of new computer software and automated immunostaining techniques, novel objective quantification methods are becoming more prevalent. The major advantages of such systems are that they reduce or eliminate subjectivity from the analysis; for instance, most staining procedures, such as in the latter two articles mentioned above, incorporate a scale that requires the differentiation between less than and greater than 50% positivity. Short of actually counting the positive cells, requiring a pathologist to make such a

determination in samples that may contain hundreds of cells is likely to generate inter- and intra-observer discrepancies. The aforementioned distinction is not trivial or semantic; for instance, according to the College of American Pathologist guidelines, only a score of 3+ for HER2 staining in breast cancer samples, defined as complete, intense, and uniform staining in > 30% of cells, will result in the recommendation to receive trastuzumab therapy[172]. This system is inherently subjective as a pathologist is required to estimate if 30% of cells are positive. Also, because the 30% sanction is based on studies that involved estimations, even if the pathologist was inclined to actually count all positive cells doing so would render the recommendation a non-sequitur. This issue, in addition to discrepancies in immunohistochemistry staining interpretation, have raised concerns regarding the legitimacy of this selection process[173,174]. In order to compensate for several of these limitations, automated computer-assisted assessment programs have been developed, and studies conclude that they can increase interobserver reproducibility and provide more dependable results[172]. An additional advantage to using an automated program is that the computer may be capable of detecting and distinguishing between similar color spectra of which the human eye cannot.

Most immunostaining appraisals involve an assessment of staining 'intensity', despite the fact that very few immunostains, with the exception of Fuelgen for DNA and phalloidin for actin, are stoichiometric[175]. As a result, immunostaining intensity can be affected by a variety of factors, including formalin fixation, storage conditions, and paraffin coating, among others[176,177].

Because these reactions are not stoichiometric, it is difficult to interpret the actual relationship between how much protein is present and the intensity of the staining. A secondary consequence of this variability is that accurate inter-study observations are often rendered impractical.

Therefore, in this study, we first developed a custom algorithm for quantifying VEGF-A immunostaining in UM specimens using a custom, automated algorithm and then determined if said expression correlated with metastasis.

Materials and Methods

Patient Samples

All patient samples (n = 29) were obtained from the Henry C. Witelson Ocular Pathology Registry, and the experiments conformed to the Declaration of Helsinki. The inclusion criteria for this study were: choroidal UM diagnosis, minimum five-year follow-up (except when metastasis were present), information regarding the presence or absence of metastases, and sufficient tumor size to obtain three non-overlapping images occupying 90% of the image at 200×.

Immunohistochemistry for VEGF-A

Immunohistochemistry was performed using the same techniques, equipment, and antibodies described in the complementary section of Chapter 3.

Image Acquisition

The details pertaining to image acquisition, including the techniques, equipment, and settings, are conveyed in the dizygotic section of Chapter 3.

Immunostaining Quantification

Immunostaining quantification could not be performed with the same algorithm used in the rabbit model (chapter 3) due to the presence of melanin in human specimens and lack thereof in albino rabbits. Therefore, the melanin had to be subtracted from the images before quantification of the immunostaining. First, brightfield and darkfield abnormalities were eliminated and the images were enhanced using the same process described in the previous chapter. Next, the hue, saturation, and brightness (HSB) were adjusted in order to isolate the positive (pink) immunostaining. HSB maps colors onto a three dimensional cylinder, with each component occupying one dimension. The specific values for isolating positive staining were determined by trial and error; however, once set, they remained consistent for all images. HSB was capable of eliminating the presence of melanin whereas color deconvolution, the technique used in chapter 3, was not as effective. The percentage of the image that was immunostained was then calculated using the built-in function, and the Analyze Particles plugin was used to determine the number of positively stained cells. A pathologist evaluated the slides to confirm that the majority of cells that were indicated as positive were UM cells. The entire java algorithm can be found in Appendix II.

Statistical Analysis

The number of positive cells and the percentage of the total image that stained positive were averaged for all three images from each UM specimen. A

student t-test was performed comparing the percentage and number of cells that were positive in patients that developed metastases and those that did not. Next, in order to determine if VEGF-A staining in the primary tumor could be used to predict metastasis, a binary logistic regression was executed with the presence of metastasis as the dependent variable and the average cell count and average positive staining fraction as the independent variables using SPSS ver. 20 (IBM). A Hosmer-Lemeshow test was performed to determine goodness-of-fit for the model. All data are presented as means ± SD.

Results

Immunohistochemistry Quantification

Twenty-nine human UM specimens met the inclusion criteria for this study, and eight of these patients had metastases (8/29; 28%). The custom immunostaining quantification algorithm was capable of identifying and isolating the positively stained cells and rendered cell counts and area stained even in samples with strong melanin expression (Figure 12).

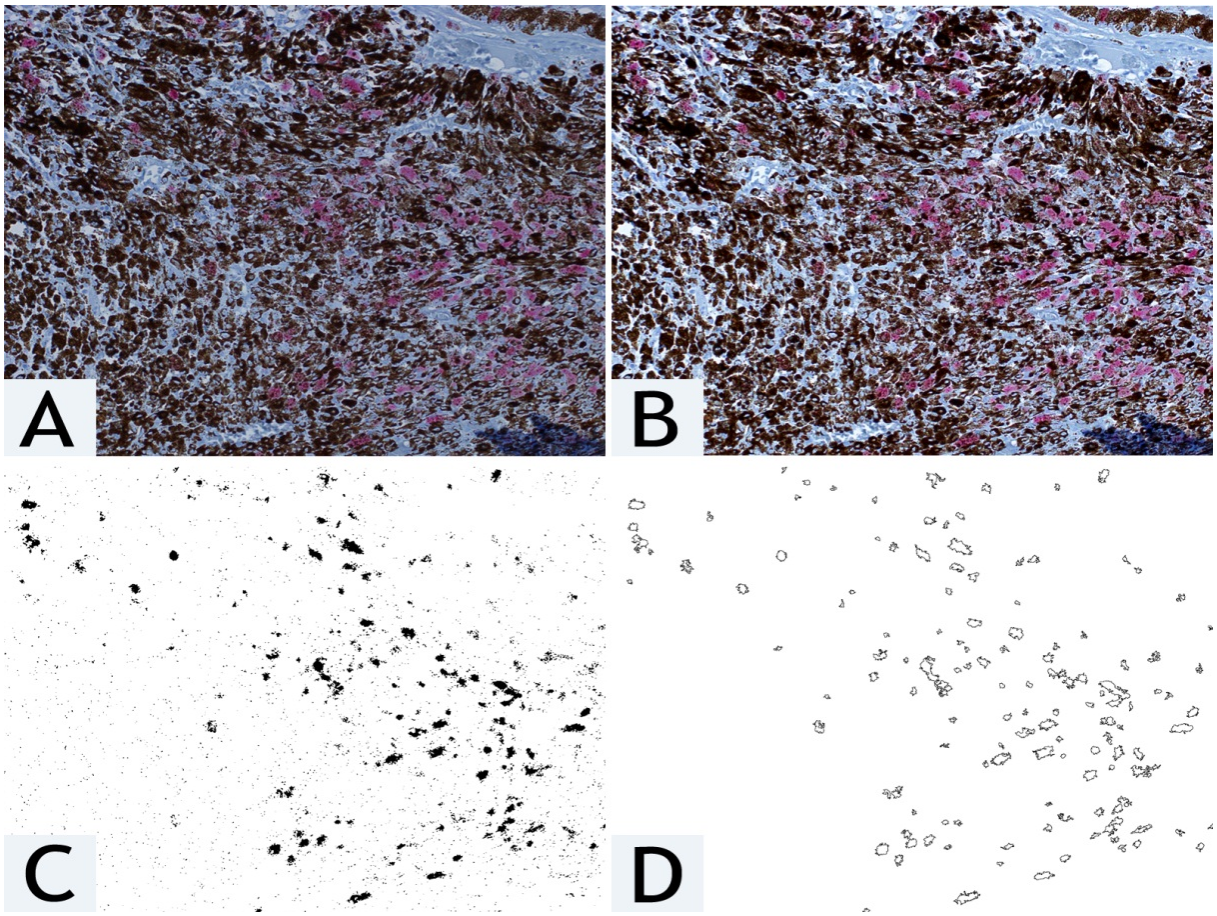

Figure 12. Representative example of the VEGF-A immunostaining quantification algorithm for human tumors. A. The original image immunostained for VEGF-A expression (pink), and counterstained with hematoxylin (blue). B. The image after correction for bright and darkfield abnormalities and enhancement. C. The binary image after hue, saturation, and brightness adjustment to isolate only the positively stained area. This image was used for the quantification of positive immunostained area. D. The image after the cells were outlined and analyzed. This image was used for the quantification of the number of positively immunostained cells. Magnification = 200×.

The three images from each patient were averaged and these values were used to generate global averages for the number of positively stained cells and the average positively stained area (24.56 ± 5.16 and 0.45% ± 0.07% and 15.67 ± 2.72 and 0.17% ± 0.03% for the non-metastatic and metastatic groups, respectively). Neither of these differences were statistically significant ($p > 0.05$).

Binary logistic regression without the addition of any variables (beginning block) obtained 74.2% accuracy for predicting metastases; this relatively high accuracy is due to the approximately three times greater ratio of non-metastatic patients compared to metastatic patients included in the sample.

The predictive accuracy of this model was improved with the addition of positive VEGF-A staining average cell count and average positive staining area; a precision of 79.3% was achieved with the input of these variables, and the model was significant (Table 4; $p < 0.05$). Hosmer-Lemeshow goodness-of-fit was greater than 0.05, indicating that the model was a good fit.

Table 4. Predictive value of VEGF-A immunostaining for the presence of metastasis in human uveal melanoma tumors with binary logistic regression.

[a]No variables added to the regression analysis (beginning block).

[b]Average positive area and average positive cell count added to the regression analysis. *p < 0.05.

		Average Positive Area ± SD	Average Positive Cells ± SD	Predicted[a]			Predicted[b]		
				Metastasis		Percentage Correct	Metastasis		Percentage Correct
				No	Yes		No	Yes	
Metastasis	No	0.17% ± 0.03%	15.67 ± 2.72	21	0	100.0	20	1	95.2
	Yes	0.45% ± 0.07%	24.56 ± 5.16	8	0	0.0	5	3	37.5
Overall (Percentage)				72.4			79.3*		

Discussion

To date, there is no consensus on whether VEGF-A expression in UM tumors correlates with important prognostic criteria, such as metastasis. This discrepancy may arise from differences attributable to the location of the tumor. For instance, in parallel studies performed by Sahin, et al., VEGF expression in posterior, but not anterior, tumors correlated with metastasis[171,178]. Furthermore, a study by Sheidow, et al. showed no correlation between VEGF expression and metastasis using a combination of both ciliary body and choroidal tumors. These results, coupled with the positive correlation revealed by our data, indicate that VEGF may be an important predictor of metastasis in posteriorly located UM tumors. Although the reason for this discrepancy requires elucidation, we hypothesize that because anterior tumors are typically smaller and are detected sooner, they may not have undergone the angiogenic switch, and thus do not express VEGF-A.

In the present study, there were several patients (2/8; 25%) with metastasis that lacked VEGF expression in primary tumors, a distinction exemplified by the absence of significant difference in either the number of positively stained cells or positive staining area between those that did and those that did not develop metastasis. Conversely, the opposite circumstance – metastasis free patients with high VEGF expression – was also identified. The latter situation is more easily explained; it may be that these patients have occult metastases. Uveal melanoma studies of tumor dormancy and CMCs suggest that all patients are apt to have metastases, albeit likely micro- or single-celled seeds[36,46]. Therefore, considering

that VEGF-A expression correlated with clinically detectable metastases in this study, these patients may be in jeopardy of developing overt metastasis and thus should be followed closely or enter into a proactive metastasis prevention treatment program. Unfortunately, our study does not provide insight into how long after VEGF-A is expressed that metastases arise; patient information related to the time of enucleation relative to clinically detectable metastases may potentially be utilized to this end. Thus, it is feasible that VEGF-A expression occurs a number of months before metastasis development, and this may account for the aforementioned discrepancy regarding high VEGF-A expression and lack of metastasis.

The opposite scenario, in which no VEGF-A expression was found in patients with metastasis, may be a result of these tumors resorting to alternative pro-angiogenic cytokines for growth. It has been previously demonstrated in a study involving 7 UM cell lines that ANG-2 was ubiquitously expressed[90]. Thus, although ANG-2 was not detected in any of our cell lines (data not shown), given the heterogeneity of in vivo tumors in patients, it is plausible that tumors void of VEGF-A expression produce ANG-2 to facilitate angiogenesis. Alternatively, it is possible that these tumors, having previously utilized VEGF-A for the angiogenic switch, now rely on other angiogenic factors, such as angiogenin and ANG-2, for growth beyond this stage[93]. Clearly, factors influencing primary tumor growth are important in UM as the largest tumor dimension remains one of the most important prognostic indicators[68,84].

It is important to identify factors in primary tumors that are linked with metastatic growth, as this can help physicians identify patients most appropriate for aggressive and experimental treatments. It is our hope that the results pertaining to VEGF-A expression in posterior UM ascertained in this chapter contribute to the body of knowledge accessible to ophthalmologists when determining standard and best practice approaches.

This study also proved the utility of using an automated system for quantifying immunohistochemistry staining in a pragmatic, perfunctory manner. This process will make inter-study comparisons possible and facilitate the production of highly valid meta-analyses. This approach is of paramount importance in UM due to the increasing rarity of enucleated specimens, which renders it difficult to acquire the minimum number of cases to ensure statistical validity. It should be noted, however, that this proposed approach is not without potential complications, as a variety of factors, ranging from fixation time, age of the paraffin block, variances in immunohistochemistry protocols, microscope settings and bulb age, type of antibody, and quality of images, among others, can affect the quality of immunohistochemistry images[174,176,177,179-181]. Nevertheless, the more traditional, subjective 3 or 7-point grading techniques also suffer from these complications. In the present study, we attempted to mitigate these variables by automating as much of the process as possible, from automated immunostaining to using an automated quantification algorithm. As a pilot study, however, several issues should be addressed prior to implementation in future studies; for instance, there was a fair degree of variability in tumor cell sizes

between patients. Thus, comparing the absolute number of positively stained cells between tumors may not be the most accurate or appropriate methodology. In fact, it was a result of this discrepancy that we decided to also incorporate the percentage of image staining in our algorithm, as we hoped that this may assuage differences in cell sizes between tumors. Secondly, although we strived for objectivity, our inclusion criteria required some subjective input; for instance, we selected only tumors that filled 90% of the image at 200x magnification. As is the case with traditional immunohistochemical grading in which slides are given a rating of 2 or 3 depending on whether greater than or less than 50% of the image stained, this is only an estimate and thus, by definition, subjective. Future approaches should incorporate even less subjectivity; now that the algorithm for identifying positive cells has been generated, it should be expanded to initially count all malignant cells in the image and then quantify the proportion of positively stained cells. This approach should rectify both of the previously aforementioned limitations of the current study.

A secondary consequence of selecting only tumors that filled 90% of a 200x magnified image is that our sample is biased towards larger tumors. As previously noted, larger tumors have already undergone the angiogenic switch and thus are more likely to express VEGF-A. Despite this fact, our model was significant; however, the inclusion of a greater range of UM tumor sizes may serve to increase our ability to predict metastasis to over 80%.

One of the limitations of this study is the lack of complete information regarding treatment prior to enucleation. As the current standard approach to

treating uveal melanomas often includes plaque radiotherapy, it can be assumed that a proportion of the tumors in our study experienced such an affront. This can confound results because it has been shown in UM, as well as in rectal cancer, that radiotherapy induces VEGF expression[88,182]. In addition, other treatment modalities, such as imatinib mesylate, are known to influence VEGF expression in UM models[166]. Thus, an opportune time for anti-VEGF therapy may be concomitant with plaque radiation therapy to prevent tumor regrowth.

There are several systems available that can effectively identify, count, and analysis various tumors. However, they often require expensive slide scanners or ancillary equipment, or use proprietary algorithms. In this study, we only used equipment available to any laboratory that performs traditional immunohistochemistry grading (such as a light microscope and camera) and we used a freeware program (ImageJ) provided by the NIH to analyze our images. The increasingly pervasive availability of our algorithm and others like it will hopefully promote and facilitate the production of even more accurate and robust immunohistochemical quantification systems.

Conclusions

We successfully developed a custom algorithm that quantified VEGF-A immunostaining in human UM specimens. Using this data, we were able to develop a statistically significant model for predicting metastasis. The automated and objective nature of this process can serve to standardize future immunohistochemical studies and facilitate large scale meta-analyses.

The correlation between VEGF-A expression and metastasis indicates that anti-VEGF agents may have clinical implications for UM sufferers. In addition, VEGF-A expression in patient samples may be used to identify candidates appropriate for aggressive anti-metastatic treatments.

Final Discussion

Despite overwhelming evidence, proof-of-concept, and researcher consensus regarding the critical importance of VEGF for the growth of intratumoral blood vessels, anti-VEGF and anti-angiogenic therapies are not as effective as first heralded. In fact, in 2011, the Food and Drug Administration (FDA) revoked their approval of Avastin for the treatment of breast cancer, stating that it has "has not been shown to be safe and effective for that use"[183]. Following on the heels of this announcement, the UK National Institute of Health and Clinical Excellence (NICE) refused to recommend Avastin use for advanced breast cancer[184]. It should be noted, however, that the decision not to recommend Avastin for breast cancer treatment is based partially on the safety concerns with systemically administered product, consequences that are substantially assuaged when administered into the eye[185,186].

Even in cancers for which the FDA continues to endorse Avastin use, including some types of colon, lung, kidney, and brain cancers, the results are far from copacetic; for instance, resistance can occur rapidly in gliomas through the exploitation of other pro-angiogenic factors, such as bFGF[187]. This corresponds well with our data: abrogation of the VEGF/VEGF-R2 signalling pathway induces compensatory upregulation of additional cytokines, although the compensatory factor differs (bFGF vs. CCL3). This phenomenon is not unique to gliomas or UM, as a similar process has been observed in chronically treated colorectal cancer cells, pancreatic cancer cells, pancreatic islet tumor cells, and renal cell carcinoma cells[101,141,188,189]. Thus, the results of the present study reinforce the

notion that, due to the plasticity of malignant cells, anti-VEGF monotherapy may be inadequate or ineffective.

The initial toxicity that a therapeutic compound exerts on malignant cells followed by tumor regrowth is generally considered either a function of the development of drug resistance or the selection for a drug-resistant clone. While both hypotheses draw considerable interest and research, the recent discovery of self-renewing, cancer stem-cells, has invigorated the latter. With respect to UM in particular, a study has identified distinct morphological populations within UM cell lines in culture, with growth patterns akin to holoclone, meroclone, and paraclone types evident in stem-cell populations[190]. In this paper, UM cells that survived the administration of the chemotherapy drug cisplatin generated more holoclones, a stem-cell like population capable of generating all types of growth patterns, compared to controls. Thus, the authors suggest that these undifferentiated holoclones are self-renewing cancer stem-cells, which were responsible for cisplatin induced resistance. This ideology extends beyond cytotoxic compounds, such as the aforementioned cisplatin; for instance, extreme hypoxia was shown to generate hypoxia-resistant clones in erythroleukemia cell lines[191]. Giuntoli et al., reports that the clonally expanded erythroleukemia cell line used in their study is composed of a spectrum of cells with differing hypoxia-sensitivities, including a resistant cohort, in addition to both actively dividing and quiescent populations[191]. Although the aforementioned study utilized an artificial chamber setting to generate hypoxic conditions, it has been broadly hypothesized that the exceedingly hypoxic environment induced by angiogenic inhibitors may

select for a similar set of clones capable of surviving in low oxygen, consequently leading to additional metastatic development[99]. This characteristic has been demonstrated in models of pancreatic neuroendocrine tumors, glioblastoma, and metastatic breast cancer, and has been proposed as a mechanism by which anti-VEGF/VEGF-R treatments increase the malignant nature of certain cell types[102,103,192]. The former hypothesis, that tumor cells develop resistance following exposure to a specific compound, is typically explained by decreased uptake of the compound, increased expulsion of the drug, or the activation of DNA repair mechanisms[193]. In the present study, however, resistance is a less likely to be involved in bevacizumab therapy, considering that the antibody does not directly enter or influence the malignant cells. Although not directly tested in the current work, it is feasible that our in vitro data indirectly represents the former manifestation; however, long-term exposure studies are required to form definitive conclusions.

Angiogenic inhibition may also facilitate the release of inflammatory cytokines, which can generate more favorable conditions for metastatic development[99,194]. In our study, this scenario was palpable: in response to bevacizumab, all three UM cell lines produced significantly greater quantities of CCL3. In a recent study assessing cytokine production in vitreous samples, it was discovered that CCL3 expression is higher in eyes harboring UM compared to controls[195]. However, as previously mentioned, there is negligible research investigating the association between UM and CCL3; in fact, the present study is the first to definitively demonstrate that UM cells produce CCL3 in any context.

Consequently, the repercussions of the amplified secretion of this powerful macrophage mitogen in UM can only be hypothesized by parsing data and results from other malignancies. Unfortunately, fundamental differences between UM and other malignancies as they pertain to the primary function of CCL3 render most comparisons unsuitable. For instance, the vast majority of studies involving CCL3 investigate its relationship with TILs or TAMs, as CCL3 is a powerful modulator of acute inflammatory responses. Therefore, in other malignancies, such as cutaneous melanoma and gastric cancer, CCL3-induced recruitment of immune cells improves prognosis and thus CCL3 is being pursued for pharmaceutical treatments[196,197]. Conversely, infiltrating macrophages and lymphocytes into the immune-privileged eye are indicators of poor prognosis in UM, suggesting that an antithetical approach toward CCL3 should be considered[160]. Hepatocellular carcinomas exhibit a similar inverse relationship with infiltrating immune cells, and recent research indicates that CCL3/CCR1 signalling contributes to disease progression[144,198]. Thus, it appears that the influence of CCL3 on malignant progression is tumor dependant; specifically, the effects of CCL3 appear intrinsically linked to the correlation between intratumoral immune system presence and outcome.

MMP-9, on the other hand, has been studied extensively in a variety of malignancies. In UM, MMP-9 has been shown to correlate with a high risk of metastasis, and is expressed primarily in more aggressive, epithelioid cells[152,199]. Although it has been previously shown that CCL3 signalling through CCR1 is capable of inducing MMP-9 activity, results corroborated by the current work, it

is of note that three of the primary molecules studied in this thesis, VEGF, MMP-9, and CCL-3, are regulated upstream by the transcription factor, nuclear factor kappa-light-chain-enhancer of activated B cells (NF-º B)[144,200,201]. Prior to determining that the majority of the increase in MMP-9 secretion was attributable to CCR3 signalling, we had considered that bevacizumab was directly affecting the transcription of all three factors by mediating NF-º B activity. However, a recent publication determining that bevacizumab does not upregulate NF-º B in endothelial cells rendered this hypothesis unlikely; however, as previously demonstrated, the effects of specific compounds and signalling pathways can differ from cell to cell, and this possibility should not be ruled out prior to studies specifically performed on UM cells[202]. On the other hand, it has been conclusively demonstrated that CCR1 signalling can activate NF-º B in monocytes, thus we propose this process as a potential candidate whereby the CCL-3 increase observed in the present study modulates MMP-9 secretion.

In summary, it is likely that in vivo treatment of UM with bevacizumab may have two-fold negative implications: increased invasiveness due to amplified MMP-9 activity and expedition or facilitation of macrophage infiltration as a result of augmented CCL3 secretion.

Most of the negative and pro-metastatic consequences of anti-VEGF/VEGF-R signalling can be mitigated and positive outcomes achieved through the implementation of multiple concurrent therapies. In the clinic, bevacizumab is often administered in combination with chemotherapeutic agents, which improves results compared to chemotherapy alone. For instance, overall

progression free survival for metastatic breast cancer patients increased when bevacizumab was added to paclitaxel or capecitabine[203]. Likewise, in advanced head and neck cancer, bevacizumab plus erlotinib with chemotherapy produced favorable results[204]. In the present study, we identified that CCL3 was upregulated as part of a compensatory response to bevacizumab treatment. To the best of our knowledge, this is the first report indicating that bevacizumab treatment can upregulate CCL3 production in any malignancy. Prior research regarding CCL3 reveals that higher levels are associated with a poor survival and, in mouse models of hepatocellular carcinoma, this signalling axis has been implicated in disease progression[144,205]. MLN-3897, a small molecule inhibitor of CCR1 (the primary CCL3 receptor), has been shown in vitro to be effective for reducing multiple myeloma cell survival and proliferation[206]. In this study, we showed that our cells produce both CCL3 and CCR1, indicating that autocrine signalling may be occurring. Therefore, this inhibitor in combination with bevacizumab may prove efficacious in in vitro and in vivo UM studies. Another approach may be to test bevacizumab with inhibitors that influence CCL3 production. For instance, ibrutinib has been shown to inhibit Bruton's tyrosine kinase (Btk) in multiple myeloma, which subsequently downregulates CCL3 secretion[207]. To date, no studies have been published investigating Btk expression in either uveal or cutaneous melanoma[208]. Another approach would be to supplement the use of chemotherapeutic agents with bevacizumab. For instance, antibodies against EGFR have been shown to raise NF-º B levels, which can cause a subsequent increase in VEGF production; thus, combining this agent with bevacizumab can

abrogate this increase[209]. Given the correlation between EGFR and metastasis in uveal melanoma, this approach presents as a potential viable option for dual or multiple therapy for UM[210,211]. In general, more studies on CCL3 and its receptors in UM are required prior to targeting as part of dual therapy with bevacizumab.

Although clinical trials using bevacizumab to reduce the size of large choroidal melanomas are underway, the inadvertent treatment of occult uveal melanoma tumors with this antibody suggests an unfavorable outcome[107]. Singh et al. reported UM progression in three cases despite the administration of bevacizumab for other pathologies; as a result, they strongly caution against the use of bevacizumab as a mono and first-line therapy[109].

It is generally hypothesized that the reason why bevacizumab therapy is ineffective is because there are no clear biomarkers to select the most appropriate cohort of patients for treatment[212]. It is logical that the best biomarker for anti-VEGF treatment would be expression of VEGF itself; however, as previously noted, there have been conflicting results in UM regarding whether or not it has prognostic relevance. In the present study, we were capable of using VEGF expression in choroidal melanomas to predict metastasis. Thus, it would be prudent to utilize this information for selecting patients that may benefit from bevacizumab treatment. As fine needle biopsies are becoming more common in UM to ascertain monosomy 3 status, these specimens could also be tested for VEGF-A expression. The purpose of this determination would be two-fold: 1) identify and select patients at higher risk of metastasis for more aggressive treatment and, 2) identify patients with active VEGF-A expression in whom

bevacizumab may have the greatest positive effect. These VEGF-A patients may then be enrolled in studies to evaluate the efficacy of bevacizumab as a mono, dual, or multiple-therapy regimen. It is likely that safety would not be an issue in these studies, in particular in the mono-therapy group, as intravitreal injections are generally well-tolerated with limited side-effects when used for other ocular pathologies.

A secondary approach to UM treatment with bevacizumab therapy, alone or in combination with other compounds, may be to shrink the tumor so that they can be treated with more conservative methods. As plaque radiotherapy is only indicated in tumors smaller than 16mm in the largest dimension due to the penetrance of the radioactive element, bevacizumab therapy may shrink the tumor to a size that is amenable to this therapy[213]. However, even with this approach, it may be important to block multiple angiogenic pathways to prevent tumor growth, as UM tumor progression was noted following bevacizumab treatment[109]. Further, bevacizumab may be useful following lamellar sclerouvectomy as a protective measure against regrowth of tumor cells that may have been overlooked during the surgical procedure.

In addition to bevacizumab, the efficacy of other anti-angiogenic compounds has been evaluated with respect to treating UM in both animal models and in culture. For instance, in 2007, Mangiameli at al. tested the ability of sorafenib to inhibit uveal melanoma cell growth and endothelial migration and tube formation in culture. Unlike bevacizumab, which is highly specific for sequestering VEGF, sorafenib functions by inhibiting a broad spectrum of RTKs,

including all VEGF-Rs, Raf, and PDGFR-^{2} [214]. Although inhibiting multiple pathways invariable increases the potential for adverse reactions, this approach may prove fruitful given the propensity of UM cells to activate compensatory pathways in the presence of bevacizumab. Indeed, Mangiameli concluded that sorafenib inhibited the migration of endothelial cells and UM growth in a xenograft model. While these results are notable, it is critical to evaluate the effects of this and other similar compounds on the functional abilities of UM cells alone, as they are capable of forming vessels in the absence of endothelial cells (vasculogenic mimicry)[58]. The latter result illustrates the effectiveness of inhibiting multiple pathways simultaneously, and this promising outcome has expedited clinical trials using sorafenib in patients with UM[215].

In a more recent study, the use of a plant saponin, astragaloside IV, effectively inhibited proliferation, migration, invasion, and the production and secretion of VEGF-A in uveal melanoma cell lines[216]. Although the exact mechanism by which this saponin exerts these effects on UM cells is unknown, it has been shown in colon cancer that this compound downregulates COX-2, which, in addition to regulating VEGF expression, is a negative prognostic indicator in UM[62,217].

One of the curious and unique aspects of UM is that even patients that underwent enucleation several years prior will still have detectable circulating malignant cells in their blood[36]. This suggests one of two rationales: 1) the cells escaped the eye before it was removed and continue to circulate indefinitely or, 2) metastatic seeds are shedding additional melanoma cells into the blood. The

former hypothesis seems highly unlikely given the toxic environment of the blood, including a high pH, exposure to the immune system, and sheer forces induced by blood flow all of which can induce anoikis[218]. However, studies have shown that CMCs may circulate in clusters surrounded by platelets and other cells in order to shield themselves, much like a polypyrenous drupe protects a seed, from both the immune system and the caustic environment of the blood[219,220]. Although the latter hypothesis for the nearly ubiquitous and perpetual detectability of CMCs in uveal melanoma patients seems more likely, it invariably invokes additional queries; for instance, where are the micrometastatic derivatives that shed these cells located? Research has indicated that the bone marrow or the liver itself may be a possible reservoir for these cells, but definitive conclusions have yet to be reached[221]. A likely contributor to the complexity in discovering these obscure reservoirs is that they are typically infinitesimal and comprised of only a handful of cells. Current techniques for identifying metastatic nodules often involve exploiting their high metabolic rate as a method of detection. For many cancers, including uveal melanoma, this is impractical because micrometastatic nodules are either dormant or divide slowly, and current in vivo imaging modalities are not sensitive enough to identify single or small clusters of metabolically inactive malignant seeds. Thus, even if a particular treatment is efficacious for treating uveal melanoma, recurrence is a valid concern. To date, there has only been one adult-to-adult living donor liver transplantation attempted for a patient with metastatic uveal melanoma. Unfortunately, despite the fact that the affected eye was removed more than three years prior to liver transplantation,

the patient developed additional hepatic metastasis within six months, from which he succumbed within eight months[222]. Thus, options for treating most UM liver metastases are limited and survival rates are subsequently low. It is therefore imperative that researchers continue to pursue and investigate novel treatment methodologies and pharmaceutical interventions in order to ease tumor burden and increase survival in the unfortunately afflicted.

In addition to in vitro studies, we also investigated VEGF-A expression in both rabbit and human UM samples by employing immunohistochemistry. Immunohistochemistry is an inherently variable and sensitive technique, which can be affected by a plethora of factors including, but not limited to, the age of the paraffin block, antibody selection, individual methods (for instance, manual vs. automated), embedding and processing variations, and scoring and result interpretations[174,176,177,179-181]. As part of our ongoing mission to objectify science, medicine, and research, there is much effort currently being expended on standardizing many of the aforementioned variables. For certain pathologies, interpretation of immunohistochemical staining, for example either a positive or negative result or staining exceeding a specific threshold, will determine the appropriate treatment course for a patient. Thus, the ability to standardize the immunostaining process, from tissue handling procedures to section evaluation, is of paramount importance. To this end, we decided to develop an automated method for quantifying VEGF-A immunostaining in UM tumors. Traditionally, immunohistochemical grading attributed to a particular sample is based on a scoring system involving classifying tumors into groups according to staining

intensity and distribution. This process, which does not deal with actual values, can place two very different tumors in the same category as intensity and distribution represent two very different protein expression profiles. Generally, intensity is indicative of average protein quantity within a subset of cells, although it is often difficult to determine the amount of protein using non-stoichiometric stains, while distribution represents a rough estimation of how many cells express the protein in question, irrespective of intensity[175,223]. By combining these two profiles and generating artificial tumor groupings, the individual implications of protein quantity and distribution are obscured; for instance, high, punctate protein expression in only a few cells may indicate that these specific cells may be capable of metastasizing[224]. Conversely, low, basal expression in a majority of cells may simply be a reflection of normal, metabolic processes, but both cohorts may be grouped together if conventional grading methods are used (high intensity/low distribution and low intensity/high distribution). This distinction is far from academic, as treatment approaches often depend on these classifications[172]. In an era in which personalized medicine is heralded, conventional grading methods and processes are generalized and archaic.

Based on the dubious link between staining intensity and protein quantity, we eliminated the assessment of intensity and focussed solely on distribution in our study. In addition, by quantitatively determining the number of cells that were positive for VEGF-A, we were capable of exploiting more robust statistical methods, which is not possible using subjective groupings. Thus, we were capable of using a regression model to retrospectively predict metastasis in patients based

on VEGF-A expression, even though there was no significant difference in the positive cell count or positive areas between those that did and those that did not develop metastases.

As enucleated specimens become more rare, ophthalmologists and researchers are resorting to alternative methods for obtaining tissue for immunohistochemical studies. Fine-needle aspiration biopsies, for instance, are becoming more common as they provide the advantage of tissue acquisition during a period more conducive to intervention compared to enucleation, the latter typically indicated when a tumor has grown too large for conventional treatments. Samples obtained for this method are typically tested for monosomy 3, which is an indicator of poor prognosis[225]. Oddly, despite a plethora of research decreeing the importance and value of prognostic factors in enucleated samples, including COX-2 and phospho-AKT, these discoveries have not been applied to fine-needle aspiration biopsies[62,65]. Although the material obtained from these biopsies is scant, it is crucial to evaluate a panel of prognostic indicators to determine which feature most accurately predicts metastasis, thereby permitting appropriately tailored intervention. Based on our ability to retrospectively predict metastasis in our sample using VEGF-A expression, and because there is a readily available pharmaceutical compound targeting this cytokine (bevacizumab), it is but a matter of due diligence to evaluate VEGF-A expression in fine-needle aspiration biopsy specimens.

Although our approach was not entirely void of subjective intervention it offers a promising start towards more objective analysis of immunohistochemical

staining. An additional advantage of this technique is that it permits more robust statistical analyses as it provides actual, spectral data as opposed to generating finite groupings. Also, it can be used for additional purposes such as absolving inter-observer disagreements[226].

Finally, while we did not test concordance between semi-quantitative immunohistochemical scoring methods and our quantitative method, previous studies using similar approaches have concluded that these methods are in accord[226-229]. It is our hope that providing the algorithm for this process that can be used with the freeware program ImageJ will serve to standardize UM immunohistochemical staining and enable meta-analysis of these increasingly rare samples.

Final Conclusion

In this thesis, we explored the role of VEGF-A in uveal melanoma, from its expression, signalling, and inhibition in vitro, to its prognostic implications in both an animal model and in human specimens. Although initially encouraged by the strong expression of VEGF-A and evidence of autocrine signalling in our cell lines, it quickly became apparent that inhibiting this pathway was no panacea for UM; the complexity, sensitivity, and redundancy of these tumor cells and their signalling processes allowed them to evade this promising treatment modality. As a result, the predicted global downregulation of the functional abilities of our UM cell lines was not realized. However, our in vitro work revealed for the first time in UM, that our cells produce CCL3, a powerful immune modulator, and secretion of this cytokine is increased following VEGF-A inhibition. We also concluded that a consequence of this increase is a concomitant increase in MMP-9, which translated into augmented invasive ability. Thus, we utilized dual-inhibition to suppress the functional characteristics of our cell lines; however, it is possible, and perhaps even likely, that in situ treatment of UM with bevacizumab may cause multiple compensatory pathways to be activated, each of which may need to be targeted in order to completely eradicate this malignant entity.

We also developed a novel, automated immunohistochemistry quantification algorithm to objectively evaluate VEGF-A staining in both a UM rabbit model and in enucleated specimens from patients with UM. In both cohorts, we were able to retrospectively predict metastatic development. The benefit of the

former may be in evaluating the efficacy of pre-clinical compounds, such as VEGF-A or CCL3 inhibitors. In patients, the ability to objectively evaluate protein expression via immunohistochemistry is a potentially significant tool for selecting patients that may respond favorably to treatment. In this case, it is conceivable that VEGF-A expression ascertained using these methods may be used as a determinant for the administration of bevacizumab or other anti-angiogenic therapies.

In conclusion, uveal melanoma is a complex, deadly disease that continually confounds researchers and clinicians. It is our hope that the research herein will contribute to eliminating the burden of this enigmatic illness.

References

1. Katz NR, Finger PT, McCormick SA, et al. Ultrasound biomicroscopy in the management of malignant melanoma of the iris. *Archives of ophthalmology.* Nov 1995;113(11):1462-1463.

2. Singh AD, Topham A. Incidence of uveal melanoma in the United States: 1973-1997. *Ophthalmology.* May 2003;110(5):956-961.

3. Albert DM. The ocular melanoma story. LIII Edward Jackson Memorial Lecture: Part II. *American journal of ophthalmology.* Jun 1997;123(6):729-741.

4. Char DH, Stone RD, Irvine AR, et al. Diagnostic modalities in choroidal melanoma. *American journal of ophthalmology.* Feb 1980;89(2):223-230.

5. Accuracy of diagnosis of choroidal melanomas in the Collaborative Ocular Melanoma Study. COMS report no. 1. *Archives of ophthalmology.* Sep 1990;108(9):1268-1273.

6. Di Cesare S, Maloney S, Fernandes BF, et al. The effect of blue light exposure in an ocular melanoma animal model. *Journal of experimental & clinical cancer research : CR.* 2009;28:48.

7. Marshall JC, Gordon KD, McCauley CS, de Souza Filho JP, Burnier MN. The effect of blue light exposure and use of intraocular lenses on human uveal melanoma cell lines. *Melanoma research.* Dec 2006;16(6):537-541.

8. Seko Y, Pang J, Tokoro T, Ichinose S, Mochizuki M. Blue light-induced apoptosis in cultured retinal pigment epithelium cells of the rat. *Graefe's archive for clinical and experimental ophthalmology = Albrecht von Graefes Archiv fur klinische und experimentelle Ophthalmologie.* Jan 2001;239(1):47-52.

9. Mainster MA. Violet and blue light blocking intraocular lenses: photoprotection versus photoreception. *The British journal of ophthalmology.* Jun 2006;90(6):784-792.

10. Schmidt-Pokrzywniak A, Jockel KH, Bornfeld N, Sauerwein W, Stang A. Positive interaction between light iris color and ultraviolet radiation in relation to the risk of uveal melanoma: a case-control study. *Ophthalmology.* Feb 2009;116(2):340-348.

11. Turaka K, Shields CL, Shah CP, Say EA, Shields JA. Bilateral uveal melanoma in an arc welder. *Graefe's archive for clinical and experimental ophthalmology = Albrecht von Graefes Archiv fur klinische und experimentelle Ophthalmologie.* Jan 2011;249(1):141-144.

12. Wang HT, Choi B, Tang MS. Melanocytes are deficient in repair of oxidative DNA damage and UV-induced photoproducts. *Proceedings of the National Academy of Sciences of the United States of America.* Jul 6 2010;107(27):12180-12185.

13. Lutz JM, Cree IA, Foss AJ. Risk factors for intraocular melanoma and occupational exposure. *The British journal of ophthalmology.* Oct 1999;83(10):1190-1193.

14. Faingold D, Marshall JC, Antecka E, et al. Immune expression and inhibition of heat shock protein 90 in uveal melanoma. *Clinical cancer research : an official journal of the American Association for Cancer Research.* Feb 1 2008;14(3):847-855.

15. Singh AD, Kalyani P, Topham A. Estimating the risk of malignant transformation of a choroidal nevus. *Ophthalmology.* Oct 2005;112(10):1784-1789.
16. Ganley JP, Comstock GW. Benign nevi and malignant melanomas of the choroid. *American journal of ophthalmology.* Jul 1973;76(1):19-25.
17. Factors predictive of growth and treatment of small choroidal melanoma: COMS Report No. 5. The Collaborative Ocular Melanoma Study Group. *Archives of ophthalmology.* Dec 1997;115(12):1537-1544.
18. Butler P, Char DH, Zarbin M, Kroll S. Natural history of indeterminate pigmented choroidal tumors. *Ophthalmology.* Apr 1994;101(4):710-716; discussion 717.
19. Shields CL, Furuta M, Mashayekhi A, et al. Clinical spectrum of choroidal nevi based on age at presentation in 3422 consecutive eyes. *Ophthalmology.* Mar 2008;115(3):546-552 e542.
20. Hawkins BS. The Collaborative Ocular Melanoma Study (COMS) randomized trial of pre-enucleation radiation of large choroidal melanoma: IV. Ten-year mortality findings and prognostic factors. COMS report number 24. *American journal of ophthalmology.* Dec 2004;138(6):936-951.
21. The Collaborative Ocular Melanoma Study (COMS) randomized trial of pre-enucleation radiation of large choroidal melanoma II: initial mortality findings. COMS report no. 10. *American journal of ophthalmology.* Jun 1998;125(6):779-796.
22. Rajpal S, Moore R, Karakousis CP. Survival in metastatic ocular melanoma. *Cancer.* Jul 15 1983;52(2):334-336.
23. Char DH. Metastatic choroidal melanoma. *American journal of ophthalmology.* Jul 1978;86(1):76-80.
24. Einhorn LH, Burgess MA, Gottlieb JA. Metastatic patterns of choroidal melanoma. *Cancer.* Oct 1974;34(4):1001-1004.
25. Mavligit GM, Charnsangavej C, Carrasco CH, Patt YZ, Benjamin RS, Wallace S. Regression of ocular melanoma metastatic to the liver after hepatic arterial chemoembolization with cisplatin and polyvinyl sponge. *JAMA : the journal of the American Medical Association.* Aug 19 1988;260(7):974-976.
26. The COMS randomized trial of iodine 125 brachytherapy for choroidal melanoma: V. Twelve-year mortality rates and prognostic factors: COMS report No. 28. *Archives of ophthalmology.* Dec 2006;124(12):1684-1693.
27. Hawkins BS. Collaborative ocular melanoma study randomized trial of I-125 brachytherapy. *Clin Trials.* Oct 2011;8(5):661-673.
28. Melia BM, Abramson DH, Albert DM, et al. Collaborative ocular melanoma study (COMS) randomized trial of I-125 brachytherapy for medium choroidal melanoma. I. Visual acuity after 3 years COMS report no. 16. *Ophthalmology.* Feb 2001;108(2):348-366.
29. Shields JA, Shields CL, Shah P, Sivalingam V. Partial lamellar sclerouvectomy for ciliary body and choroidal tumors. *Ophthalmology.* Jun 1991;98(6):971-983.
30. Robertson DM, Campbell RJ, Weaver DT. Residual intrascleral and intraretinal melanoma: a concern with lamellar sclerouvectomy for uveal melanoma. *American journal of ophthalmology.* Nov 15 1991;112(5):590-593.
31. Gunduz K, Bechrakis NE. Exoresection and endoresection for uveal melanoma. *Middle East African journal of ophthalmology.* Jul 2010;17(3):210-216.
32. Melia M, Moy CS, Reynolds SM, et al. Quality of life after iodine 125 brachytherapy vs enucleation for choroidal melanoma: 5-year results from the

Collaborative Ocular Melanoma Study: COMS QOLS Report No. 3. *Archives of ophthalmology.* Feb 2006;124(2):226-238.

33. Geisse LJ, Robertson DM. Iris melanomas. *American journal of ophthalmology.* Jun 15 1985;99(6):638-648.

34. Singh AD, Topham A. Survival rates with uveal melanoma in the United States: 1973-1997. *Ophthalmology.* May 2003;110(5):962-965.

35. Singh AD, Rennie IG, Kivela T, Seregard S, Grossniklaus H. The Zimmerman-McLean-Foster hypothesis: 25 years later. *The British journal of ophthalmology.* Jul 2004;88(7):962-967.

36. Callejo SA, Antecka E, Blanco PL, Edelstein C, Burnier MN, Jr. Identification of circulating malignant cells and its correlation with prognostic factors and treatment in uveal melanoma. A prospective longitudinal study. *Eye (Lond).* Jun 2007;21(6):752-759.

37. Schuster R, Bechrakis NE, Stroux A, et al. Prognostic relevance of circulating tumor cells in metastatic uveal melanoma. *Oncology.* 2011;80(1-2):57-62.

38. Ly LV, Odish OF, Wolff-Rouendaal D, Missotten GS, Luyten GP, Jager MJ. Intravascular presence of tumor cells as prognostic parameter in uveal melanoma: a 35-year survey. *Investigative ophthalmology & visual science.* Feb 2010;51(2):658-665.

39. Harbour JW, Onken MD, Roberson ED, et al. Frequent mutation of BAP1 in metastasizing uveal melanomas. *Science.* Dec 3 2010;330(6009):1410-1413.

40. Petrausch U, Martus P, Tonnies H, et al. Significance of gene expression analysis in uveal melanoma in comparison to standard risk factors for risk assessment of subsequent metastases. *Eye (Lond).* Aug 2008;22(8):997-1007.

41. van Gils W, Lodder EM, Mensink HW, et al. Gene expression profiling in uveal melanoma: two regions on 3p related to prognosis. *Investigative ophthalmology & visual science.* Oct 2008;49(10):4254-4262.

42. Worley LA, Onken MD, Person E, et al. Transcriptomic versus chromosomal prognostic markers and clinical outcome in uveal melanoma. *Clinical cancer research : an official journal of the American Association for Cancer Research.* Mar 1 2007;13(5):1466-1471.

43. Economou MA, All-Ericsson C, Bykov V, et al. Receptors for the liver synthesized growth factors IGF-1 and HGF/SF in uveal melanoma: intercorrelation and prognostic implications. *Acta ophthalmologica.* Nov 2008;86 Thesis 4:20-25.

44. Topcu-Yilmaz P, Kiratli H, Saglam A, Soylemezoglu F, Hascelik G. Correlation of clinicopathological parameters with HGF, c-Met, EGFR, and IGF-1R expression in uveal melanoma. *Melanoma research.* Apr 2010;20(2):126-132.

45. Economou MA, All-Ericsson C, Bykov V, et al. Receptors for the liver synthesized growth factors IGF-1 and HGF/SF in uveal melanoma: intercorrelation and prognostic implications. *Investigative ophthalmology & visual science.* Dec 2005;46(12):4372-4375.

46. Logan PT, Fernandes BF, Di Cesare S, Marshall JC, Maloney SC, Burnier MN, Jr. Single-cell tumor dormancy model of uveal melanoma. *Clinical & experimental metastasis.* 2008;25(5):509-516.

47. Spagnolo F, Caltabiano G, Queirolo P. Uveal melanoma. *Cancer treatment reviews.* Aug 2012;38(5):549-553.

48. Frenkel S, Nir I, Hendler K, et al. Long-term survival of uveal melanoma patients after surgery for liver metastases. *The British journal of ophthalmology.* Aug 2009;93(8):1042-1046.

49. Mariani P, Piperno-Neumann S, Servois V, et al. Surgical management of liver metastases from uveal melanoma: 16 years' experience at the Institut Curie. *European journal of surgical oncology : the journal of the European Society of Surgical Oncology and the British Association of Surgical Oncology.* Nov 2009;35(11):1192-1197.

50. Kodjikian L, Grange JD, Baldo S, Baillif S, Garweg JG, Rivoire M. Prognostic factors of liver metastases from uveal melanoma. *Graefe's archive for clinical and experimental ophthalmology = Albrecht von Graefes Archiv fur klinische und experimentelle Ophthalmologie.* Oct 2005;243(10):985-993.

51. Shields JA, Shields CL, De Potter P, Singh AD. Diagnosis and treatment of uveal melanoma. *Seminars in oncology.* Dec 1996;23(6):763-767.

52. Laver NV, McLaughlin ME, Duker JS. Ocular melanoma. *Archives of pathology & laboratory medicine.* Dec 2010;134(12):1778-1784.

53. Callender GR. Malignant melanotic tumors of the eye: A study of the histologic types on 111 cases. *Trans Am Acad Ophthalmol Otolaryngol.* 1931;36:131-142.

54. McLean IW, Foster WD, Zimmerman LE, Gamel JW. Modifications of Callender's classification of uveal melanoma at the Armed Forces Institute of Pathology. *American journal of ophthalmology.* Oct 1983;96(4):502-509.

55. Gamel JW, McLean IW. Quantitative analysis of the Callender classification of uveal melanoma cells. *Archives of ophthalmology.* Apr 1977;95(4):686-691.

56. Folberg R, Rummelt V, Parys-Van Ginderdeuren R, et al. The prognostic value of tumor blood vessel morphology in primary uveal melanoma. *Ophthalmology.* Sep 1993;100(9):1389-1398.

57. Maniotis AJ, Folberg R, Hess A, et al. Vascular channel formation by human melanoma cells in vivo and in vitro: vasculogenic mimicry. *The American journal of pathology.* Sep 1999;155(3):739-752.

58. Folberg R, Hendrix MJ, Maniotis AJ. Vasculogenic mimicry and tumor angiogenesis. *The American journal of pathology.* Feb 2000;156(2):361-381.

59. Folberg R, Maniotis AJ. Vasculogenic mimicry. *APMIS : acta pathologica, microbiologica, et immunologica Scandinavica.* Jul-Aug 2004;112(7-8):508-525.

60. Coleman K, Baak JP, van Diest PJ, Mullaney J. Prognostic value of morphometric features and the callender classification in uveal melanomas. *Ophthalmology.* Oct 1996;103(10):1634-1641.

61. Bakalian S, Marshall JC, Faingold D, Logan P, Antecka E, Burnier MN, Jr. Expression of nm23-H1 in uveal melanoma. *Melanoma research.* Oct 2007;17(5):284-290.

62. Figueiredo A, Caissie AL, Callejo SA, McLean IW, Gold P, Burnier MN, Jr. Cyclooxygenase-2 expression in uveal melanoma: novel classification of mixed-cell-type tumours. *Canadian journal of ophthalmology. Journal canadien d'ophtalmologie.* Aug 2003;38(5):352-356.

63. All-Ericsson C, Girnita L, Seregard S, Bartolazzi A, Jager MJ, Larsson O. Insulin-like growth factor-1 receptor in uveal melanoma: a predictor for metastatic disease and a potential therapeutic target. *Investigative ophthalmology & visual science.* Jan 2002;43(1):1-8.

64. Scala S, Ierano C, Ottaiano A, et al. CXC chemokine receptor 4 is expressed in uveal malignant melanoma and correlates with the epithelioid-mixed cell type. *Cancer immunology, immunotherapy : CII.* Oct 2007;56(10):1589-1595.
65. Saraiva VS, Caissie AL, Segal L, Edelstein C, Burnier MN, Jr. Immunohistochemical expression of phospho-Akt in uveal melanoma. *Melanoma research.* Aug 2005;15(4):245-250.
66. Niederkorn JY, Wang S. Immunology of intraocular tumors. *Ocular immunology and inflammation.* Feb 2005;13(1):105-110.
67. Aronow M, Biscotti, C., Chan, C., Singh, A. The Role of Biopsy in the Assessment of Uveal Melanoma. *Retinal Physician.* 2012;9(June):13-17.
68. Shammas HF, Blodi FC. Prognostic factors in choroidal and ciliary body melanomas. *Archives of ophthalmology.* Jan 1977;95(1):63-69.
69. Folkman J, Merler E, Abernathy C, Williams G. Isolation of a tumor factor responsible for angiogenesis. *The Journal of experimental medicine.* Feb 1 1971;133(2):275-288.
70. Ferrara N, Davis-Smyth T. The biology of vascular endothelial growth factor. *Endocrine reviews.* Feb 1997;18(1):4-25.
71. Shibuya M, Claesson-Welsh L. Signal transduction by VEGF receptors in regulation of angiogenesis and lymphangiogenesis. *Experimental cell research.* Mar 10 2006;312(5):549-560.
72. Hanahan D, Folkman J. Patterns and emerging mechanisms of the angiogenic switch during tumorigenesis. *Cell.* Aug 9 1996;86(3):353-364.
73. Takahashi S. Vascular endothelial growth factor (VEGF), VEGF receptors and their inhibitors for antiangiogenic tumor therapy. *Biological & pharmaceutical bulletin.* 2011;34(12):1785-1788.
74. Carmeliet P, Ferreira V, Breier G, et al. Abnormal blood vessel development and lethality in embryos lacking a single VEGF allele. *Nature.* Apr 4 1996;380(6573):435-439.
75. Holmes K, Roberts OL, Thomas AM, Cross MJ. Vascular endothelial growth factor receptor-2: structure, function, intracellular signalling and therapeutic inhibition. *Cellular signalling.* Oct 2007;19(10):2003-2012.
76. Goto F, Goto K, Weindel K, Folkman J. Synergistic effects of vascular endothelial growth factor and basic fibroblast growth factor on the proliferation and cord formation of bovine capillary endothelial cells within collagen gels. *Laboratory investigation; a journal of technical methods and pathology.* Nov 1993;69(5):508-517.
77. Weis SM, Cheresh DA. Pathophysiological consequences of VEGF-induced vascular permeability. *Nature.* Sep 22 2005;437(7058):497-504.
78. Shibuya M, Yamaguchi S, Yamane A, et al. Nucleotide sequence and expression of a novel human receptor-type tyrosine kinase gene (flt) closely related to the fms family. *Oncogene.* Apr 1990;5(4):519-524.
79. Terman BI, Carrion ME, Kovacs E, Rasmussen BA, Eddy RL, Shows TB. Identification of a new endothelial cell growth factor receptor tyrosine kinase. *Oncogene.* Sep 1991;6(9):1677-1683.
80. Matthews W, Jordan CT, Gavin M, Jenkins NA, Copeland NG, Lemischka IR. A receptor tyrosine kinase cDNA isolated from a population of enriched primitive hematopoietic cells and exhibiting close genetic linkage to c-kit. *Proceedings of*

the National Academy of Sciences of the United States of America. Oct 15 1991;88(20):9026-9030.

81. Pajusola K, Aprelikova O, Korhonen J, et al. FLT4 receptor tyrosine kinase contains seven immunoglobulin-like loops and is expressed in multiple human tissues and cell lines. *Cancer research.* Oct 15 1992;52(20):5738-5743.

82. Galland F, Karamysheva A, Pebusque MJ, et al. The FLT4 gene encodes a transmembrane tyrosine kinase related to the vascular endothelial growth factor receptor. *Oncogene.* May 1993;8(5):1233-1240.

83. Ferrara N, Gerber HP, LeCouter J. The biology of VEGF and its receptors. *Nature medicine.* Jun 2003;9(6):669-676.

84. Folkman J. Tumor angiogenesis: therapeutic implications. *The New England journal of medicine.* Nov 18 1971;285(21):1182-1186.

85. Lai GG, Penson RT. Bevacizumab and ovarian cancer. *Drugs Today (Barc).* Sep 2011;47(9):669-681.

86. Lin EY, Li JF, Gnatovskiy L, et al. Macrophages regulate the angiogenic switch in a mouse model of breast cancer. *Cancer research.* Dec 1 2006;66(23):11238-11246.

87. Murakami M, Zheng Y, Hirashima M, et al. VEGFR1 tyrosine kinase signaling promotes lymphangiogenesis as well as angiogenesis indirectly via macrophage recruitment. *Arteriosclerosis, thrombosis, and vascular biology.* Apr 2008;28(4):658-664.

88. Boyd SR, Tan D, Bunce C, et al. Vascular endothelial growth factor is elevated in ocular fluids of eyes harbouring uveal melanoma: identification of a potential therapeutic window. *The British journal of ophthalmology.* Apr 2002;86(4):448-452.

89. Missotten GS, Notting IC, Schlingemann RO, et al. Vascular endothelial growth factor a in eyes with uveal melanoma. *Archives of ophthalmology.* Oct 2006;124(10):1428-1434.

90. Ijland SA, Jager MJ, Heijdra BM, Westphal JR, Peek R. Expression of angiogenic and immunosuppressive factors by uveal melanoma cell lines. *Melanoma research.* Oct 1999;9(5):445-450.

91. el Filali M, Missotten GS, Maat W, et al. Regulation of VEGF-A in uveal melanoma. *Investigative ophthalmology & visual science.* May 2010;51(5):2329-2337.

92. Crosby MB, Yang H, Gao W, Zhang L, Grossniklaus HE. Serum vascular endothelial growth factor (VEGF) levels correlate with number and location of micrometastases in a murine model of uveal melanoma. *The British journal of ophthalmology.* Jan 2011;95(1):112-117.

93. Boyd SR, Tan DS, de Souza L, et al. Uveal melanomas express vascular endothelial growth factor and basic fibroblast growth factor and support endothelial cell growth. *The British journal of ophthalmology.* Apr 2002;86(4):440-447.

94. Sheidow TG, Hooper PL, Crukley C, Young J, Heathcote JG. Expression of vascular endothelial growth factor in uveal melanoma and its correlation with metastasis. *The British journal of ophthalmology.* Jul 2000;84(7):750-756.

95. Presta LG, Chen H, O'Connor SJ, et al. Humanization of an anti-vascular endothelial growth factor monoclonal antibody for the therapy of solid tumors and other disorders. *Cancer research.* Oct 15 1997;57(20):4593-4599.

96. Sandler A, Gray R, Perry MC, et al. Paclitaxel-carboplatin alone or with bevacizumab for non-small-cell lung cancer. *The New England journal of medicine.* Dec 14 2006;355(24):2542-2550.
97. Miller K, Wang M, Gralow J, et al. Paclitaxel plus bevacizumab versus paclitaxel alone for metastatic breast cancer. *The New England journal of medicine.* Dec 27 2007;357(26):2666-2676.
98. Holash J, Davis S, Papadopoulos N, et al. VEGF-Trap: a VEGF blocker with potent antitumor effects. *Proceedings of the National Academy of Sciences of the United States of America.* Aug 20 2002;99(17):11393-11398.
99. Shojaei F. Anti-angiogenesis therapy in cancer: current challenges and future perspectives. *Cancer letters.* Jul 28 2012;320(2):130-137.
100. Jain RK. Normalization of tumor vasculature: an emerging concept in antiangiogenic therapy. *Science.* Jan 7 2005;307(5706):58-62.
101. Casanovas O, Hicklin DJ, Bergers G, Hanahan D. Drug resistance by evasion of antiangiogenic targeting of VEGF signaling in late-stage pancreatic islet tumors. *Cancer cell.* Oct 2005;8(4):299-309.
102. Paez-Ribes M, Allen E, Hudock J, et al. Antiangiogenic therapy elicits malignant progression of tumors to increased local invasion and distant metastasis. *Cancer cell.* Mar 3 2009;15(3):220-231.
103. Ebos JM, Lee CR, Cruz-Munoz W, Bjarnason GA, Christensen JG, Kerbel RS. Accelerated metastasis after short-term treatment with a potent inhibitor of tumor angiogenesis. *Cancer cell.* Mar 3 2009;15(3):232-239.
104. Cairns RA, Kalliomaki T, Hill RP. Acute (cyclic) hypoxia enhances spontaneous metastasis of KHT murine tumors. *Cancer research.* Dec 15 2001;61(24):8903-8908.
105. Pennacchietti S, Michieli P, Galluzzo M, Mazzone M, Giordano S, Comoglio PM. Hypoxia promotes invasive growth by transcriptional activation of the met protooncogene. *Cancer cell.* Apr 2003;3(4):347-361.
106. Yang H, Jager MJ, Grossniklaus HE. Bevacizumab suppression of establishment of micrometastases in experimental ocular melanoma. *Investigative ophthalmology & visual science.* Jun 2010;51(6):2835-2842.
107. Treatment with intravitreal Avastin for large uveal melanomas. In: Trials C, ed2008.
108. Piperno-Neumann S. SV, Bidard F-C., Mariani P., Plancher C., Asselain B., Vago-Ady N., Desjardins L. BEVATEM: Phase II single-center study of bevacizumab in combination with temozolomide in patients (pts) with first-line metastatic uveal melanoma (MUM): First-step results. *American Society of Clinical Oncology.* Vol 30: J Clin Oncol; 2012.
109. Lima BR, Schoenfield LR, Singh AD. The impact of intravitreal bevacizumab therapy on choroidal melanoma. *American journal of ophthalmology.* Feb 2011;151(2):323-328 e322.
110. Eremina V, Quaggin SE. Biology of anti-angiogenic therapy-induced thrombotic microangiopathy. *Seminars in nephrology.* Nov 2010;30(6):582-590.
111. Stewart MW. The expanding role of vascular endothelial growth factor inhibitors in ophthalmology. *Mayo Clinic proceedings. Mayo Clinic.* Jan 2012;87(1):77-88.
112. Avery RL, Pearlman J, Pieramici DJ, et al. Intravitreal bevacizumab (Avastin) in the treatment of proliferative diabetic retinopathy. *Ophthalmology.* Oct 2006;113(10):1695 e1691-1615.

113. Spaide RF, Laud K, Fine HF, et al. Intravitreal bevacizumab treatment of choroidal neovascularization secondary to age-related macular degeneration. *Retina.* Apr 2006;26(4):383-390.
114. Iturralde D, Spaide RF, Meyerle CB, et al. Intravitreal bevacizumab (Avastin) treatment of macular edema in central retinal vein occlusion: a short-term study. *Retina.* Mar 2006;26(3):279-284.
115. Avery RL. Regression of retinal and iris neovascularization after intravitreal bevacizumab (Avastin) treatment. *Retina.* Mar 2006;26(3):352-354.
116. Pieramici DJ, Avery RL, Castellarin AA, Nasir MA, Rabena M. Case of anterior uveitis after intravitreal injection of bevacizumab. *Retina.* Sep 2006;26(7):841-842.
117. Meyer CH, Mennel S, Schmidt JC, Kroll P. Acute retinal pigment epithelial tear following intravitreal bevacizumab (Avastin) injection for occult choroidal neovascularisation secondary to age related macular degeneration. *The British journal of ophthalmology.* Sep 2006;90(9):1207-1208.
118. Wu L, Martinez-Castellanos MA, Quiroz-Mercado H, et al. Twelve-month safety of intravitreal injections of bevacizumab (Avastin): results of the Pan-American Collaborative Retina Study Group (PACORES). *Graefe's archive for clinical and experimental ophthalmology = Albrecht von Graefes Archiv fur klinische und experimentelle Ophthalmologie.* Jan 2008;246(1):81-87.
119. Klettner A, Roider J. Comparison of bevacizumab, ranibizumab, and pegaptanib in vitro: efficiency and possible additional pathways. *Investigative ophthalmology & visual science.* Oct 2008;49(10):4523-4527.
120. Martin DF, Maguire MG, Ying GS, Grunwald JE, Fine SL, Jaffe GJ. Ranibizumab and bevacizumab for neovascular age-related macular degeneration. *The New England journal of medicine.* May 19 2011;364(20):1897-1908.
121. Steinbrook R. The price of sight--ranibizumab, bevacizumab, and the treatment of macular degeneration. *The New England journal of medicine.* Oct 5 2006;355(14):1409-1412.
122. Martin DF, Maguire MG, Fine SL, et al. Ranibizumab and Bevacizumab for Treatment of Neovascular Age-Related Macular Degeneration: Two-Year Results. *Ophthalmology.* May 1 2012.
123. De Waard-Siebinga I, Blom DJ, Griffioen M, et al. Establishment and characterization of an uveal-melanoma cell line. *International journal of cancer. Journal international du cancer.* Jul 17 1995;62(2):155-161.
124. Marshall JC, Caissie AL, Callejo SA, Antecka E, Burnier Jr MN. Cell proliferation profile of five human uveal melanoma cell lines of different metastatic potential. *Pathobiology : journal of immunopathology, molecular and cellular biology.* 2004;71(5):241-245.
125. Diebold Y, Blanco G, Saornil MA, Fernandez N, Lazaro MC. Morphologic and immunocytochemical characterization of four human uveal cell lines (melanoma- and melanocytes-derived). *Current eye research.* May 1997;16(5):487-495.
126. Lopez-Velasco R, Morilla-Grasa A, Saornil-Alvarez MA, et al. Efficacy of five human melanocytic cell lines in experimental rabbit choroidal melanoma. *Melanoma research.* Feb 2005;15(1):29-37.

127. Strober W. Trypan blue exclusion test of cell viability. *Current protocols in immunology / edited by John E. Coligan ... [et al.].* May 2001;Appendix 3:Appendix 3B.
128. Maloney SC, Marshall JC, Antecka E, et al. SPARC is expressed in human uveal melanoma and its abrogation reduces tumor cell proliferation. *Anticancer research.* Aug 2009;29(8):3059-3064.
129. Abramoff MD, Magalhaes, P.J., Ram, S.J. Image Processing with ImageJ. *Biophotonics International.* 2004;11(7):36-42.
130. Kaczmarek E, Gorna A, Majewski P. Techniques of image analysis for quantitative immunohistochemistry. *Rocz Akad Med Bialymst.* 2004;49 Suppl 1:155-158.
131. Pfaffl MW. A new mathematical model for relative quantification in real-time RT-PCR. *Nucleic acids research.* May 1 2001;29(9):e45.
132. Cools-Lartigue J, Marshall JC, Caissie AL, Saraiva VS, Burnier MN, Jr. Secretion of hepatocyte growth factor and vascular endothelial growth factor during uveal melanoma-monocyte in vitro interactions. *Melanoma research.* Jun 2005;15(3):141-145.
133. Barak V, Pe'er J, Kalickman I, Frenkel S. VEGF as a biomarker for metastatic uveal melanoma in humans. *Current eye research.* Apr 2011;36(4):386-390.
134. Biswas P, Sengupta S, Choudhary R, Home S, Paul A, Sinha S. Comparative role of intravitreal ranibizumab versus bevacizumab in choroidal neovascular membrane in age-related macular degeneration. *Indian journal of ophthalmology.* May-Jun 2011;59(3):191-196.
135. Wu WC, Yeh PT, Chen SN, Yang CM, Lai CC, Kuo HK. Effects and complications of bevacizumab use in patients with retinopathy of prematurity: a multicenter study in taiwan. *Ophthalmology.* Jan 2011;118(1):176-183.
136. Lefevre G, Babchia N, Calipel A, et al. Activation of the FGF2/FGFR1 autocrine loop for cell proliferation and survival in uveal melanoma cells. *Investigative ophthalmology & visual science.* Mar 2009;50(3):1047-1057.
137. de Jong JS, van Diest PJ, van der Valk P, Baak JP. Expression of growth factors, growth-inhibiting factors, and their receptors in invasive breast cancer. II: Correlations with proliferation and angiogenesis. *The Journal of pathology.* Jan 1998;184(1):53-57.
138. Boocock CA, Charnock-Jones DS, Sharkey AM, et al. Expression of vascular endothelial growth factor and its receptors flt and KDR in ovarian carcinoma. *Journal of the National Cancer Institute.* Apr 5 1995;87(7):506-516.
139. Jackson MW, Roberts JS, Heckford SE, et al. A potential autocrine role for vascular endothelial growth factor in prostate cancer. *Cancer research.* Feb 1 2002;62(3):854-859.
140. Gaudry M, Bregerie O, Andrieu V, El Benna J, Pocidalo MA, Hakim J. Intracellular pool of vascular endothelial growth factor in human neutrophils. *Blood.* Nov 15 1997;90(10):4153-4161.
141. Fan F, Samuel S, Gaur P, et al. Chronic exposure of colorectal cancer cells to bevacizumab promotes compensatory pathways that mediate tumour cell migration. *British journal of cancer.* Apr 12 2011;104(8):1270-1277.
142. Forooghian F, Kertes PJ, Eng KT, Agron E, Chew EY. Alterations in the intraocular cytokine milieu after intravitreal bevacizumab. *Investigative ophthalmology & visual science.* May 2010;51(5):2388-2392.

143. Skehan P, Storeng R, Scudiero D, et al. New colorimetric cytotoxicity assay for anticancer-drug screening. *Journal of the National Cancer Institute.* Jul 4 1990;82(13):1107-1112.

144. Yang X, Lu P, Fujii C, et al. Essential contribution of a chemokine, CCL3, and its receptor, CCR1, to hepatocellular carcinoma progression. *International journal of cancer. Journal international du cancer.* Apr 15 2006;118(8):1869-1876.

145. Molhoek KR, Griesemann H, Shu J, Gershenwald JE, Brautigan DL, Slingluff CL, Jr. Human melanoma cytolysis by combined inhibition of mammalian target of rapamycin and vascular endothelial growth factor/vascular endothelial growth factor receptor-2. *Cancer research.* Jun 1 2008;68(11):4392-4397.

146. Emlet DR, Brown KA, Kociban DL, et al. Response to trastuzumab, erlotinib, and bevacizumab, alone and in combination, is correlated with the level of human epidermal growth factor receptor-2 expression in human breast cancer cell lines. *Molecular cancer therapeutics.* Oct 2007;6(10):2664-2674.

147. Asnaghi L, Ebrahimi KB, Schreck KC, et al. Notch signaling promotes growth and invasion in uveal melanoma. *Clinical cancer research : an official journal of the American Association for Cancer Research.* Feb 1 2012;18(3):654-665.

148. Jubb AM, Oates AJ, Holden S, Koeppen H. Predicting benefit from anti-angiogenic agents in malignancy. *Nature reviews. Cancer.* Aug 2006;6(8):626-635.

149. Jubb AM, Browning L, Campo L, et al. Expression of vascular Notch ligands Delta-like 4 and Jagged-1 in glioblastoma. *Histopathology.* Apr 2012;60(5):740-747.

150. Darrington E, Zhong M, Vo BH, Khan SA. Vascular endothelial growth factor A, secreted in response to transforming growth factor-beta1 under hypoxic conditions, induces autocrine effects on migration of prostate cancer cells. *Cellular & molecular immunology.* Jun 18 2012.

151. Valleala H, Hanemaaijer R, Mandelin J, et al. Regulation of MMP-9 (gelatinase B) in activated human monocyte/macrophages by two different types of bisphosphonates. *Life sciences.* Sep 26 2003;73(19):2413-2420.

152. El-Shabrawi Y, Ardjomand N, Radner H. MMP-9 is predominantly expressed in epithelioid and not spindle cell uveal melanoma. *The Journal of pathology.* Jun 2001;194(2):201-206.

153. Maurer M, von Stebut E. Macrophage inflammatory protein-1. *The international journal of biochemistry & cell biology.* Oct 2004;36(10):1882-1886.

154. Harlin H, Meng Y, Peterson AC, et al. Chemokine expression in melanoma metastases associated with CD8+ T-cell recruitment. *Cancer research.* Apr 1 2009;69(7):3077-3085.

155. Ly LV, Bronkhorst IH, van Beelen E, et al. Inflammatory cytokines in eyes with uveal melanoma and relation with macrophage infiltration. *Investigative ophthalmology & visual science.* Nov 2010;51(11):5445-5451.

156. Park JE, Keller GA, Ferrara N. The vascular endothelial growth factor (VEGF) isoforms: differential deposition into the subepithelial extracellular matrix and bioactivity of extracellular matrix-bound VEGF. *Molecular biology of the cell.* Dec 1993;4(12):1317-1326.

157. Lentzsch S, Gries M, Janz M, Bargou R, Dorken B, Mapara MY. Macrophage inflammatory protein 1-alpha (MIP-1 alpha) triggers migration and signaling cascades mediating survival and proliferation in multiple myeloma (MM) cells. *Blood.* May 1 2003;101(9):3568-3573.

158. Bruns AF, Herbert SP, Odell AF, et al. Ligand-stimulated VEGFR2 signaling is regulated by co-ordinated trafficking and proteolysis. *Traffic.* Jan 2010;11(1):161-174.

159. Le Y, Zhou Y, Iribarren P, Wang J. Chemokines and chemokine receptors: their manifold roles in homeostasis and disease. *Cellular & molecular immunology.* Apr 2004;1(2):95-104.

160. Makitie T, Summanen P, Tarkkanen A, Kivela T. Tumor-infiltrating macrophages (CD68(+) cells) and prognosis in malignant uveal melanoma. *Investigative ophthalmology & visual science.* Jun 2001;42(7):1414-1421.

161. Lu P, Li L, Wu Y, Mukaida N, Zhang X. Essential contribution of CCL3 to alkali-induced corneal neovascularization by regulating vascular endothelial growth factor production by macrophages. *Molecular vision.* 2008;14:1614-1622.

162. Jeong JH, Chun YS, Kim ES, Kim JC. Compensatory growth factor and cytokine response in tears after subconjunctival bevacizumab injection. *Cornea.* Oct 2011;30(10):1071-1077.

163. White VA, Chambers JD, Courtright PD, Chang WY, Horsman DE. Correlation of cytogenetic abnormalities with the outcome of patients with uveal melanoma. *Cancer.* Jul 15 1998;83(2):354-359.

164. de la Cruz PO, Jr., Specht CS, McLean IW. Lymphocytic infiltration in uveal malignant melanoma. *Cancer.* Jan 1 1990;65(1):112-115.

165. Marshall JC, Fernandes BF, Di Cesare S, et al. The use of a cyclooxygenase-2 inhibitor (Nepafenac) in an ocular and metastatic animal model of uveal melanoma. *Carcinogenesis.* Sep 2007;28(9):2053-2058.

166. Fernandes BF, Di Cesare S, Neto Belfort R, et al. Imatinib mesylate alters the expression of genes related to disease progression in an animal model of uveal melanoma. *Anal Cell Pathol (Amst).* 2011;34(3):123-130.

167. Burnier MN, Jr., McLean IW, Gamel JW. Immunohistochemical evaluation of uveal melanocytic tumors. Expression of HMB-45, S-100 protein, and neuron-specific enolase. *Cancer.* Aug 15 1991;68(4):809-814.

168. Landini G. How to correct background illumination in brightfield microscopy. 2006-2010. http://imagejdocu.tudor.lu/doku.php?id=howto:working:how_to_correct_background_illumination_in_brightfield_microscopy. Accessed July 6, 2012.

169. Ruifrok AC, Johnston DA. Quantification of histochemical staining by color deconvolution. *Analytical and quantitative cytology and histology / the International Academy of Cytology [and] American Society of Cytology.* Aug 2001;23(4):291-299.

170. Blanco PL, Marshall JC, Antecka E, et al. Characterization of ocular and metastatic uveal melanoma in an animal model. *Investigative ophthalmology & visual science.* Dec 2005;46(12):4376-4382.

171. Sahin A, Kiratli H, Soylemezoglu F, Tezel GG, Bilgic S, Saracbasi O. Expression of vascular endothelial growth factor-A, matrix metalloproteinase-9, and extravascular matrix patterns and their correlations with clinicopathologic parameters in posterior uveal melanomas. *Japanese journal of ophthalmology.* Sep-Oct 2007;51(5):325-331.

172. Masmoudi H, Hewitt SM, Petrick N, Myers KJ, Gavrielides MA. Automated quantitative assessment of HER-2/neu immunohistochemical expression in breast cancer. *IEEE transactions on medical imaging.* Jun 2009;28(6):916-925.

173. Clark GM. Should selection of adjuvant chemotherapy for patients with breast cancer be based on erbB-2 status? *Journal of the National Cancer Institute.* Sep 16 1998;90(18):1320-1321.
174. Kay EW, Walsh CJ, Cassidy M, Curran B, Leader M. C-erbB-2 immunostaining: problems with interpretation. *Journal of clinical pathology.* Sep 1994;47(9):816-822.
175. Zhu Z, Jiang W, Thompson HJ. Effect of energy restriction on the expression of cyclin D1 and p27 during premalignant and malignant stages of chemically induced mammary carcinogenesis. *Molecular carcinogenesis.* Apr 1999;24(4):241-245.
176. McGinley JN, Knott KK, Thompson HJ. Effect of fixation and epitope retrieval on BrdU indices in mammary carcinomas. *The journal of histochemistry and cytochemistry : official journal of the Histochemistry Society.* Mar 2000;48(3):355-362.
177. Jacobs TW, Prioleau JE, Stillman IE, Schnitt SJ. Loss of tumor marker-immunostaining intensity on stored paraffin slides of breast cancer. *Journal of the National Cancer Institute.* Aug 7 1996;88(15):1054-1059.
178. Sahin A, Kiratli H, Tezel GG, Soylemezoglu F, Bilgic S. Expression of vascular endothelial growth factor a, matrix metalloproteinase 9 and extravascular matrix patterns in iris and ciliary body melanomas. *Ophthalmic research.* 2007;39(1):40-44.
179. Press MF, Hung G, Godolphin W, Slamon DJ. Sensitivity of HER-2/neu antibodies in archival tissue samples: potential source of error in immunohistochemical studies of oncogene expression. *Cancer research.* May 15 1994;54(10):2771-2777.
180. Busmanis I, Feleppa F, Jones A, et al. Analysis of cerbB2 expression using a panel of 6 commercially available antibodies. *Pathology.* Jul 1994;26(3):261-267.
181. Solomides CC, Zimmerman R, Bibbo M. Semiquantitative assessment of c-erbB-2 (HER-2) status in cytology specimens and tissue sections from breast carcinoma. *Analytical and quantitative cytology and histology / the International Academy of Cytology [and] American Society of Cytology.* Apr 1999;21(2):121-125.
182. Nozue M, Isaka N, Fukao K. Over-expression of vascular endothelial growth factor after preoperative radiation therapy for rectal cancer. *Oncology reports.* Nov-Dec 2001;8(6):1247-1249.
183. FDA. FDA Commissioner announces Avastin decision In: Administration USFaD, ed2011.
184. NICE. Avastin (bevacizumab) is not recommended for the treatment of metastatic breast cancer in new guidance from NICE. In: Excellence NIfHaC, ed2011.
185. Spaide RF, Fisher YL. Intravitreal bevacizumab (Avastin) treatment of proliferative diabetic retinopathy complicated by vitreous hemorrhage. *Retina.* Mar 2006;26(3):275-278.
186. Smit DP, Meyer D. Intravitreal bevacizumab: an analysis of the evidence. *Clin Ophthalmol.* Sep 2007;1(3):273-284.
187. Arbab AS. Activation of alternative pathways of angiogenesis and involvement of stem cells following anti-angiogenesis treatment in glioma. *Histology and histopathology.* May 2012;27(5):549-557.

188. Jia Z, Zhang J, Wei D, et al. Molecular basis of the synergistic antiangiogenic activity of bevacizumab and mithramycin A. *Cancer research.* May 15 2007;67(10):4878-4885.
189. Huang D, Ding Y, Zhou M, et al. Interleukin-8 mediates resistance to antiangiogenic agent sunitinib in renal cell carcinoma. *Cancer research.* Feb 1 2010;70(3):1063-1071.
190. Kalirai H, Damato BE, Coupland SE. Uveal melanoma cell lines contain stem-like cells that self-renew, produce differentiated progeny, and survive chemotherapy. *Investigative ophthalmology & visual science.* Oct 2011;52(11):8458-8466.
191. Giuntoli S, Rovida E, Gozzini A, et al. Severe hypoxia defines heterogeneity and selects highly immature progenitors within clonal erythroleukemia cells. *Stem Cells.* May 2007;25(5):1119-1125.
192. Lucio-Eterovic AK, Piao Y, de Groot JF. Mediators of glioblastoma resistance and invasion during antivascular endothelial growth factor therapy. *Clinical cancer research : an official journal of the American Association for Cancer Research.* Jul 15 2009;15(14):4589-4599.
193. Persidis A. Cancer multidrug resistance. *Nature biotechnology.* Jan 1999;17(1):94-95.
194. Kim S, Takahashi H, Lin WW, et al. Carcinoma-produced factors activate myeloid cells through TLR2 to stimulate metastasis. *Nature.* Jan 1 2009;457(7225):102-106.
195. Nagarkatti-Gude N, Bronkhorst IH, van Duinen SG, Luyten GP, Jager MJ. Cytokines and chemokines in the vitreous fluid of eyes with uveal melanoma. *Investigative ophthalmology & visual science.* 2012;53(11):6748-6755.
196. Nakasone Y, Fujimoto M, Matsushita T, et al. Host-derived MCP-1 and MIP-1alpha regulate protective anti-tumor immunity to localized and metastatic B16 melanoma. *The American journal of pathology.* Jan 2012;180(1):365-374.
197. He S, Wang L, Wu Y, Li D, Zhang Y. CCL3 and CCL20-recruited dendritic cells modified by melanoma antigen gene-1 induce anti-tumor immunity against gastric cancer ex vivo and in vivo. *Journal of experimental & clinical cancer research : CR.* 2010;29:37.
198. Zhou J, Ding T, Pan W, Zhu LY, Li L, Zheng L. Increased intratumoral regulatory T cells are related to intratumoral macrophages and poor prognosis in hepatocellular carcinoma patients. *International journal of cancer. Journal international du cancer.* Oct 1 2009;125(7):1640-1648.
199. Klisovic DD, Klisovic MI, Effron D, Liu S, Marcucci G, Katz SE. Depsipeptide inhibits migration of primary and metastatic uveal melanoma cell lines in vitro: a potential strategy for uveal melanoma. *Melanoma research.* Jun 2005;15(3):147-153.
200. Liu N, Sun Q, Chen J, et al. MicroRNA-9 suppresses uveal melanoma cell migration and invasion through the NF-kappaB1 pathway. *Oncology reports.* Sep 2012;28(3):961-968.
201. Grove M, Plumb M. C/EBP, NF-kappa B, and c-Ets family members and transcriptional regulation of the cell-specific and inducible macrophage inflammatory protein 1 alpha immediate-early gene. *Molecular and cellular biology.* Sep 1993;13(9):5276-5289.

202. Tabruyn SP, Memet S, Ave P, et al. NF-kappaB activation in endothelial cells is critical for the activity of angiostatic agents. *Molecular cancer therapeutics.* Sep 2009;8(9):2645-2654.
203. Croom KF, Dhillon S. Bevacizumab: a review of its use in combination with paclitaxel or capecitabine as first-line therapy for HER2-negative metastatic breast cancer. *Drugs.* Nov 12 2011;71(16):2213-2229.
204. Yoo DS, Kirkpatrick JP, Craciunescu O, et al. Prospective trial of synchronous bevacizumab, erlotinib, and concurrent chemoradiation in locally advanced head and neck cancer. *Clinical cancer research : an official journal of the American Association for Cancer Research.* Mar 1 2012;18(5):1404-1414.
205. Hamed H, Zaki S. Role of CCL3 protein (monocyte inflammatory protein-1 alpha) in lymphoid malignancy. *The Egyptian journal of immunology / Egyptian Association of Immunologists.* 2007;14(1):63-72.
206. Vallet S, Raje N, Ishitsuka K, et al. MLN3897, a novel CCR1 inhibitor, impairs osteoclastogenesis and inhibits the interaction of multiple myeloma cells and osteoclasts. *Blood.* Nov 15 2007;110(10):3744-3752.
207. Tai YT, Chang BY, Kong SY, et al. Bruton's tyrosine kinase inhibition is a novel therapeutic strategy targeting tumor in the bone marrow microenvironment in multiple myeloma. *Blood.* Jun 11 2012.
208. O'Connell MP, Weeraratna AT. Hear the Wnt Ror: how melanoma cells adjust to changes in Wnt. *Pigment cell & melanoma research.* Dec 2009;22(6):724-739.
209. Gan HK, Lappas M, Cao DX, Cvrljevdic A, Scott AM, Johns TG. Targeting a unique EGFR epitope with monoclonal antibody 806 activates NF-kappaB and initiates tumour vascular normalization. *Journal of cellular and molecular medicine.* Sep 2009;13(9B):3993-4001.
210. Ma D, Niederkorn JY. Role of epidermal growth factor receptor in the metastasis of intraocular melanomas. *Investigative ophthalmology & visual science.* Jun 1998;39(7):1067-1075.
211. Wu X, Zhou J, Rogers AM, et al. c-Met, epidermal growth factor receptor, and insulin-like growth factor-1 receptor are important for growth in uveal melanoma and independently contribute to migration and metastatic potential. *Melanoma research.* Apr 2012;22(2):123-132.
212. Ebos JM, Kerbel RS. Antiangiogenic therapy: impact on invasion, disease progression, and metastasis. *Nature reviews. Clinical oncology.* Apr 2011;8(4):210-221.
213. Nag S, Quivey JM, Earle JD, Followill D, Fontanesi J, Finger PT. The American Brachytherapy Society recommendations for brachytherapy of uveal melanomas. *International journal of radiation oncology, biology, physics.* Jun 1 2003;56(2):544-555.
214. Wilhelm SM, Carter C, Tang L, et al. BAY 43-9006 exhibits broad spectrum oral antitumor activity and targets the RAF/MEK/ERK pathway and receptor tyrosine kinases involved in tumor progression and angiogenesis. *Cancer research.* Oct 1 2004;64(19):7099-7109.
215. clinicaltrials.gov. A Study of Sorafenib in Patients With Chemonaive Metastatic Uveal Melanoma (STREAM). http://clinicaltrials.gov/show/NCT013770252011.
216. Wenjing Z, Minwang, M., Dong, W., Dongrun, T. Inhibition of angiogenesis and metastasis of uveal melanoma cells by astragaloside IV. *Journal of Medicinal Plants Research.* August, 2012 2011;6(31):4609-4614.

217. Law PC, Auyeung KK, Chan LY, Ko JK. Astragalus saponins downregulate vascular endothelial growth factor under cobalt chloride-stimulated hypoxia in colon cancer cells. *BMC complementary and alternative medicine.* Sep 19 2012;12(1):160.

218. Naumov GN, MacDonald IC, Weinmeister PM, et al. Persistence of solitary mammary carcinoma cells in a secondary site: a possible contributor to dormancy. *Cancer research.* Apr 1 2002;62(7):2162-2168.

219. Paterlini-Brechot P, Benali NL. Circulating tumor cells (CTC) detection: clinical impact and future directions. *Cancer letters.* Aug 18 2007;253(2):180-204.

220. Borsig L, Wong R, Hynes RO, Varki NM, Varki A. Synergistic effects of L- and P-selectin in facilitating tumor metastasis can involve non-mucin ligands and implicate leukocytes as enhancers of metastasis. *Proceedings of the National Academy of Sciences of the United States of America.* Feb 19 2002;99(4):2193-2198.

221. Eide N, Faye RS, Hoifodt HK, et al. Immunomagnetic detection of micrometastatic cells in bone marrow in uveal melanoma patients. *Acta ophthalmologica.* Nov 2009;87(8):830-836.

222. Zhao J, Yan LN, Li B. Adult-to-adult living donor liver transplantation for malignant metastatic melanoma to the liver. *Hepatobiliary & pancreatic diseases international : HBPD INT.* Jun 2010;9(3):329-332.

223. Choudhury KR, Yagle KJ, Swanson PE, Krohn KA, Rajendran JG. A robust automated measure of average antibody staining in immunohistochemistry images. *The journal of histochemistry and cytochemistry : official journal of the Histochemistry Society.* Feb 2010;58(2):95-107.

224. Lazova R, Camp RL, Klump V, Siddiqui SF, Amaravadi RK, Pawelek JM. Punctate LC3B expression is a common feature of solid tumors and associated with proliferation, metastasis, and poor outcome. *Clinical cancer research : an official journal of the American Association for Cancer Research.* Jan 15 2012;18(2):370-379.

225. Shields CL, Ganguly A, Bianciotto CG, Turaka K, Tavallali A, Shields JA. Prognosis of uveal melanoma in 500 cases using genetic testing of fine-needle aspiration biopsy specimens. *Ophthalmology.* Feb 2011;118(2):396-401.

226. Matos LL, Stabenow E, Tavares MR, Ferraz AR, Capelozzi VL, Pinhal MA. Immunohistochemistry quantification by a digital computer-assisted method compared to semiquantitative analysis. *Clinics (Sao Paulo).* Oct 2006;61(5):417-424.

227. Gustavson MD, Bourke-Martin B, Reilly D, et al. Standardization of HER2 immunohistochemistry in breast cancer by automated quantitative analysis. *Archives of pathology & laboratory medicine.* Sep 2009;133(9):1413-1419.

228. Turashvili G, Leung S, Turbin D, et al. Inter-observer reproducibility of HER2 immunohistochemical assessment and concordance with fluorescent in situ hybridization (FISH): pathologist assessment compared to quantitative image analysis. *BMC cancer.* 2009;9:165.

229. Jacobs TW, Gown AM, Yaziji H, Barnes MJ, Schnitt SJ. HER-2/neu protein expression in breast cancer evaluated by immunohistochemistry. A study of interlaboratory agreement. *American journal of clinical pathology.* Feb 2000;113(2):251-258.

Appendix I

//Rabbit Immunostaining Quantification Java Macro

```
title = getTitle;
```

//To correct image for bright and darkfield anomalies

```
  imageCalculator("Subtract create", "Brightfield.TIF","Darkfield.TIF");
  selectWindow("Result of Brightfield.TIF");
  rename("Divisor");
  imageCalculator("Subtract create", title,"Darkfield.TIF");
  selectWindow("Result of "+title);
  rename("Numerator");
 run("Calculator Plus", "i1=Numerator i2=Divisor operation=[Divide: i2 = (i1/i2)
x k1 + k2] k1=255 k2=0 create");
  selectWindow("Result");
  rename(title+ " Corrected");
selectWindow("Numerator");
run("Close");
selectWindow("Divisor");
run("Close");
selectWindow(title);
run("Close");
selectWindow(title+" Corrected");
run("Select All");
run("Copy");
```

//To enhance contrast to separate color spectra

```
run("Enhance Contrast", "saturated=1 equalize");
```

//To separate and isolate positive immunostaining

```
run("Colour Deconvolutions", "vectors=VEGF_A hide");

run("Despeckle");

selectWindow(title+" Corrected-Red");
```

//To threshold the positive staining image

```
setAutoThreshold();

getThreshold(min, max);

setThreshold(0, 150);

run("Make Binary");
```

//To analyze and count the number of immunostained cells

```
run("Watershed");

selectWindow(title+" Corrected-Red");

run("Analyze Particles...", "size=70-Infinity circularity=0.00-1.00 show=Outlines
display summarize");
```

//To measure the immunostained area

```
  run("Set Measurements...", "area area_fraction limit display redirect=None
decimal=3");

  run("Measure")
```

Appendix II

//Human Uveal Melanoma Immunostaining Quantification Java Macro

```
title = getTitle;


// To adjust for bright and darkfield anomalies
imageCalculator("Subtract create", "Brightfield.TIF","Darkfield.TIF");
selectWindow("Result of Brightfield.TIF");
rename("Divisor");
imageCalculator("Subtract create", title,"Darkfield.TIF");
selectWindow("Result of "+title);
rename("Numerator");
run("Calculator Plus", "i1=Numerator i2=Divisor operation=[Divide: i2 = (i1/i2)
x k1 + k2] k1=255 k2=0 create");
selectWindow("Result");
rename(title+ " Corrected");
selectWindow("Numerator");
run("Close");
selectWindow("Divisor");
run("Close");
selectWindow(title);
run("Close");


//To enhance contrast to separate color spectra
run("Enhance Contrast", "saturated=1");
```

// To adjust Color Threshold (Hue, Saturation, Brightness) so that only positive immunostaining remains

```
selectWindow(title+" Corrected");

min=newArray(3);

max=newArray(3);

filter=newArray(3);

a=getTitle();

run("HSB Stack");


selectWindow(title+" Corrected");


run("Convert Stack to Images");

selectWindow("Hue");

rename("0");

selectWindow("Saturation");

rename("1");

selectWindow("Brightness");

rename("2");

min[0]=190;

max[0]=255;

filter[0]="pass";

min[1]=100;

max[1]=255;

filter[1]="pass";

min[2]=82;
```

```
max[2]=255;
filter[2]="pass";
for (i=0;i<3;i++){
  selectWindow(""+i);
  setThreshold(min[i], max[i]);
  run("Convert to Mask");
  if (filter[i]=="stop")  run("Invert");
}
imageCalculator("AND create", "0","1");
imageCalculator("AND create", "Result of 0","2");
for (i=0;i<3;i++){
  selectWindow(""+i);
  close();
}
selectWindow("Result of 0");
close();
selectWindow("Result of Result of 0");
rename(a);
```

//To measure the immunostained area

```
selectWindow(title+" Corrected");
run("Set Measurements...", "area area_fraction limit display redirect=None
decimal=3");
run("Measure");
selectWindow("Results");
```

//To analyze and count the number of immunostained cells

selectWindow(title+" Corrected");

run("Analyze Particles...", "size=70-Infinity circularity=0.00-1.00 show=Outlines display summarize");

THE END